Impact of fish farming on benthic communities and the natural condition

A geochemical and micropaleontological study

Carsten Sørlie

Master Thesis
Environmental geology – Environmental stratigraphy
60 credits

Institute of Geosciences
The faculty of Mathematical and Natural Sciences

UNIVERSITY OF OSLO

10/2018

Impact of fish farming on benthic communities and the natural condition

A geochemical and micropaleontological study

Carsten Sørlie

Master Thesis
Environmental geology – Environmental stratigraphy
60 credits

Institute of Geosciences
The faculty of Mathematical and Natural Sciences

UNIVERSITY OF OSLO

10/2018

2018

Impact of fish farming on the benthic community and the natural condition

Carsten Sørlie

http://www.duo.uio.no/

Trykk: Reprosentralen, Universitetet i Oslo

Abstract

This study investigated fish farm impact on the benthic environment at in a northern Norwegian fjord by analysing temporal changes in geochemical concentrations and micropaleontological assemblages from pre fish farming times to present day. Sediment cores were collected at two deep basins in inner Øksfjord and radiometrically dated by the Pb-210 method. The radio nuclide concentrations and grain size distribution analysis indicated redeposited sediment layers in different core depth intervals in each core. Excluding the redeposited layers, the sedimentation accumulation rates were stable and showed no increase post fish farm establishment. Normalized total organic carbon and total nitrogen content in the sediments, together with stable C- and N-isotope ratios were analysed to interpret the sources of organic material. An increase in nTOC and TN concentrations in recent sediments indicated increased organic material deposition in recent times, which was substantiated by increased abundance of species indicative of organic enrichment. The stable isotopes signal and C/N ratio was found to relatively stable, indicating little input of terrestrially sourced organic material at the locations. Heavy metal concentrations were analysed and displayed no significant increases post fish farm establishment. Foraminiferal assemblages were analysed in terms of relative abundance of species, foraminiferal concentration, foraminiferal accumulation rate and similarity of assemblages. Although, the species composition in recent assemblages in both locations indicated increased available nutrients post fish farm establishment, all assemblages were classified as having *good* or *background* ecological quality status (EcoQS) based on diversity, thus indicating no heavy impact on the benthic community post fish farm establishment.

Acknowledgments

I would like to thank my supervisor Elisabeth Alve for the opportunity to join this project and all the help and guidance she has given me. I would especially thank co-supervisor Siliva Hess for all the excellent help with the foraminiferal species analysis, and the proof reading of my thesis, even on the weekend. A great thanks to co-supervisor Jane Dolven and Ph.D. student Anouk Klootwijk as well, for providing valuable insights and guidance on the subject.

I would also like to thank the crew of 'Brattholmen' from Grieg Seafood for a safe and enjoyable cruise in Øksfjord, and Odd Leknes of Grieg Seafood for providing raw data on the fish farm production.

A special thanks to the always helpful and very competent laboratory technician Mufak Said Naoroz at the Department of Geosciences, UiO, for his guidance and help in the lab.

Finally I would like to thank my father, Jan Erik Sørlie, for support and help through the whole process.

Table of contents

Table of Figures

1. Introduction

Norway has one of the longest coastline in the world, stretching approximately 29 000 km when including the bays and fjords. The fjords of Norway are worldwide popular tourist attractions because of their often spectacular scenery, with high and steep mountainsides, lush vegetation and turquoise glacial-waters. In addition to being a tourist hot spot, the fjords are also home to a large part of Norway's increasing aquaculture production. The fjords serve as ideal naturally sheltered harbours for aquaculture production which provide an in situ environment resembling the natural habitat of Atlantic finfish species, mainly Atlantic salmon (*Salmo salar*) and rainbow trout (*Salmo trutta*). Norway's aquaculture production has experienced a significant increase in production volume since the first farms were established in the seventies, and the production volume has tripled since 1998 to 2017 (Directorate of fisheries, 2018). 1130 licenses for aquaculture of Atlantic salmon and rainbow trout were issued in 2017, producing 1 284 585 tons of slaughtered fish for export and using 1 829 236 tons of fish feed (Directorate of fisheries, 2018). This large production volume also results in a large discharge of nutrients, solid waste and medicine used in production to the marine environment which can alter the seafloor geochemistry and the benthic community structure (Kutti et al., 2008, Kutti et. al, 2007, Perreira et al., 2004).

Of the total amount of fish feed used in fish farming, an estimated 12.5 % is released as faecal matter and 5 % as uneaten food pellets (Kutti, 2008), which for 2017 would amount to 320 116 tons of particulate organic matter (POM) released to the marine environment. Most of the POM settles rapidly in the close vicinity of the fish cages, but in higher current environments there is the possibility of widespread horizontal dispersion (Silvert et al., 1996; Findlay et al., 1995, Ervik, et al., 2007). Simulations of POM dispersal from fish farming predict that >75% are deposited at near-field sites (<500 m from source), while 2.7% are dispersed to far-field sites (<2 km from source) (Johnsen et al, 2016). The increased influx in POM raises concerns regarding the possible environmental consequences on the fjord ecology. In addition to the added organic material deposited directly from the fish cages on the ocean floor, the amount of available nutrients (Nitrogen and Phosphorous) increases and can result in phytoplankton blooms (Gowen et al, 1992). When the algae die, they sink to the ocean floor where microbes degrade the material with a variety of electron acceptors. This

could cause a depletion of the oxygen in the sediment pore water and generate sulphides by sulphate reaction, which is the dominant anaerobic process in coastal waters (Holmer & Kristensen, 1992). Most benthic organisms are sensitive to fluctuations in available nutrients and oxygen concentrations, and even small variations may greatly affect abundance and species diversity (Valdemarsen et al., 2015; Kutti et al., 2007a; Kutti, 2007b; Gustafsson et al., 1999). Earlier studies of benthic communities in fjords with varying influx of organic material show different responses depending on the hydrodynamic conditions and the distance of the study location to the waste source. Valdemarsen et al. (2015) found severely reduced diversity in benthic macrofauna in the vicinity of a low-current fish cage location, and a more stimulated community with moderate environmental impact in a high current cage location. Likewise, in Bjørnafjord (Hordaland, Norway), a moderately enriched infauna community was observed at a location with traced farm waste 1 km away from the fish cage (Kutti et al. 2007a, Kutti 2007b). The rate and volume of the dispersal of organic waste depends largely on current velocities, water depth and the sink-rate and dissipation rate of the detritus (Husa et al., 2016). At locations with low current velocity (<5 cm/s), most of the organic matter is deposited directly below and in close vicinity of the cages, while higher velocities (> 10 cm/s) results in low deposition close to the cages, where the majority of the particles are spread with currents and deposited away from the cage location (Husa et al., 2016). In addition to released POM, there is also the risk of chemical pollution. Antifouling agents used to impregnate the cage nets are often copper-based. Copper is toxic for a range of marine organisms and has antimicrobial effect which prevents algae and other marine organisms attaching to the cage nets (Grass et al., 2011). The Norwegian Environmental Directorate estimates that 85% of the copper used in antifouling agents leaches to the marine environment (Skarbøvik et al., 2014). In 2013, which had a similar total production volume as today, this amounted to approximately 1000 tons (Husa et al., 2016). Environmental monitoring studies (MOM–C, see chapter 2.3) of fish farms in Norway between 2011-2015, found that 20 % of the fish farms had copper concentrations considered toxic (Husa et. al, 2016 and references therein).

In order to monitor the environmental impact from fish farming in Norway, the Norwegian aquaculture law was introduced in 2005 (lovdata.no, 2018). This requires aquaculture companies to perform regular environmental studies to monitor variations in selected pollutants and benthic fauna compositions in surface sediments close to the aquaculture

installation (MOM-C, MOM-B, see chapter 2.3). The monitoring classifies results according to the European Water Framework Directive (WFD, European Commission 2000) and the Marine Strategy Framework Directive (MSFD, European Parliament, 2008). The WFD and MSFD provide tools for determining the ecological quality status (EcoQS) for chemical pollutants and biological indicators, classifying them in five ecological quality groups from *poor* to *background*. Although the MOM-C and MOM-B studies monitor yearly geochemical and faunal assemblage fluctuations, they lack retrospective ability. To recognize a potential environmental impact from fish farming activity, we need to have knowledge of the pristine natural conditions in the fjord pre-anthropogenic aquaculture times. Sediments deposited and preserved in fjords provide a continuous stratigraphic chronology of several environmental parameters which can serve as the basis for interpreting paleoecological and paleoenvironmental conditions. Thus, by collecting and analyzing sediment cores, it is possible to study temporal changes in the depositional environment and compare past with present-day conditions.

The use of benthic foraminifera as bio-indicators to assess the environmental quality is less established than the use of the traditional macrofauna assemblage. However, several recent studies have proven the ability of benthic foraminiferal assemblage analysis as a valuable tool for determining *in situ* reference conditions (Dolven et al. 2013; Alve, 1995; Alve et al., 2009; Hess et al. 2013; Coccioni 2009; Sjetne, 2017; Vågen, 2018; Torper, 2014). Benthic foraminifera are among the most abundant unicellular organisms in the marine soft bottom habitat. When the organism dies, the remaining shell (test) is often preserved within the sediments. Foraminifera inhabit most marine habitats and display distinct species assemblages in often narrow niched living conditions. The distribution patterns are mainly governed by environmental parameters such as depth, salinity, temperature, oxygen, food availability and energy environment. The quick response time in communities, due to even small changes in the environment, can result in notable changes in assemblage composition. This makes foraminiferal assemblage analysis a valuable tool for interpreting environmental quality changes.

In this study, sediment cores were collected in the deep basins in inner Øksfjord where there are 5 active (or recently active) fish farms. The basins were selected to better understand the environmental impact on a larger fjord area. Two cores from different basins were collected for laboratory analysis and radiometrically dated to establish a chronology of the sediment

layers. Physical properties such as particle size distribution and water content were analyzed to interpret the depositional environment, while stable isotopes of ^{13}C and ^{15}N in the sediments and concentrations of total organic carbon (TOC) and nitrogen (TN) were measured to interpret carbon and nitrogen sources. Heavy metal concentrations were measured and classified according to the Norwegian classification system (Norwegian Environmental Agency, 2016). Micropaleontological (benthic foraminiferal) assemblages at different core depths were studied to record changes in the benthic community over time. The overall objective for the study is to evaluate and interpret the environmental impact from fish farming activity on the benthic environment in a northern Norwegian fjord (Øksfjord) by studying microfaunal and geochemical variations over time from past to present (up-core). The following sub-objectives and questions were established to answer the overall objective:

1. Defining the natural reference conditions in the benthic environment.

2. Identifying significant trends and/or increases in pollutants after the fish farm establishment. Do they indicate organic loading from fish farm waste? Are there increased values of heavy metals in the sediments?

3. Considering changes in assemblages of benthic foraminifera in the sediments through time. Do they indicate increased nutrient availability or decreased oxygen concentration as a result of increased organic material in the sediments?

4. Investigating differences in the environmental parameters at the two sites. How does the depositional and hydrological setting influence fish farm impact?

By investigating these objectives, this study aims to contribute to the understanding of the natural environmental conditions of a northern Norwegian fjord, and to evaluate fish farm impact on the benthic environment at far-field sites.

2. Study area

Øksfjord (70°10'N, 22°16'E) is a partially sheltered glacially formed fjord in Loppa municipality in Finnmark County in northern Norway. It is approximately 28 km long with an inner orientation from E-W before turning S-N in the outer part. The fjord connects semi-directly with the Barents Sea in the north, partially sheltered by Stjerneøya north of the mouth (Figure 2.1). Population is scarce around the fjord with the majority (504 people, SSB 2017) living in Øksfjord, which is the administrative center of Loppa municipality. Øksfjord was historically an important regional fishing village with a fish processing and a fish oil factory. The latter closed in 1980, and the only notable industry present today is the aquaculture activity in the fjord.

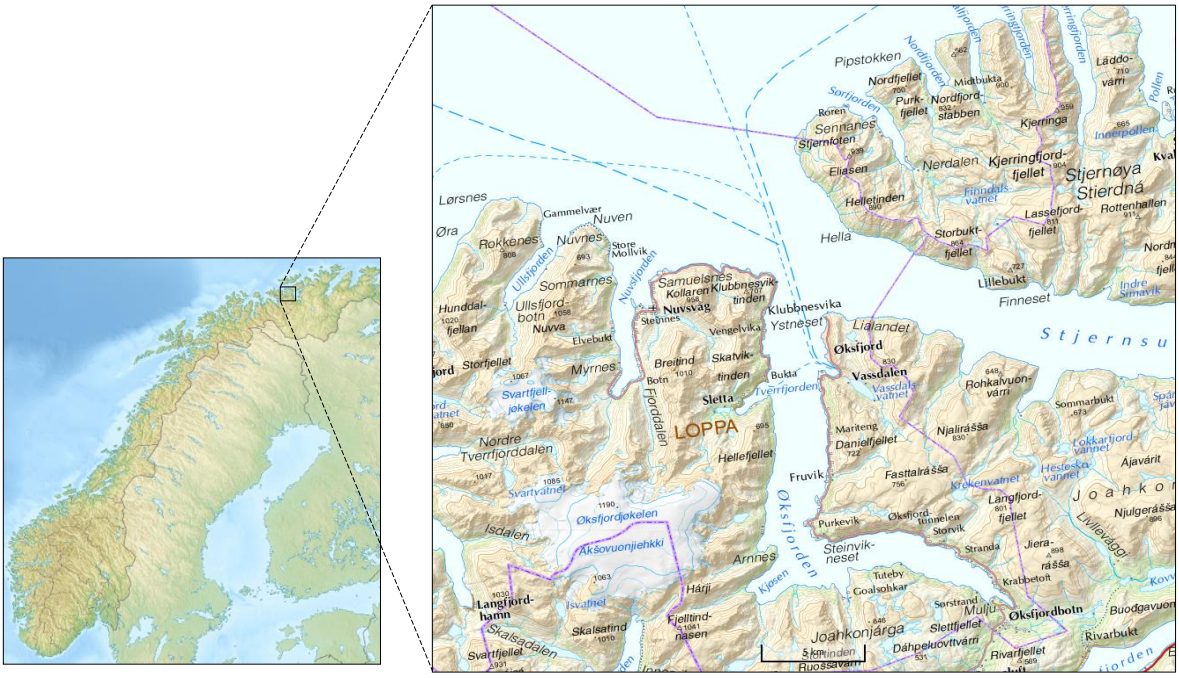

Figure 2.1: Geographical location of Øksfjord, Loppa municipality (Finnmark, Norway) (modified after kartverket.no, 2018)

2.1 Geomorphology and geology

The morphology of the area is dominated by steep mountain sides which connect with 4 main basins in the fjord, three of which are in the inner part of the fjord (D2, D3 and D4, Figure 2.1.2). The bedrock is part of the Sørøy-Seiland-series of the upper part of the Kalak Nappe Complex formed during the Caledonian orogeny (Sturt et al. 1975). This complex consists of

various types of igneous and metamorphic rocks, mainly gabbro, gabbro gneiss and gneisses and some ultramafic peridotite intrusions (NGU 2018, Figure 2.1.1). Gabbro and gneiss are resilient rocks which are not easily erodible (Rea et al. 1996), which will influence the sedimentation accumulation rate in the fjord (Syvetksi et al, 1986).

Figure 2.1.1: Geological map of Øksfjord (modified after NGU, 2018)

The study area in question is the inner and middle part of the fjord, which is separated from the outer fjord by a sill between Bardineset and Langstrand/Arneset at approximately 130 meters depth (Figure 2.1.2). Grain size in the fjord sediments varies from silty clays and sands in the basins, to exposed rock faces with rocks and shelly sands and gravel along in the steeper part of the fjord walls (Emaus & Velvin, 2011-2105). The basin sediments are mainly of silty fraction (Emaus & Velvin, 2011-2015). The fjord serves as catchment for only small streams and rivers scarcely spread around the perimeter (NVE map catalog – river net). The glacier Øksfjordjøkulen (1190 m) towers above the western boundary of the fjord (Figure 2.1), but the freshwater glacial input is low since only a small part of the glacier discharges

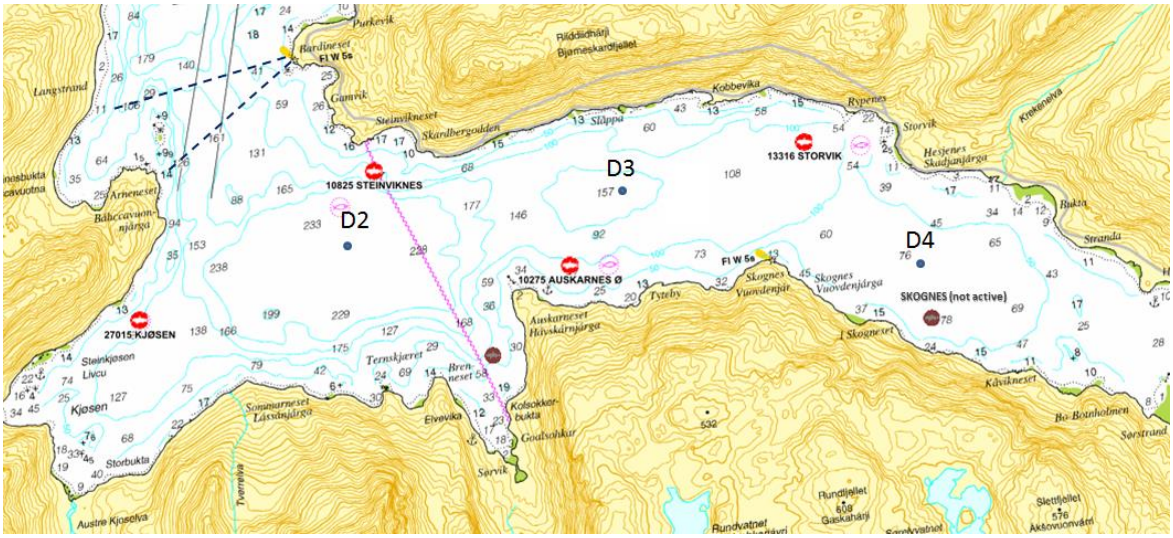

Figure 2.1.2: Nautical and topographical map of inner Øksfjord. Sill is approximately marked with dotted lines. Blue dots = Basins D2, D3 and D4; red fish logo = Fish farms (modified after Kartverket, 2018)

into Øksfjord (NVE map catalog - Glaciers in Norway). The generally steep gradient from the mountain tops to the fjord basins makes the fjord especially prone to landslides and avalanches, and the eastern and northern parts of the inner fjord from Øksfjordbotn to Øksfjord are given a landslide and avalanche risk assessment classification of 3 (potential area for rock and snow avalanches, NVE), due to the especially steep gradient of the topography along this area. Øksfjord also has the largest historic record of landslides and avalanches in Loppa municipality with 10 notable occurrences and 11 deaths since the year 1800 in the village of Øksfjord alone (NGI/Loppa municipality, 2014).

2.3 Hydrography

Fjords receive various amounts of natural sediment input. This includes river- and wind-transported terrestrial sources, open ocean sources, and internal fjord sources, of which fluvial input accounts for most (>90%, Syvetski et al., 1987). Norwegian fjords only locally receive meltwater from glaciers, so the main fluvial discharge occurs during snow melting in early spring and summer and during the high rainfall peak in autumn (Syvetkski et al., 1987). Fjords are narrow and deep estuaries carved by glacial processes with a sill in the mouth (Stiegbrandt, 2012). They contain variably stratified water bodies with three distinguishable water masses which restrict vertical circulation (Stiegbrandt, 2012). The surface water (0-5 m) is variably brackish due to seasonal variations of freshwater input form rivers and precipitation, which varies greatly from fjord to fjord. Below the surface layer, there is an intermediary layer reaching down to sill depths, which mirrors the ocean waters outside the sill (Stiegbrandt, 2012). Below the sill depth, there is dense basin water with restricted renewal, which in some cases can result in extended periods of hypoxic or anoxic conditions in the basin water which may be detrimental to benthic communities (Valdemarsen et al., 2011). The fjord currents are driven by winds, tides, river-runoff and density differences between the water masses, so-called estuarine circulation (Sætre, 2007). The surface water is mainly transported offshore, while the circulation within the intermediary layer is driven by density differences between the coastal water and offshore waters. Tidal currents are often strongest in narrow straits and above shallow sills, while wind currents may be occasionally strong in the open fjord. Local winds force the surface current approximately in the wind direction at a speed of 3 to 8 % percent of the wind speed (Stiegbrandt, 2012), and is mainly predominant in the upper 10-20 meters. The complex circulation patterns of fjords are thus

largely dependent the geomorphology such as sill depth, basin depth, and freshwater input and how the fjord is connected to the open ocean. The resulting dispersal patterns of nutrients, dissolved oxygen and sediments are therefore difficult to predict, and can be quite different from one particular fjord to another.

The general water type in Øksfjord is classified by the Norwegian Environmental Agency as a type 3 (protected coastal waters, salinity ≥ 30) in the Barents Sea region (Veileder 02:218) with a tidal range of approximately 3 meters (vann-nett.no, 2018). The surface current flows north-south in over the west part of the sill, turns east along the coast and generally flows in an anti-clockwise circular pattern through the inner fjord before it flows out over the east side

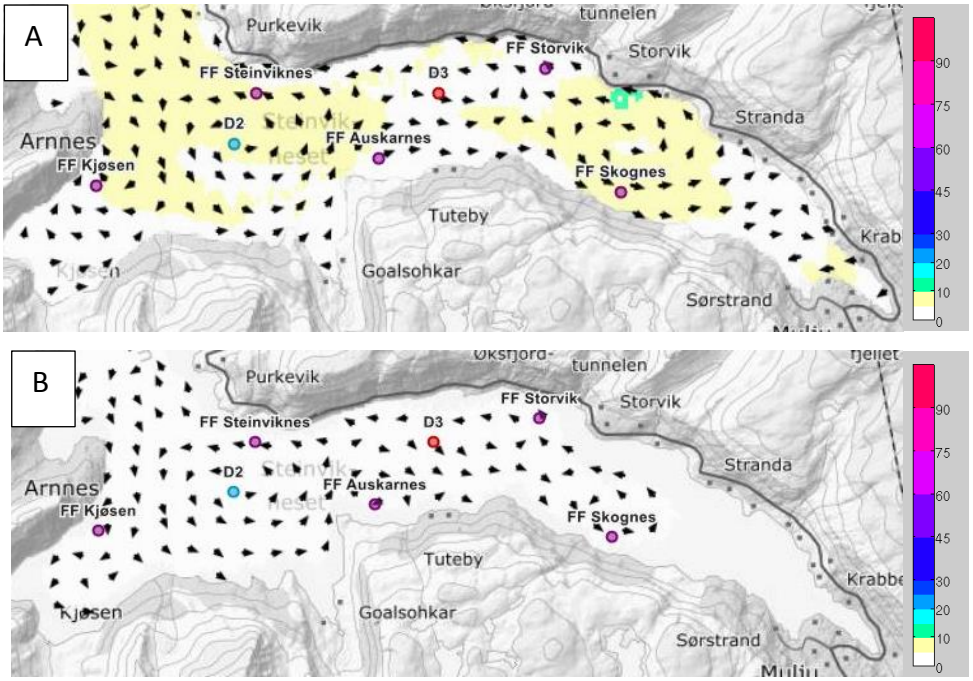

Figure 2.3.1: A: Hydrodynamic model of Øksfjord at 5 m water depth. B: Hydrodynamic model of Øksfjord at 50 m water depth. Color represents mean yearly current velocity and vectors represent yearly mean current direction. Fish farms are marked as purple, basins as blue (D2) and red (D3) (Modified after kart.akvaplan.niva.no/os, 2018)

of the sill (Figure 2.3.1 A and B). The mean yearly current velocity lies in the range of 5-15 cm/s at 5 meters depth, and between 0-5 cm/s at 50 m depth. The surface current velocity is higher in in basin D4 and in the D2 basin towards the sill (Figure 2.3.1-A). In the basin D2, the circulation pattern resembles an eddy, as the inflowing water seems to be dragged in a circular pattern by the outflowing water (Figure 2.3.1 A and B). CTD measurements recorded in September 2017 in the two basins D2 and D3 for this study, showed similar salinity values in the surface and bottom waters at both sites (33 and 35, respectively, Figure 2.3.2). The

CTD salinity values recorded in September are most likely in the lower seasonal range as the fjord has received larger amounts of freshwater in the form of meltwater during the summer months. At both sites, D2 and D3, oxygen concentrations classified as *very good* (>4.5 ml/l, Veileder 02:2013 – revised 2015) throughout the water column, with minimum values of 5.2 ml/l at D2 and 5.8 ml/l at D3 in the deepest part of the water columns (Figure 2.3.2). Surface temperature at both stations was 9.4 °C and reached a stable temperature of 5.6 °C at approximately 150 meters water depth (Figure 2.3.2).

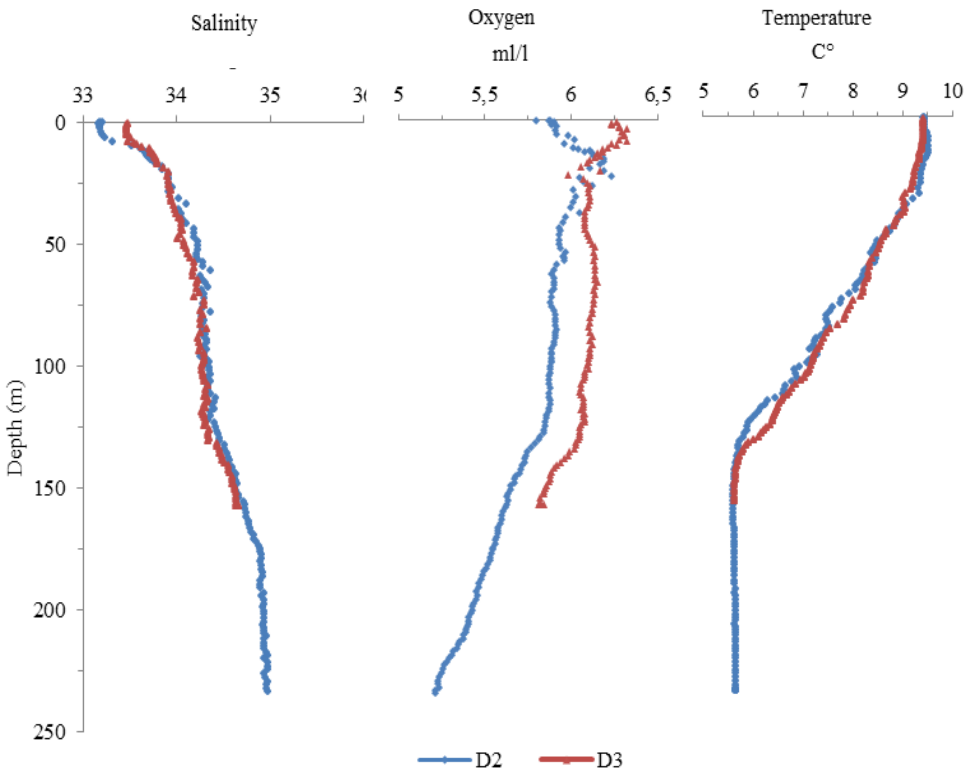

Figure 1.3.2: Oxygen concentrations (ml-O2/l), salinity and temperature (C°) from CDT measurements at stations D2 (154 m depth) and D3 (233 m depth) in September 2017.

2.4 Fish farming history

Fish farming history Fish farming in Øksfjord was established in 1994, and has since 2005 been operated by Grieg Seafood AS, which increased the production volume greatly compared with the production volume pre 2005 (T. Haugen, pers. comm., 2018). In the inner part of the fjord, there are five fish farms which are active today or were active in the recent past; Skognes, Storvik, Auskarnes, Steinviknes and Kjøsen (Figure 2.1.2). The fish farms all consist of 10 fish cages which are moored to the main ainchoring point. The farms produced a total of 62.7 million kg of salmon and used 75.5 million kg of fish feed from 2005 to 2017 (Grieg Seafood, 2018, Appendix x). Production volume has been relatively stable since 2007, ranging from approx. 6000-8000 tons, with the exception of a low production volume in 2016 (Figure 2.2). This decrease in production was due to was fallowing of the all the stock at all farm locations in 2015. This was part of new production strategy as measure to reduce lice infections (Odd Leknes, pers. comm., 2018). This also explains the relatively few production days in 2015 and 2016 (Figure 2.3). Fish farm Skognes has not been in use since 2013 as the permit was revoked due to deteriorating environmental conditions below the farm (Velvin & Emaus, 2013).

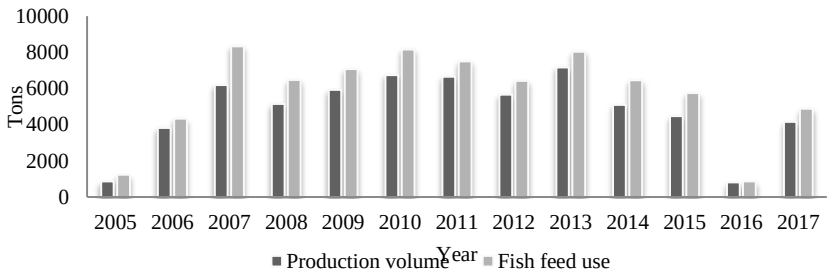

Figure 2.4.1: Total production volume vs. fish feed usage 2005-2017 (Odd Leknes, Grieg Seafood AS, 2018)

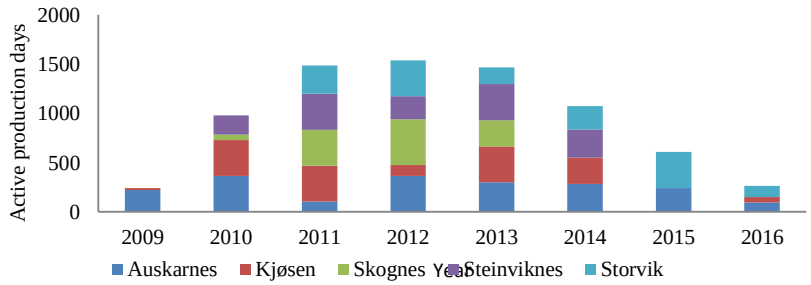

Figure 2.4.2: Active production days for each fish farm per year 2009-2016 (Odd Leknes, Grieg Seafood AS, 2018)

2.5 Previous environmental monitoring

Yearly monitoring since 2006/2007 (MOM-B and MOM-C) have been performed by Akvaplan-NIVA in accordance to Norwegian Standard 9410. MOM-B is a yearly independent study of each fish farm location, while MOM-C studies all stations and include the deep basins. Both studies include sediment sample collection and laboratory analysis for total organic carbon (TOC), total phosphor (TOT-P), grain size distribution, heavy metal concentrations (Zn, Cu) and a quantitative macrobenthos analysis. All results are classified in accordance to the Norwegian Pollution Control Authority's classification system (Chapter 3, table).

The MOM-C-studies from 2007 measured low TOC values in all deep basins and at three selected fish farms. There was also no indication of loading effects on the soft bottom macrobenthos (Dahl- Hansen and Velvin, 2007). The MOM-C-studies from 2008 and 2009 showed that the bottom water oxygen concentration inside the sill at Bardineset was not stagnant. In the MOM-C-study from 2010, there was no change in diversity of benthos in the deep basins, or changes in oxygen concentration in the water column inside the sill. At Results from the MOM-C-studies from 2011-2015 are summarized in Table 2.51.1. The results for deep basins stations D2 and D3 are generally classified as *background* or *good*, except the soft bottom benthos indices which are *good* to *moderate.* All the results and their corresponding ecological quality status from the MOM-C-studies in basins D2 and D3 by Akvaplan-NIVA are summarized in Table 2.5.1.

Table 2.5.1: Selected heavy metals concentrations and diversity indices and their corresponding classification status from yearly MOM-B and MOM-C-studies from basins D2 and D3 in inner Øksfjord 2011-2015 (Akvaplan-NIVA, 2012-2016). The classification assigned to the results in this table is based the most current guidelines as seen in Table 3, and may differ from the original classification at the time of study.

Station/EcoQS	H'	ES100	Zn (mg/kg)	Cu (mg/kg)	TOC (mg/g)
D2 2011	3.6	19	28.9	26.7	22.4
D2 2012	3.3	17.4	58	41.1	22.3
D2 2013	3.2	18.9	54.9	45.8	21
D2 2014	3.28	18.7	71.9	43.8	21.9
D2 2015	3.06	15.8	71.4	39.2	26.3
D3 2011	3.4	25	19.4	8.9	23
D3 2012	2.6	16.2	39.2	22.7	12.2
D3 2013	2.7	21.5	31.5	19.3	15.1
D3 2014	3.03	22.7	38.2	18.7	12.8
D3 2015	2.96	25.1	35.1	17.3	11.9

In addition to the environmental monitoring related to the fish farms, the Norwegian Environmental agency classifies the ecological quality of coastal water regions in accordance to the European Water Framework Directive (WFD) based on several biological, physio-chemical and hydromorphological quality elements. The quality status in Øksfjord is based on the MOM-C and MOM-B studies related to the fish farming, but can also include other relevant studies in the fjord. In this classification system, Øksfjord is separated into three water body (in Norwegian *type*), one for each basin: *Øksfjordbotn* (D4), *Øksfjord indre* (D3) and *Øksfjord midtre* (D4)(vann-nett, 2018). Each is classified separately, and the current ecological quality status (vannportalen, 2018) for the water bodies relevant for this study can be seen in Table 2.5.2.

Table 2.5.2: Ecological quality status (EcoQS) as of 2018 of the water bodies Øksfjord midtre and Øksfjord indre in inner Øksfjord.

Basin	Øksfjord midtre (D2)	Øksfjord indre (D3)
EcoQS	Good	Background

3. Methods and materials

3.1 Sample collection and preparations

Sediment cores from the inner part of Øksfjord were collected during a cruise with Grieg Seafood's boat 'Brattholmen' on 07.-08. September 2017. Sediments were collected with a twin gravity corer for soft sediments called a Gemini corer (8 cm inner diameter, Figure 3.1.1). Several deployments were made at each station, until at least 4 replicate cores were retrieved. Sediment cores were collected successfully at the two basins D2 and D3 inside the sill. D2 is located at the deepest part inside the sill at 250 meter water depth, D3 further east at approximately 162 meter water depth. After visual inspection on deck, the most homogenous and undisturbed cores from each site were chosen for further investigations. Two

Figure 3.1.1: Gemini corer on deck in Øksfjord.

replicate cores from each station were sub-sampled. Water depths, Coordinates and core-names for the collected cores can be seen in Table 3.1.1 Several attempts to collect cores closer to the fish cages (Steinviknes and Storvik, Figure 2.1.2) were unsuccessful since gravel and large rocks inhibited the corer to close during collection.

Table 3.1.1: Station details

Station	**D2**	**D2**	**D3**	**D3**
Core name	D2-6A	D2-6B	D3-3A	D3-3B
Coordinates	N70°08.6456 E22°17.7542	N70°08.6456 E22°17.7542	N70°08.7908 E22°22.5421	N70°08.7908 E22°22.5421
Depth (m)	240	240	157	157
Used for	Analysis	Logging	Logging	Analysis

The cores selected for further analysis were extruded by a piston and sliced horizontally into samples at an interval of 1 cm from 0-20 cm, and at 2 cm intervals from 20 cm to the bottom of the core. The samples were stored in a freezer (-20 C) at the end of each day. A sample of the food pellets in use at the fish farm was also collected and placed in a freezer for further analyses. Cores from site D2 and D3 were selected for further laboratory analysis because of their central placement between the fish farms.

In the laboratory, all samples were freeze-dried using a Christ Alpha 1-4LD pluss and a Christ Alpha 1-4 freeze dryer unit to ensure minimal disturbance. Total weights of each sample were taken before and after drying to determine the water content.

3.2 Sediment dating

Approximately 7 grams of carefully homogenized dry sediment were placed in plastic cups and shipped to P.G. Appleby and G.T. Piliposian at the Environmental Radioactivity Research Centre at the University of Liverpool for radiometric dating. Pb-210 has a half-life of 22.3 years and is therefore suitable for dating young sediments. When applying the Pb-210 method, it is assumed that the sediments are receiving a constant input of Pb-210 from the atmosphere. Pb-210 that was incorporated into the sediments 22.3 years ago will be only one

half as radioactive as when initially deposited. This logic can be extended to calculate the age of sediments at other depths in the sediment column and/or the rate of sediment accumulation. Cs-137 is a fission product which is released into the environment during nuclear testing or nuclear accidents, and provides date "markers" based on known nuclear activity. The first appearance of Cs-137 in sediments marks the date the concentrations were deposited in detectable limits for the first time, 1954. Likewise it is possible to date the sediments deposited during the maximum fallout from nuclear testing in 1963. The chronology model is based on combining the Pb-210- and Cs-137-method.
For detailed description of the technical procedures and the different models, see Appendix A.

3.3 Grain size distribution

A Beckman Coulter LS13 320 was used to determine the grain size distribution, based on laser diffraction measuring distribution in the area of 0.4 μ m - 2000 μ m. The basis for the analysis is that light from the laser scatters at different angles depending on the size of the particle. In brief, a small particle has a high angle of broken light, while large particles have a low angle.
Approximately 0.8 – 1.2 g of representative sediment, excluding large shell and organic matter particles, was extracted from each sample. The sediments were then deflocculated adding Calgon $(NaPO_3)_6$ and treated with ultrasound for 2 minutes in a sonic bath to break up faecal pellets and flocculated sediments, after which the solution was poured directly into the sample vessel of the machine until the concentration showed 8-12% obscuration. The procedure was run twice for each sample, using the mean value for the results.

3.4. Total organic content (TOC), total nitrogen (TN) and stable isotopes ($\delta^{15}N$ and $\delta^{13}C$)

Approximately 1 g of pulverized sediment and fish food was sent to Iso-Analytical Laboratories in Crewe, UK, for analysis. For analysis of the sediment samples an Elemental Analyzer - Isotope Ratio Mass Spectrometry (EA-IRMS) was used. Tin capsules containing sample and reference material are loaded into an auto-sampler on a Europa Scientific elemental analyzer and dropped in sequence into a furnace where they were combusted in an oxygen rich environment. The gases produced on combustion are filtered through several

reduction stages before the resultant CO_2 and N_2 chromatographic peaks enters the ion source of the Europa Scientific 20-20 IRMS. Gas species of different mass are separated in a magnetic field then simultaneously measured using a Faraday cup collector array to measure the isotopomers of CO_2 at m/z 44, 45, and 46 and isotopomers of N_2 at m/z 28, 29, and 30. (See Appendix B for detailed description). TOC values were normalized to fine particulate material (<63 µg, nTOC) according to Rygg (1995).

3.5 Heavy metals analysis

The heavy metals analysis was performed according to the Norwegian Standard(NS4770/1994). The technique used to measure the concentration of trace elements was by Inductively Coupled Plasma Mass-Spectrometry (ICP-MS). Approximately 1 gram of sediments was pulverized in an agate mortar and weighed with 4 decimals. The sediment powder was transferred to labeled 50 ml polypropylene centrifuge tubes where 20 ml of distilled nitric acid (7 M HNO_3) was added. Then the tubes were heated in an autoclave for minimum 30 minutes to extract the bioavailable fraction of the metals. The cold samples were centrifuged for 10 minutes at 4000 rpm to separate the dissolved extraction from the sediment. 0.25 ml of the dissolved fraction was extracted from the clear solution and diluted 40 times with 1% distilled HNO_3 and analyzed. The samples were analyzed for copper (Cu), lead (Pb), Zinc (Zn), cadmium (Cd) and mercury (Hg) concentration. Hg was analyzed semi-quantitatively since the machine was not able to calibrate for Hg. Veileder M-608:2016 was used to identify the EcoQs of the concentrations (Table 3.7.1).

3.6 Micropaleontological analysis

Approximately 2 grams of dry sediment from each sample were used for foraminiferal analyses. The sediments were washed with a 63 µm brass sieve. The residues >63µm were subsequently dried at 45 °C in a controlled environment. Approximately 250 individuals were picked and sorted by species with a binocular microscope and subsequently counted and catalogued (final total count for each sample was between 200-250 specimens). Foraminiferal abundance was normalized to individuals per gram dry sediment. Benthic foraminiferal accumulation rates (BFAR, ind/g/yr) were calculated applying the sedimentation rates provided by the radiometric dating analysis (Herguera and Berger, 1991). Percentages of

species in each sample were also calculated. All counts are presented in Appendix D-G. Due to the difficulty in separating *Stainforthia fusiformis* and *Stainforthia feylingi*, these two species were grouped in the analysis as *Stainforthia* group.

PRIMER (Plymouth Routines In Multivariate Ecological Research) version 6.1.13. (Clarke and Gorley, 2006) software was used to calculate diversity indices Shannon-Wiener H' (Shannon and Weaver, 1949) and Hurlberts ES(100) (Hurlbert, 1971). PRIMER was also used to determine similarities in relative abundance within each core and between the two cores, based on Bray-Curtis similarity coefficient (Bray-Curtis, 1957), Results are expressed as cluster analyses and non-metric multidimensional scaling (MDS) ordinations (Clark et al., 2001).

Samples for analysis were selected throughout the cores to both determine the reference conditions and to identify possible environmental changes due to fish farm activity.

Determination of the Ecological Quality Status (EcoQS) of the samples is based on the Norwegian classification system (Veileder 02:2013-revised 2015, Table 3.7.1).

3.7 Ecological Quality Status (EcoQS)

All results were classified according to the most recent Norwegian classification system. Relevant parameters can be seen in Table x.

Table 3.7.1: Norwegian classification system for selected parameters. Diversity indices based on H' and ES(100) (Veileder 02:2013, revised 2015), heavy metal concentrations (Veileder M-608:2016)(Note there is no *good* classification assigned for Cu) and oxygen concentrations in deep water (Veileder 02:2013 - revised 2015)

EcoQS	Background	Good	Moderate	Poor	Bad
H'	>3.8	3.0-3.8	1.9-3.0	0.9-1.9	<0.9
ES(100)	>25	17-25	10-17	5-10	<5
Cd mg/kg	<0.2	0.2-2.5	2.5-16	16-157	>157
Cu mg/kg	<20	-	20-84	84-147	>147
Hg mg/kg	<0.05	0..05-0.52	0.52-.075	0.75-1.45	>1.45
Pb mg/kg	<25	25-150	150-1480	14480-2000	>2000
Zn mg/kg	<90	90-139	139-750	750-6690	>6690
TOC (%)	<2.0	2.0-2.7	2.7 - 3.4	3.4-4.1	>4.1
Oxygen in deepwater (for salinity 34 mg/l, T = 6 C)	>4.5	4.5-3.5	3.5-2.5	2.5-1.5	<1.5

4. Results

4.1 Physical properties

Core D2-6A

The core consisted of mainly brownish green, silty sediment (Figure 4.1.1.B) from 0-5 cm with some Polychaeta tubes present in these layers. The surface sediments were undisturbed and consisted of fine, fluffy material. From around 7 cm the color turned more greyish, and in 10-12 cm there was a notable coarser shell-sand layer. From 12 cm and down core, the sediments were gradually darker grey and fine silty. Some black smears and sulfuric odor was noticed during the slicing of the pseudo replicate core on deck.

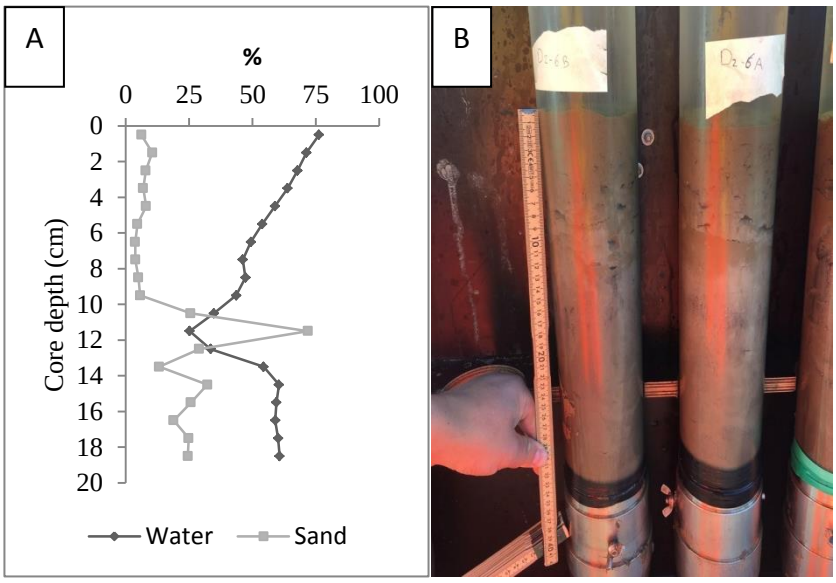

Figure 4.1.1: A: Sand and water content in D2-6A. B: Inspection of cores D2-6A and D2-6B on deck.

The water content decreased from 76 % in the surface layer to a minimum of 25 % at 12 cm (Figure 4.4.1.A). From 12 to 15 cm the percentage increases from 25 to 61 %. Beneath this core depth the water content decreases marginally down core to 61% % at the bottom of the core. The sand content was relatively stable from 0-10 cm core depth with an average value of 6.2 %. Below the sand content increases, with a maximum of 72 % in 11-12 cm core depth, to relative stable values of approx. 20-25 % in the bottom 3 cm of the core. The differential grain size distribution shows three distinct different trends within the core, with a mainly silty

fraction from 0-10 cm, a notable increase in sand in 10-13 cm, and silty material in 13-19 cm with a slightly coarser fraction than in 0-10 cm (Figure 4.1.2).

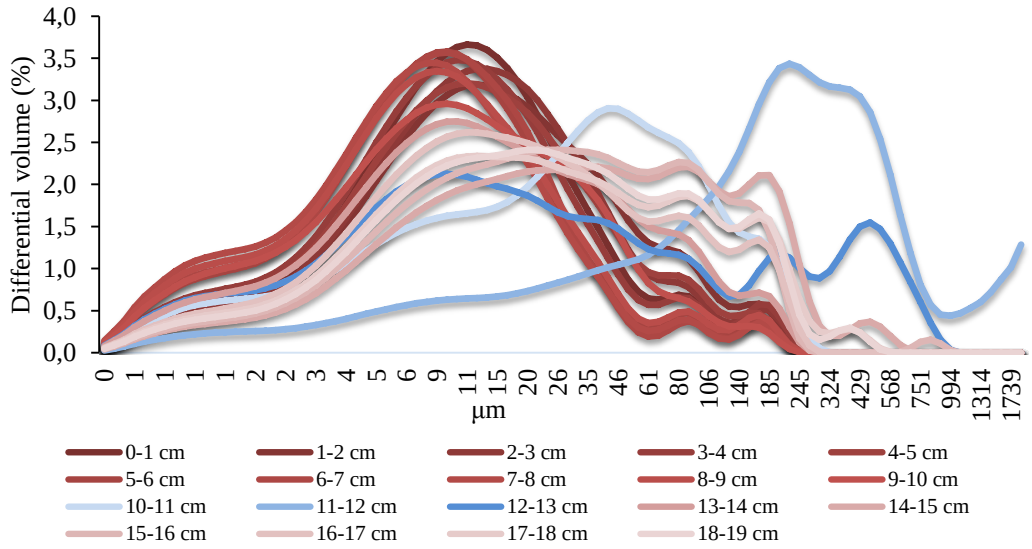

Figure 4.1.2: Differential grain size distribution of core D2-6A.0-10 cm = dark reds; 10-13 cm = blues; 13-19 cm = light reds.

Core D3-3B

The sediments observed in the core liner of D3-3B (14 cm length) consisted of homogenous greenish-brown, silty material, fluffy on top with some Polychaeta tubes (Figure 4.1.3.B). From the observation of the sliced pseudo replicate core D3-3A, the sediments consisted of mostly greenish-brown, silty material, with a gradual darkening of colour down core. Some shell fragments, pieces of wood and an angular rock (1-2 cm length) were observed in the layers 6-14 cm.

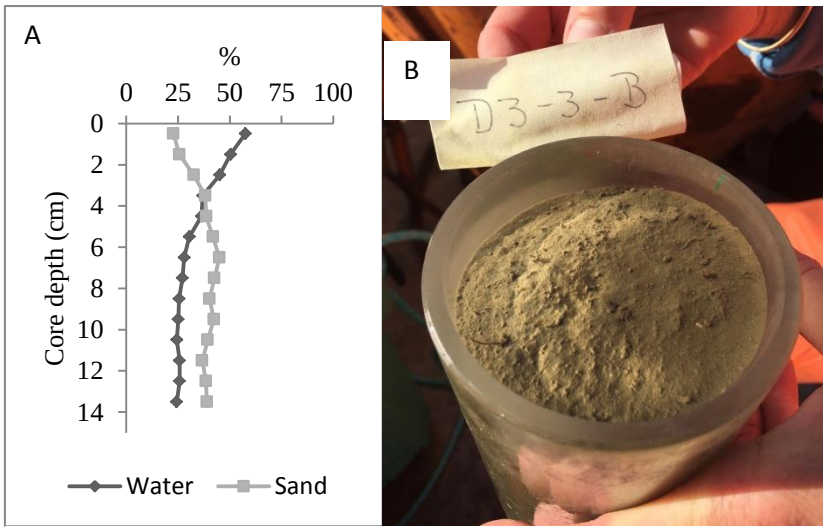

Figure 4.1.3: A: Sand and water content in D3-3B. B: Inspection of water/surface sediments of deck.

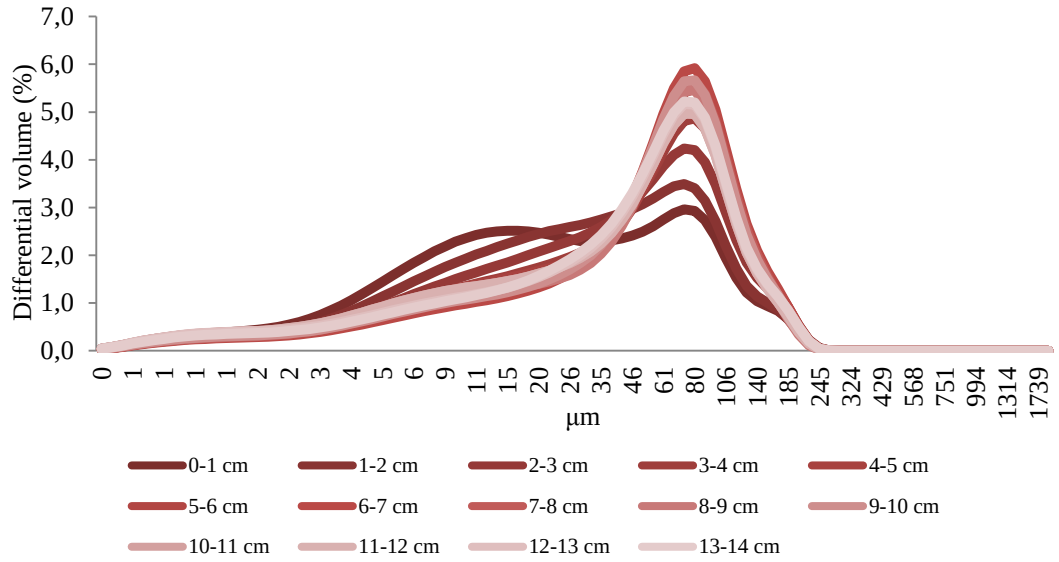

Figure 4.1.4: Differential grain size distribution of core D3-3B.

The water content displayed a maximum of 58 % at the surface layer and a steady decrease down core to 26 % at 9 cm (Figure 4.1.3.A). From 9 to 14 cm core depth the water content was stable with a mean value of 25 %. The sand content showed a minimum of 23 % at the surface layer and a gradual increase down core to 45 % at 7 cm. From 7 to 14 cm core depth the sand content ranged between 37 and 43 %. The differential grain size distribution in the core showed mainly sandy and silty fractions with a slightly higher volume of finer material in 0-3 cm (Figure 4.1.4).

4.2 Radiometric dating

Core D2-6A

There were largely similar trends in both Pb-210 and Cs-137 activity (Figure 4.2.1.A). The Pb-210/Ra-22 equilibrium in this core is reached at a depth of around 25 cm. There were two defined peaks in unsupported Pb-210, one at 14-15 cm and one at 2-4 cm which is thought to be the result of the artificial fallout from nuclear testing in the early 1960's (maximum fallout in 1963). Between these two peaks the activity reached minimum values at 6-13 cm. Below 14 cm core depth, the activity declined more or less exponentially. The Cs-137 activity largely exhibited similar trends (Figure 4.2.1.A). The maximum value of the Cs-137/Pb-210

activity ratio, which often is a good indicator of the 1963 date, was placed between between 7-10 cm (Appendix A).

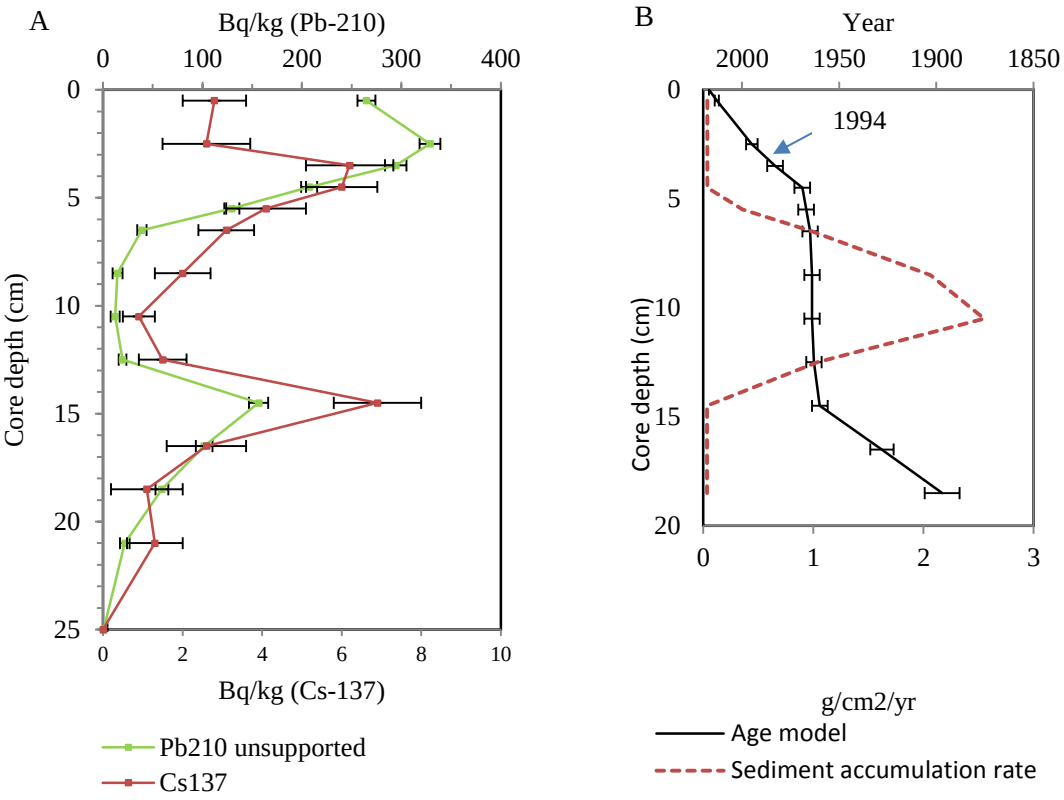

Figure 4.2.1: A: Unsupported Pb210 and Cs137 activity vs. core depth in core D2-6A. B: Age model and sediment accumulation rate of core D2-6A. Blue arrow marks the year of fish farm upstart.

The chronology model gave a stable sediment accumulation rate (SAR) of 0.034 g/cm^2/yr from 1868-1960 (21-14 cm) and 0.037 g/cm^2/yr from 1967 (4-5 cm) to present day (Figure 15B). Calculated SARs in layers 5-14 cm displayed a notable increase, reaching a maximum value of at 2.553 g/cm^2/yr at 10-11 cm which was dated to 1964. All layers 5-14 cm were dated to the 1960's in the model. The deepest layers of the core (18-19 cm) was dated to 1897, and sediments found in 3-4 cm were dated to the year the aquaculture first started in Øksfjord, 1994 (Figure 4.2.1.B).

Core D3-3B

In this core, the Pb-210/Ra-22 equilibrium was reached at 6 cm core depth. The Pb-210 concentrations decrease exponentially (Figure 4.2.2.A), which gave a relatively uniform SAR, calculated to 0.058 g/cm^2/yr (Figure 4.2.2.B, Appendix A). Cs-137 concentrations were very

low, and there was no clearly defined peak for the 1963 artificial fallout, although there was a slight increase at 4-5 cm. The Pb-210 model placed 1963 somewhere between 3.5-4 cm. The age model dated the sediments in 5-6 cm to 1926, and the year 1994 of aquaculture start between 2-3 cm (Figure 16B).

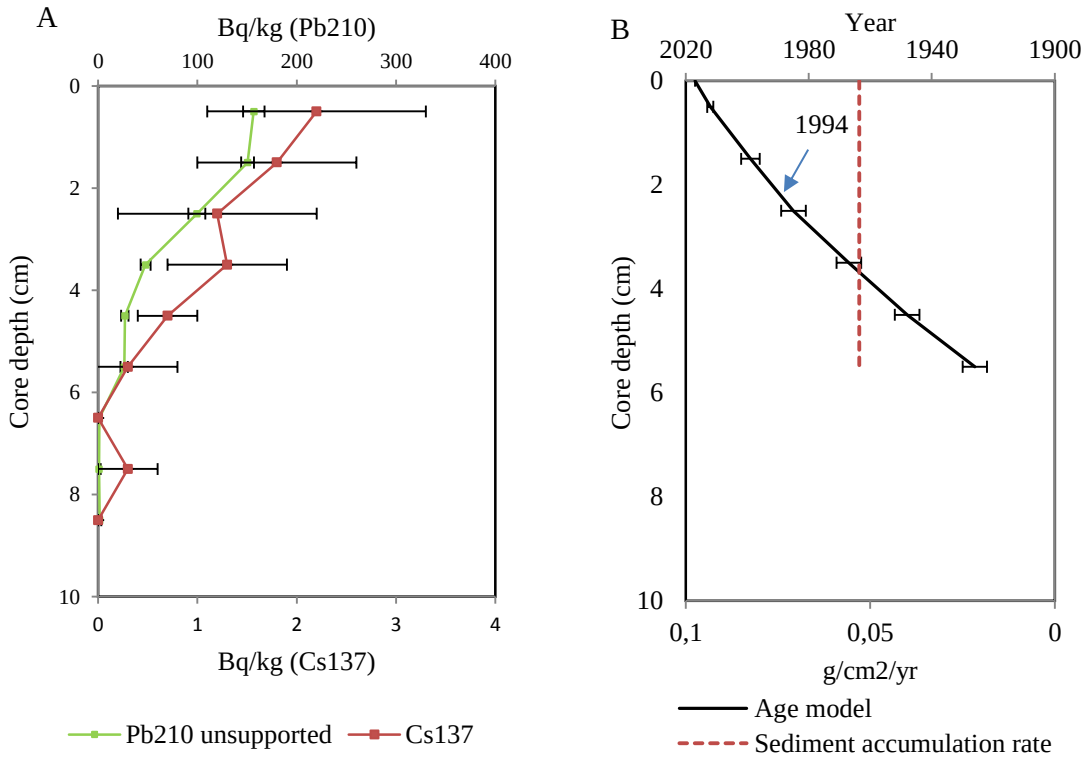

Figure 4.2.2: A: Unsupported Pb210 and Cs137 activity vs. core depth in core D3-3B. B: Age model and sediment accumulation rate of core D3-3B. Blue arrow marks the year of fish farm upstart.

The full report of the sediment dating results of core D2-6A and D3-3B provided by P.G. Appleby and G.T. Piliposian can be seen in Appendix A.

4.3 Total organic carbon, total nitrogen and stable sediment isotopes ($\delta^{13}C$ and $\delta^{15}N$)

Core D2-6A

Normalized total organic carbon (nTOC) and nitrogen (TN) showed largely the same trends throughout the core (Figure 4.3.1). Below 5-14 cm they both displayed relatively stable values with an average of 3.6 % (EcoQS *poor*) and 0.5 %, respectively. In 5-13 cm there was a

significant decrease in concentrations reaching a minimum in 9-10 cm (nTOC, 0.9 %) and 11-12 cm (TN, 0.3 %) and a subsequent increase in layers 0-5 cm, with average concentrations of 2.6 % nTOC (EcoQS *moderate*) and 0.4 % TN (Figure 4.3.1). The stable isotopes $\delta^{13}C$ displayed relatively stable concentrations throughout the core with a mean concentration of 22.2 ‰ except for a decrease in layer 10-11 cm to -23.2 ‰. $\delta^{15}N$ also showed relatively stable values throughout the core with a mean value of 5.2 ‰. There were however some fluctuations in concentrations in 7-13 cm with a high value of 5.7 ‰ found in layer 9-10 cm (Figure 4.3.1).

The carbon/nitrogen ratio (C/N) were relatively stable throughout the core with an average value of 6.8 (Figure 4.3.1). There was a slight increase in C/N in layers 10-13 cm which had a mean value of 7.8.

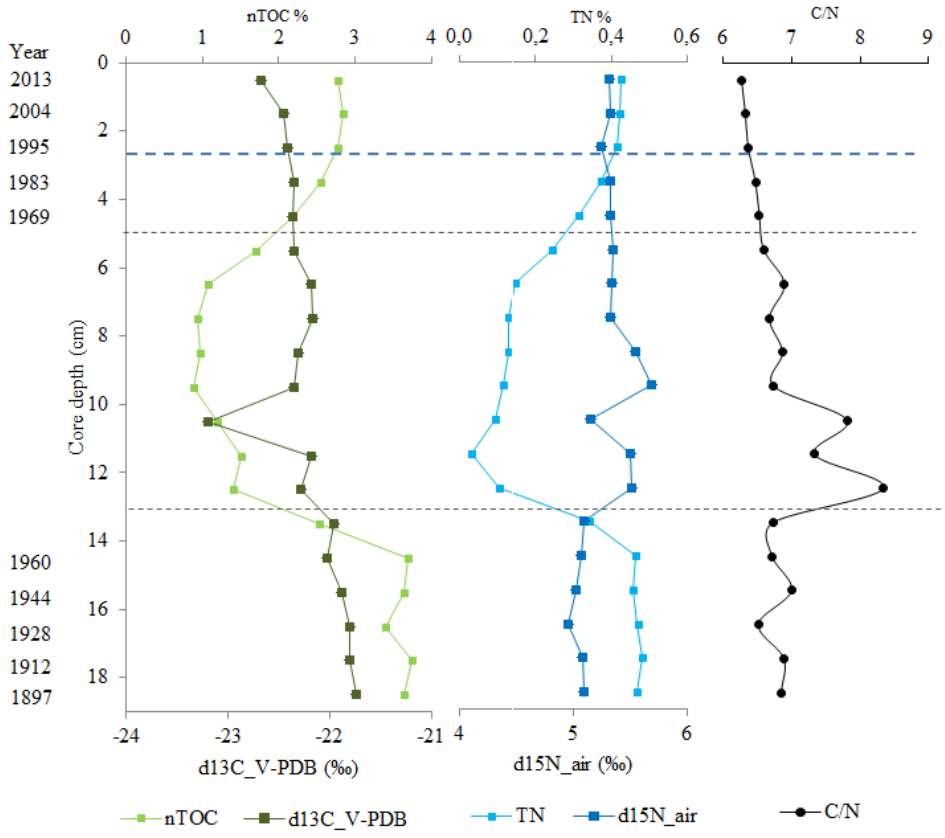

Figure 4.3.1: nTOC content and stable carbon isotope ratio, TN content and stable nitrogen isotope ratio, Carbon/nitrogen ratio of core D2-6A. Blue-dotted line marks the start of fish farming in 1994, grey lines mark the redeposited layer interval.

Core D3-3B

Normalized total organic carbon (nTOC) concentrations showed a slight increase up core with minimum values of 1.1 % at 12-13 cm and the highest values of 1.7 % in 0-3 cm. All concentrations were within the *background* classification (Table 3.7.1). Total nitrogen (TN) concentrations displayed stable values below 6 cm with an average value of 0.09 %. From 6 cm TN increasesd and reached the highest concentration in the top cm with 0.24 %. (Figure 4.3.2). The $\delta^{13}C$ signal was relatively stable from bottom of the core to 4-5 cm with average value of -22 ‰ and a decreasing trend from 4-0 cm. $\delta^{15}N$ values were stable through the core with a mean value of 5.2 ‰ with a slight increase from 3-0 cm. The C/N ratio was relatively stable through the core with a mean ratio of 5.9. The highest value of 7.1 was found in 13-14 cm, and the lowest of 4.8 in the layer directly above (12-13 cm).

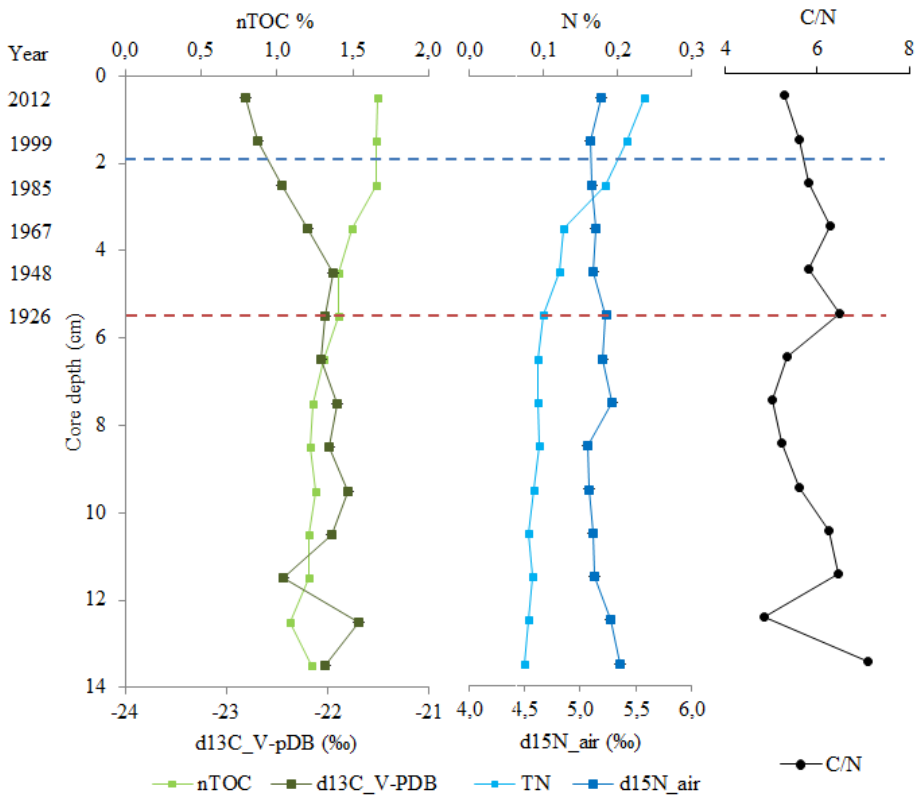

Figure 4.3.2: nTOC content (%) and stable carbon isotope ratio, TN content (%) and stable nitrogen isotope ratio, carbon/nitrogen ratio of core D3-3BA. Blue-dotted line marks the upstart of fish farming in 1994. Red-dotted line marks the dating horizon.

4.4 Heavy metals concentration

Core D2-6A

The main trends for Cu, Pb, Zn and Hg showed relatively stable concentrations in 19 -14 cm and 5 – 0 cm core depth (Figure 19). In the layers with increased sedimentation rate (5-13 cm) there was a decrease in metal concentrations which reach minimum values at 11.5 cm (sandy layer). Pb, Zn and Cd were classified as *good* or *background* throughout the core, while Cu was classified as *moderate* except for in 11-12 cm which classified as *background*. Concentrations above and below this layer interval were largely stable, and with no increasing or decreasing trends.

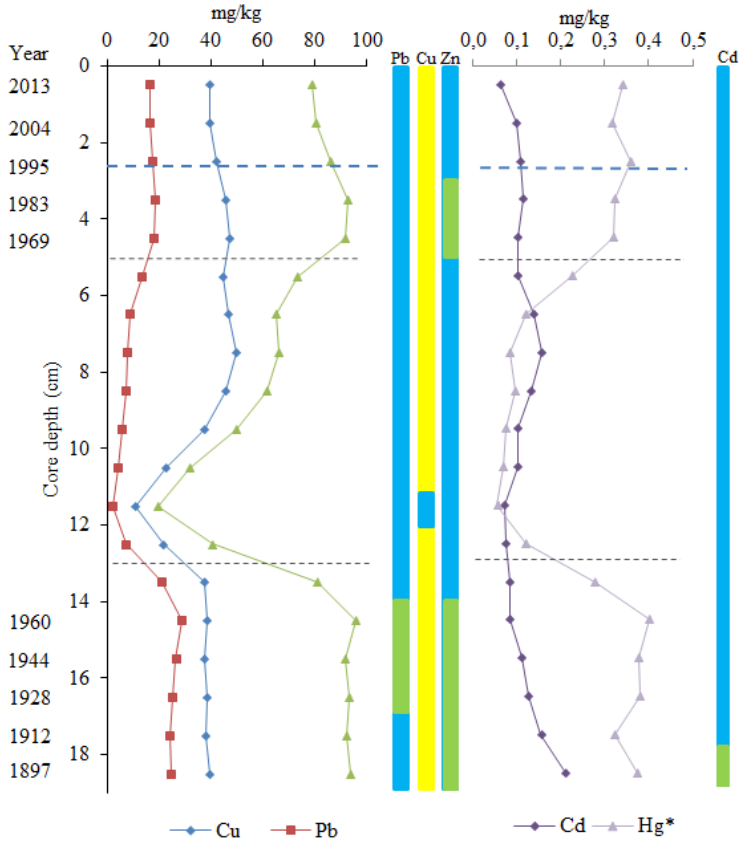

Figure 4.4.1: Heavy metal concentrations and their corresponding environmental class, core D2-6A. Blue-dotted line marks the start of fish farming in 1994. Grey lines border the layers with SAR. Hg* is only measured semi-quantitatively, so only relative trends should be considered.

Core D3-3B

All metal concentrations for D3-3B displayed trends of stable concentrations from the bottom of the core up to 6 cm core depth, a slight increase from 6 to 1 cm, and a slight decrease in

concentrations from 1 cm to the surface layer (Pb from 3 cm) (Figure 4.3.2). Cu, Pb, Zn and Cd concentrations were classified as *background* throughout the core, except the maximum value for Cu at 2-3 cm which was marginally over in the *moderate* classification (Figure 20). There were no significant increases in heavy metal concentrations in the recent sediments.

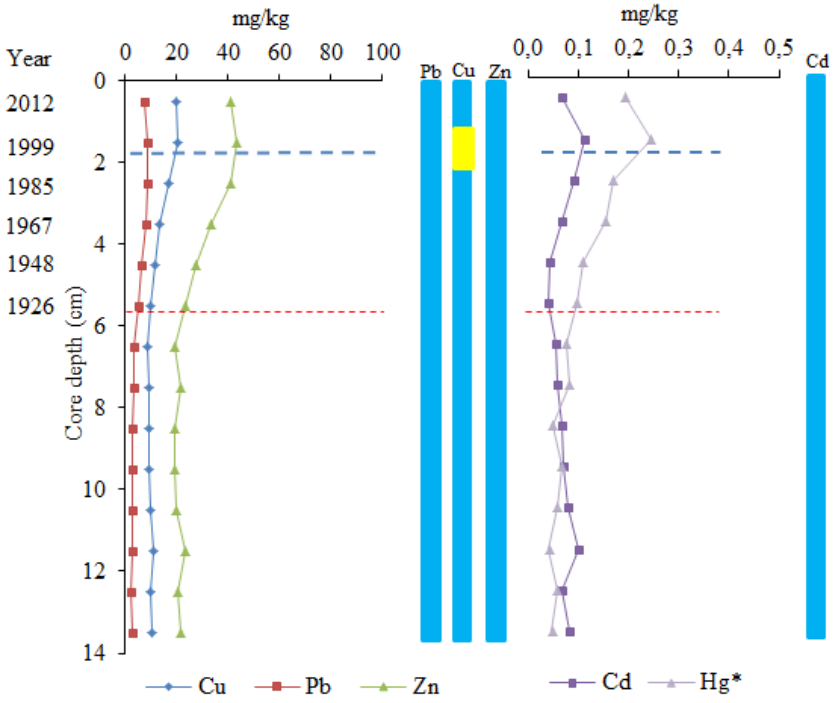

Figure 4.4.2: Heavy metal concentrations and their corresponding environmental classification, D3-3B. Hg* is only measured semi-quantitatively, so only relative trends should be considered. Blue-dotted line marks the start of fish farming in 1994. Red-dotted marks the dating horizon.

4.5 Micropaleontological analysis

Core D2-6A

All results can be seen in Figure 21. Foraminiferal abundance was generally high throughout the core with an average concentration of 2197 individuals per gram dry sediment. The lowest concentration was found in 16-17 cm (1208 ind/g) and the highest in 2-3 cm (3350 ind/g). The benthic foraminiferal accumulation rate (BFAR) showed high values of 5018 ind/cm^2/yr in the 11-12 cm layer and 866 ind/cm^2/yr. The average value of BFAR excluding these two layers is 73 ind/cm^2/y, with the lowest rate found in 16-17 cm (41 ind/cm^2/yr) and highest rate in 2-3 cm (124 ind/cm^2/yr. Based on the diversity indices H'($\log_2$) and ES(100), all analyzed samples indicated *good* or *high* ecological quality standard (EcoQS) with the

highest diversity found in 0-3 cm (Figure 21). Relative abundance of agglutinated species versus calcareous species displayed a significant down-core decrease. There was also an increase in fragments of agglutinated species observed down-core during the picking process.

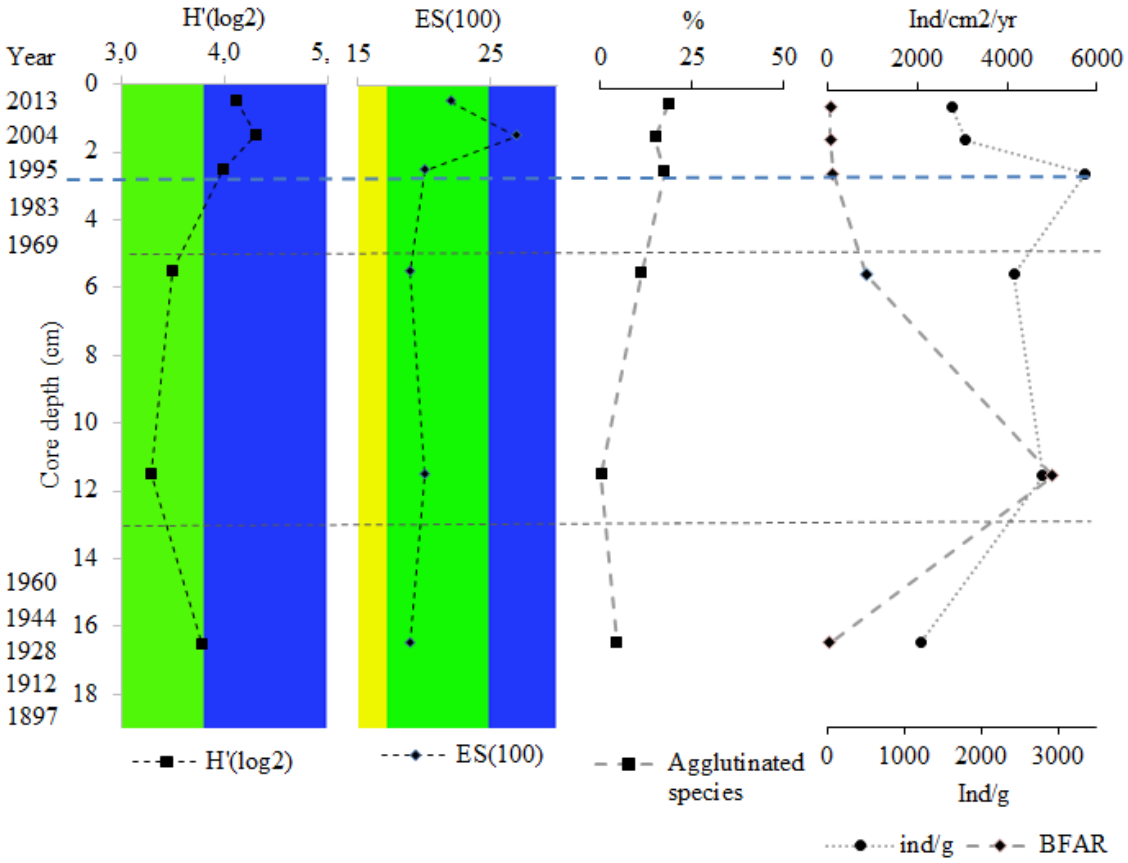

Figure 4.5.1: Selected foraminiferal parameters in core D2-6A. Blue-dotted line marks the start of fish farming in 1994. Grey lines border the layers with increased SAR.

Core D3-3B

All results can be seen in Figure 22. Foraminiferal concentration and BFAR displayed a close relationship because of the stable sedimentation rate in the dated layers (0-6 cm). Both showed a significant up core increase with lowest values in 5-6 cm (315 ind/g and 16.6 ind/cm^2/y) and highest in the surface layer (3368 ind/g and 176.9 ind/cm^2/y). The low concentration in the two deepest analyzed layers was also clearly evident during picking. Diversity indices were all classified as either *good* or *background* with the lowest diversity found in 11-12 cm for both H'log$_2$ (*good*) and ES(100)(*good*) (Figure 4.5.2). Highest diversity was found in 5-6 cm from where it decreases slightly up core. Relative abundance of

agglutinated species increased from 0-1 cm to a maximum in 2-3 cm (34.4 %), and then decreased down core, with a minimum abundance of 2.3 % at 11-12 cm.

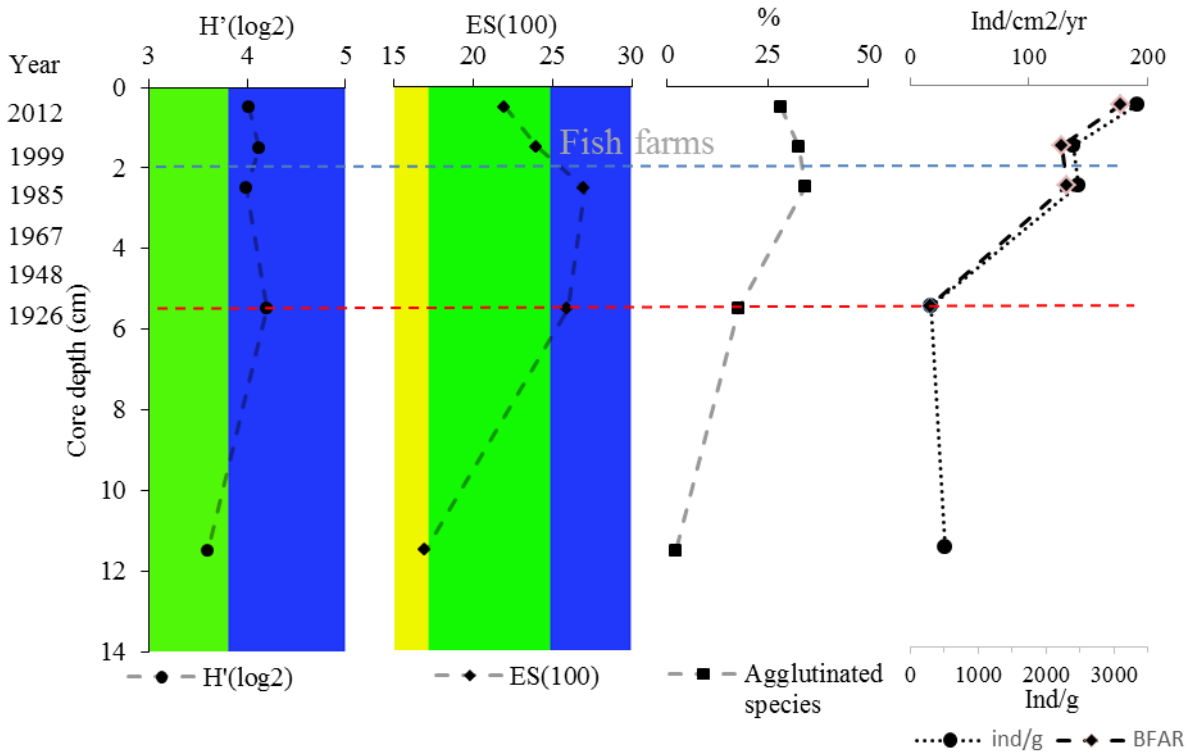

Figure 4.5.2: Selected foraminiferal parameters in core D3-3B. Blue-dotted line marks the start of fish farming in 1994. Red-dotted line marks the dating horizon.

4.5.1 Assemblage composition

The MDS analysis resulted in two main similarity groups, one for each core. Assemblages from 2013 (0-1 cm), 2004 (1-2 cm), 1995 (2-3 cm) and 1928 (16-17 cm) of core D2-6A grouped together, likewise assemblages from 2012 (0-1 cm), 1999 (1-2 cm), 1985 (2-3 cm) and 1926 (5-6 cm) of core D3-3, both with a similarity above 60 % (Figure 4.5.3). In the D2-6A, assemblages from 2004 and 1995 displayed the greatest similarity (>70%, Figure 23). In the D3-3B, the assemblages from 2012 and 1999 also showed over 70% similarity. The two assemblages (1967 and 1963) from the redeposited layer in D2-6A, and the ND (no dating)-assemblage of D3-3B plot each separately (Figure 4.5.3).

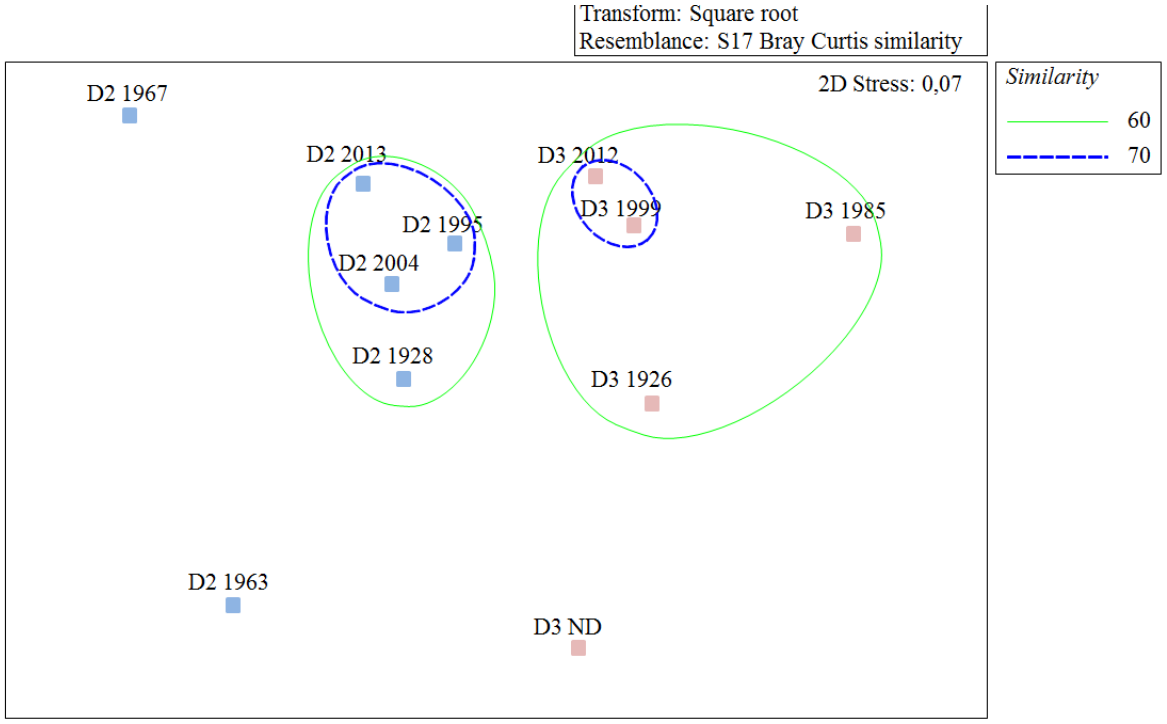

Figure 4.5.3: Two-dimensional MDS-ordination plot based on foraminiferal assemblages (relative abundance of species) of core D2-6B and core D3-3B. Numbers behind the core codes indicate the year. ND=not dated.

Core D2-6A

Bulimina marginata was relatively abundant in core D2-6A, with the lowest abundance found in the 1928 assemblage (3.5 %) and highest in the 1963 assemblage (25.5 %)(Figure 4.5.4-A). The most recent assemblages showed an increasing trend in *B. marginata* from 1985 to 2012 The *Stainforthia* group was also abundant with an average of 8.7 % with lowest abundances in the 1963 and 1967 assemblages (average of 3.1%)(Figure 4.5.4-B). *Cassidulina reniforme* (Figure 4.5.4-D) and *Cassidulina laevigata* (Figure 4.5.4-C) were also abundant throughout the core with averages of 11.5 % and 9 %, respectively. Of note was also the significant increase of *Brizalina skagerrakensis* in the 2012 assemblage (14.1%) compared to the older assemblages (average 2.2 %)(Figure 4.5.4-I). The 1963 assemblage displayed some prominent differences from the others. Most notably is the high abundance of *Cibicides refulgens* 39.1 %)(Figure 4.5.4-G) and *Trifarina angulosa* (10.9 %)(Figure 4.5.4-H) compared to the other assemblages (average of 2.1 % and 0.5 %, respectively). The 1967 assemblage also plotted separately, where the most notable variance in species composition was the absence of *Pullenia osloensis (Figure 4.5.4-F), C. refulgens* and *T. angulosa,* and the lower abundance of the *Stainforthia* group.

Core D3-3B

In the 4 dated assemblages of core D3-3B (1926, 1985, 1999 and 2012), *B. marginata* was abundant with an average of 21.8 %. The lowest abundance of *B. marginata* was found in the 1926 assemblage (13 %). The *Stainforthia* group was also abundant with an average of 13.8 %, with highest abundances occurring in the more recent assemblages. Other species with similar mean abundances were *Hyalinea balthica* (4 %), *P. osloensis* (3.9 %) and *C. laevigata* (3.1 %). *C. reniforme* displayed a decreasing trend in abundance since 1926 with the lowest abundance found in the 2012 assemblage.

The ND assemblage differs from the other assemblages most notably by a higher abundance of *H. balthica* (14.4 %) and *C. reniforme* (25.5%), a somewhat lower abundance of *B. marginata* and *Stainforthia* group, and the absence of *C. laevigata.*

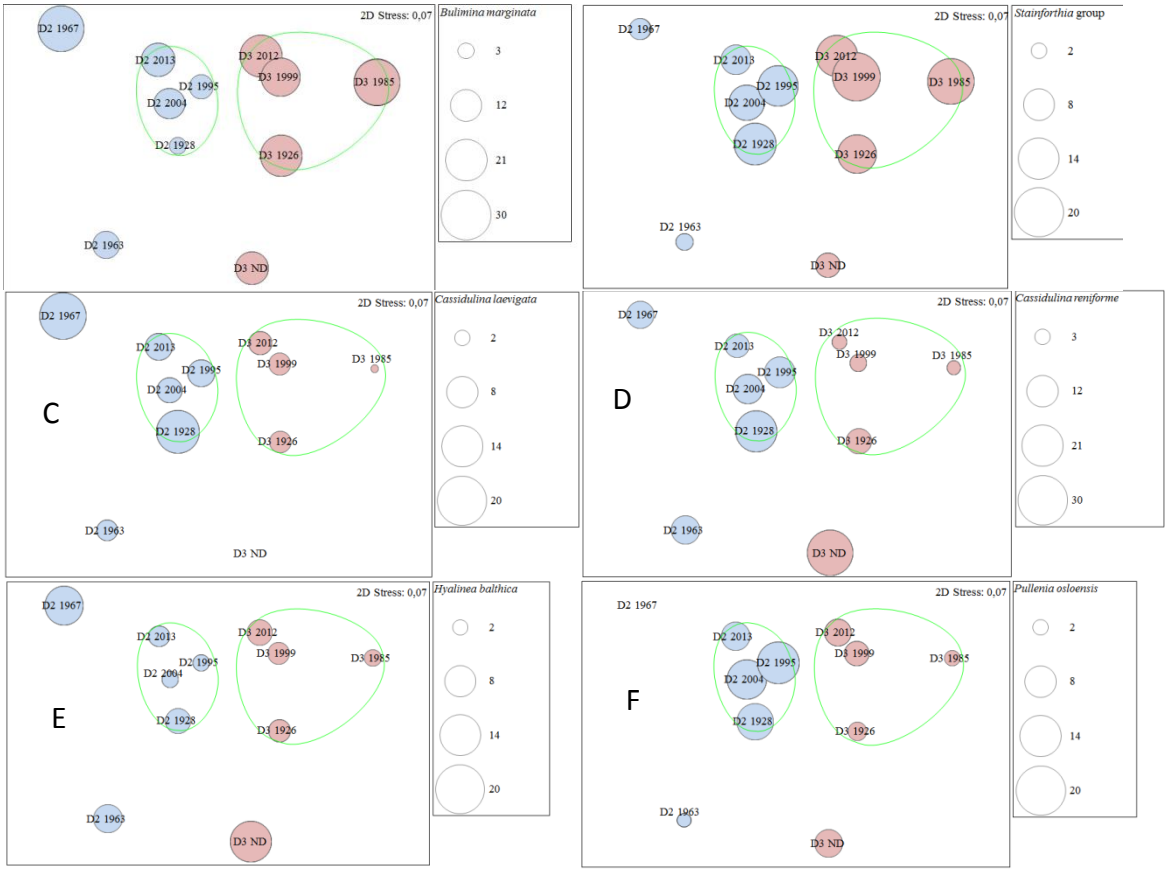

Figure 4.5.4: A-F: MDS-diagram showing relative occurrence of A: *B. marginata*; B: The *Satinforthia* group; C: *C. laevigata*; D: *C. reniforme*; E: *H. balthica*; F: *P. osloensis*. Green line groups assemblages based on 60 % similarity. Red spheres = D3-3B samples, blue spheres = D2-6A samples. Note: Sphere size which indicates relative abundance value is not the same for all plots. 0 % = no circle.

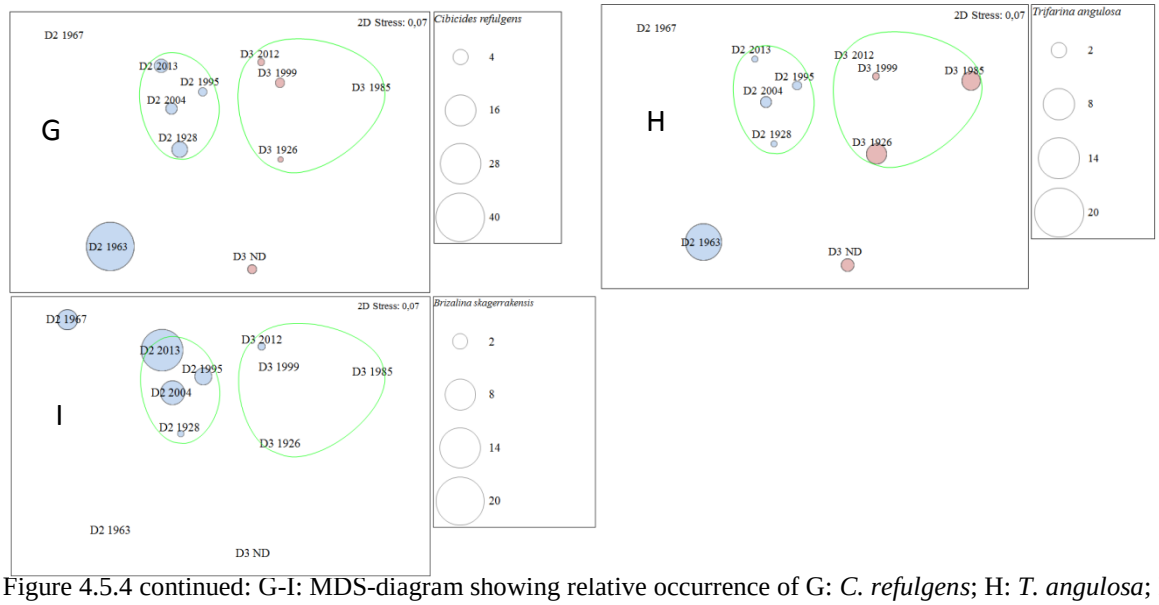

Figure 4.5.4 continued: G-I: MDS-diagram showing relative occurrence of G: *C. refulgens*; H: *T. angulosa*; I: *B. skagerrakensis*. Green line groups assemblages based on 60 % similarity. Red spheres = D3-3B samples, blue spheres = D2-6A samples. Note: Sphere size which indicates relative abundance value is not the same for all plots. 0 % = no circle.

5. Discussion

5.1 Age model – depositional settings and processes

Both cores displayed results for all parameters which deviate from expected results found in stable depositional environments.. Dating using Pb-210 and Cs-137 in marine depositional environments such as fjords may be challenging due to depositional processes that distort the record. A common issue is the mixing of sediments due to bioturbation or re-deposition caused by slumping, sliding or gravity flows (Syvetksi et al., 1987). Sediment mixing typically flattens out the radionuclide concentrations in the affected layers, giving the impression of an accelerated sedimentation rate (Appleby, 1978).

The relatively uniform sediment accumulation rates (SAR) in both analyzed cores indicate low natural SARs in the inner part of Øksfjord, which are comparable to other northern Norwegian fjords (Table 5.1.1). The low SARs are likely due to the relative low freshwater water and sediment input from rivers to the fjord, the scarce vegetation in the surrounding area, and the mainly metamorphic rock lithology (gabbro), which is generally very resilient and not easily erodible (Rea et al., 1996).

Table 5.1.1: Sediment accumulation rates (SAR) in other Norwegian fjords given as minimum and maximum values.

Fjord	**SAR min-max (g/cm^2/yr)**
Malangen (Hald et al., 2011)	0.04-0.17
Kaldfjord (Vågen, 2018)	0.043-0.085
Øksfjord D2 (this study)	0.034-0.037
Øksfjord D3 (this study)	0.053

5-14 cm

*Core D2-6A*Core D2-6A had wo defined peaks in the Cs-137 record, one at 13-16 cm and one at 3-5 cm, which implied that both were from the period of maximum Cs-137 fallout during the early 1960's. Likewise, the similarity in Pb-210 concentrations in layers 4 cm and 14 cm indicated that both layers were similar in age (1963-1967). Both records therefore suggest that the sediments in the layers 5-13 cm have been deposited over a relatively short time period, most likely as a sudden event in the early 1960s. This was substantiated by the chronology model for layers 5-14 cm which all have statistical errors which could date the interval to 1965 (Appendix A, Table 5). In addition, the geochemical parameters and microfaunal assemblage composition in 5-14 cm displayed notable irregularities in this sediment layer interval compared to the sediments above and below (Figure 4.3.1, Figure 4.4.1, Figure 4.5.4:A-I). A rapid deposition of this scale is most likely the result of a gravity-driven submarine depositional process, possibly a slide, slump or a debris flow, since steep-sided fjords are more prone to these depositional processes (Syvitski et al., 1987). Grain size distribution in layers 5-10 cm showed a high content of silt while layers 10-14 cm showed a significantly increase in the sand fraction, with the largest sand content in the 11-12 cm layer. A turbidity flow deposition may explain this fining upwards succession. As the flow moves downslope and eventually loses energy and settles in the basin, the coarser sediments are deposited first, and the less dense finer particles settling on top. The uniform distribution of mainly silt in 5-10 cm suggests that this may be a mixture of re-suspended *in situ* and transported material. (Figure 4.1.4)

Core D3-3B

The increase and variance in grain size distribution down core suggested a disruption of the normal *in situ* depositional energy, since stable depositional settings would yield a relatively uniform grain size distribution down core. There were also some anomalies regarding the radionuclide concentrations in this core. Although the Pb-210 record suggested a stable sediment accumulation rate from 0-6 cm, the record disappeared abruptly below 6 cm core depth (Figure 4.2.1-A). The unsupported 210-Pb concentrations were also generally very low compared to the concentrations found in the most recent deposits in core D2-6A (Figure 4.2.1-A, Figure 4.2.2-A). In addition, there were no detectable Cs-137 peaks from the artificial fallout maximum in 1963. The lack of Pb-210 concentrations below 6 cm could suggest that these sediments were deposited so far back in time that the radionuclides have almost completely disintegrated. A possible explanation could be that the sediments below 6 cm are, as in the 5-14 cm layer in core D2-6A, redeposited. However, if the sediments above 5- 6 cm (dated to 1926) were deposited under stable depositional conditions, one would expect to see the maximum artificial fallout peaks from the early1960's, which are absent. A possible explanation could be a slumping or sliding event that has dislocated and removed the most recent sediment layers. This would create "false" chronology since the Pb-210 dating method dates the sediments down core in relation the concentrations in the top layer, which is assumed to be modern day. Therefore, if a submarine slide occurred directly before the core collection, older sediments would be exposed, and the Pb-210 concentrations in the water/surface sediments would be interpreted to present day, while in reality they would be significantly older. Based on this, the suggested chronology for core D3-3B (Figure 4.2.1-B) is highly uncertain.

The following discussion applies the suggested age models to the results obtained for both cores to help determine reference conditions and evaluate possible fish farming impact on the benthic environment. The oldest analysed layers were dated to 1897 in core D2-6A (18-19 cm) and 1926 in core D3-3B (5-6 cm). The layers 5-14 cm in core D2-6A are interpreted as redeposited sediments and are not given weight in the discussion as they do not represent the *in situ* environmental conditions. This sediment interval is given the name *redeposited layer* in the following chapters. It should also be noted that since dating below 6 cm in core D3-3B proved to be difficult, the geochemical results obtained in core D3-3B in layers 7-14 cm are not discussed in this chapter unless they exhibit notable trends. The lack of major industrial

activity and other possible pollutant waste sources from anthropogenic activities from pre-fish farming times in inner Øksfjord, substantiates that 1897 (D2-6A) and 1926 (D3-3B) are of an adequate age defining natural, un-impacted conditions. However, since the first fish farms were established as recent as 1994, and because of the low sedimentation rate, only results from 0-3 cm in core D2-6A and 0-2 cm in core D3-3B represent environmental conditions since the establishment of fish farming activities in the inner Øksfjord. Statistically, this provides a weak basis for establishing trends and variations due to fish farm impact, and interpretations as such should therefore be considered with this in mind.

5. 2 Sources of organic matter and heavy metals

The C/N ratio and stable isotope $\delta^{13}C$ and $\delta^{15}N$ signatures in the sediments are valuable proxies used to separate autochthonous and allochthonous organic material as they provide a basis for differentiating marine derived OM and terrestrially derived OM. Marine derived organic matter (OM) usually has C/N ratios between 4 to 6, a $\delta^{13}C$ signature of -20 ‰ to -22 ‰ and a $\delta^{15}N$ signature of 4 ‰ of 8 ‰, while terrestrial derived organic matter usually has a C/N ratio of over 20, $\delta^{13}C$ signatures of -27 ‰ and a $\delta^{15}N$ signature of 0.4 ‰ (Meyers, 1994; Meyers 1997; Peters et al., 1978).

Core D2-6A

In core D2-6A, the values of the C/N ratio, $\delta^{13}C$ and $\delta^{15}N$ were all in the range which indicates that the OM is of mainly marine origin. However, the slightly higher mean value of C/N found in 10-13 cm, and the decrease in $\delta^{13}C$ in 10-11 cm and the increase in $\delta^{15}N$ in layers 9-13 cm point to a slight influx of terrestrial derived OM in these layers. This indicates that the redeposition event originally started closer to the shore in sediments with a higher concentration of terrestrially sourced OM than in the basin sediments. It is also possible that an avalanche originally started on land and ended in the fjord causing submarine debris flow processes. In both cases some of the terrestrially derived OM would be brought further out in the fjord and possibly deposit in the basin.

The nTOC and TN concentrations were of relatively similar values in the sediments deposited before and after the redeposited layer, although there seems to have been a larger influx of carbon pre 1960 (14-19 cm, EcoQS *poor*) compared to 1969 to present day (0-5 cm, EcoQS

moderate). Since there has been little or no industry in the inner fjord this difference is likely due to natural variations in carbon influx and/or slight changes in the depositional environment. The slight increase in nTOC and TN from 1969 to present day observed in recent sediments could indicate increased deposition of organic matter in recent years compared to the natural influx.
Pb, Zn, Cd concentrations were all in relatively stable conditions (excluding redeposited layer) and were classified as mainly *background* quality which implies a stable natural deposition and little or no anthropogenic deposition. The Cu values were stable throughout the core (excluding redeposited layer) and classified as *moderate* quality. The said stable values, and the fact that there are no significant variations in Cu concentrations indicate that the natural deposition of Cu in this basin is relatively high.

The generally higher concentrations of nTOC and TN, and heavy metal concentrations in core D2-6A compared to core D3-3B, could be due to the circular circulation pattern (eddy) in this part of the fjord. The eddy is clearly evident also at 50 m water depth (Akvaplan NIVA, Strømmodellering, APN Finnmark Hav) which suggests it may extend even deeper in the water column. This could increase the residence time of suspended particulate matter, and subsequently lead to an increased deposition of fine material to the D2 basin floor compared to the D3 basin.

Core D3-3B

The values of C/N ratio and the stable ^{13}C and ^{15}N sediment isotopes were all in the range which indicate that the OM found throughout the core is mainly of marine origin. The steady decrease in $\delta^{13}C$ concentrations since 1948 to present day could indicate a shift to higher terrestrial sourced OM. However, this is contradicted by the relatively stable $\delta^{15}N$ values and the decreasing C/N ratio in this time period. The nTOC values were classified as *background* throughout the core with a slight increase in concentrations from 1926 to present day. The scarce anthropogenic activity in the inner fjord makes it difficult to interpret this as anything else than natural fluctuations due to changes in the depositional environment.
The heavy metals were all classified as background, except for Cu in the 1-2 cm layer which was classified as *moderate*. The value of 20.2 mg/kg is marginally higher than the background (<20 mg/kg) classification, and since he EcoQS classification system does not include a *good* classification for copper, the classification of *moderate* is somewhat misleading.

5.3 Foraminiferal assemblages

5.3.1 Redeposited assemblages

Analysis of benthic foraminifera in dated sediments provides a tool for reconstructing reference conditions and identifying alterations in assemblages through time. However, an accurate comparison and interpretation of assemblages from different time periods assumes that the assemblages found in the fossil record represent the living assemblages at the time of burial. Many depositional processes could have influenced the distribution of species composition observed in the fossil record. There were notable differences in species composition, concentration, diversity and BFAR in the assemblages in the redeposited sediment layers from core D2-6A (samples from 1963 (11-12 cm) and 1967 (16-17 cm)) and core D3-3B (sample ND (11-12 cm)); Figure MDS). This combined with the differences in physical properties and geochemical concentrations, and the interpretation of depositional events, suggested that all three samples were contain foraminiferal assemblages influenced by redepositional events. This was especially evident for the sample D2 1963. The extremely high value of BFAR found in this assemblage was the result of the artificially high sediment accumulation rates calculated for the redeposited layer by the dating models, and gave therefore a "false" BFAR. The sample D2 1963 plotted separately in the MDS-similarity plot, and the species composition displayed some significant dissimilarities from the other assemblages in the core, i.e. the absence of *B. skagerakensis* and the low occurrence of *P. osloensis* and the *Stainforthia* group. Redeposition of sediments could mix older and younger assemblages and may result in the high abundance of allochthonous species, such as *C. refulgens* and *T. angulosa* in sample D2 1963. *C. refulgens* is usually abundant in shallower, high-energy environments and sandy sediments where they live attached to hard substrates (Murray, 1991). Likewise, the abundance of *T. angulosa* has been shown to decrease with water depth (Kihle, 1971). The abundance of *T. angulosa* in sample D2 1963 was actually more similar to the dated D3 core assemblages which are located in the shallower basin (150 m). .

The assemblage of sample D2 1967 comes from 5-6 cm core depth and might represent the first deposition layer after the redeposition event . The assemblage is still impacted by increased sedimentation of fin grained material and is more similar to the *in situ* assemblages of the younger sediments in the core. Since exact placement of the borders of the redeposited

layer is difficult, it is possible that this layer consists of both redeposited sediments and in situ deposits, and the foraminifera assemblage could thus be a mix of the two.
The physical properties of the sediments in core D3-3B, as well as the dating results indicate that the D3 ND (no date) sample assemblage may be a redeposited assemblage. The irregular sand content and increased grain size distribution and the disappearance of the Pb-210 signal below 6 cm could indicate that the sediments below are redeposited and older (see chapter 5.1). The lower diversity of this assemblage and the significantly lower foraminifera concentration (ind/g) point to a different depositional setting compared for the younger assemblages from 1985, 1999 and 2012.
The low foraminiferal concentration and BFAR in the D3 1926 sample, which is similar to the values found in the D3 ND assemblage, and the fact that it borders the disappearance of the Pb-210 concentrations, could indicate that this layer (5-6 cm) also was influenced by redepositional events. However, the relatively similar species composition and the stable SAR compared to the more recent sediments substantiate not interpreting this as a redeposited assemblage. This should be kept in mind when discussing the *in situ* assemblages in the following chapter.

5.3.2 *In situ* foraminiferal assemblages (excluding the redeposited assemblages)

The foraminiferal compositions assumed to be representative for the un-impacted depositional environment (*in situ*) in both cores display many of the same characteristics. In both cores, the diversity indices indicate *background* or *good* ecological quality status (EcoQS), and the concentration of foraminifera is relatively high (with the exception of the low concentration in the D3 1926 assemblage). In core D2-6A, diversity, foraminiferal concentration and BFAR are higher in the more recent assemblages (1995, 2007, 2013) compared to the 1928 assemblage. This could indicate an increase in available food supply to the benthic system since the establishment of fish farm activity in the inner Øksfjord in 1994. There are some stratigraphic trends which substantiates this theory. The steady increase in abundance of *B. skagerrakensis* in the assemblages could suggest an increase in phytodetritus deposited to the ocean floor in this area, as this species has been shown to respond positively to fresh organic matter (Alve et al, 2011; Duffield et al., 2015). The nTOC and TN also show a slight increasing trend in the sediments post 1969 (Figure 4.3.1). This could indicate increased phytoplankton blooms in this part of the fjord during this time. This is also substantiated by the increase in abundance in the *B. marginata*, which is thought to flourish in organic

enriched environments (Alve et. al, 2016). An increase in organic material could also be indicated by the steady decrease in abundance of *C. reniforme* since 1928. *C. reniforme* is classified as a Group I "Sensitive species" species by the Foram-AMBI sensitivity index (Alve et al., 2016) which characterizes species as sensitive to organic matter enrichment. However, although there may be an enrichment of organic detritus to the ocean floor in recent time, it does not seem be of a magnitude which caused oxygen depletion. The abundance of *B. skagerrakensis*, which has been shown to be intolerant of low oxygen concentrations (Duffield et al. 2015) suggests the sediments are well-oxygenated which is underlined by the observed oxygen concentrations during the sampling campaign (Figure 1.3.2).

In core D3-3B, the diversity indices indicate *good* to *background* EcoQS, and it is difficult to observe any significant trends. The increase in foraminifera concentration and BFAR from 1995 and 2007 to 2012, may indicate increased food supply to the benthic system also in this basin. The increase in abundance of the *Stainforthia* group in the three youngest assemblages compared to the assemblage from 1926 could substantiate this, as *Stainforthia fusiformis* is an opportunistic species which proliferates in organic material enriched environments (Alve, 2002).

In both cores a significant down core decrease in agglutinated species abundance is observed (Figure x). As seen in numerous studies, calcareous species dominate the fossil record in fjords and marginal marine environments (Torper 2015, Enoksen 2011, Sjetne 2016). The notable decrease in agglutinated species was also evident in the before mentioned studies. Agglutinated species are often fragile and more prone to taphonomic processes than most calcareous species (Alve 1996; Majewski & Zajaczkovski 2007; Hald & Steinsund 1996), which may explain the down core decrease. The cluster analysis and MDS ordinations used to analyze similarities between assemblages were also run with only the calcareous species. This resulted in the same groups and outliers, and no significant variations in relative abundance of the dominant species (Appendix E).

5.6 Impact of fish farming on the benthic environment

The overall objective for the study is to evaluate and interpret the environmental impact from fish farming activity on the benthic environment by studying microfaunal and geochemical variations over time from past to present. To assess the degree of impact in the inner Øksfjord, it is necessary to have knowledge about the *in situ* natural conditions, which means the environmental condition before aquaculture activity was established in this area. The uncertainties of the radiometric dating, most likely caused by redepositional events, made solid interpretations of the reference conditions slightly difficult. The relatively low sediment accumulation rates in Øksfjord resulted in six dated data points (from 1926 to 2012) in core D3-3B, of which only three represent the environmental development after the establishment of fish farming. In core D2-6A only two data points have post fish farming age. This provides a statistically very weak basis for determining and interpreting the impact of fish farming at the studied sites. The following discussion should therefore be considered with this in mind.

Of special interest for this study was the Cu concentration record in the sediments. Antifouling agents used to impregnate the cage nets are often copper-based. It is well known that Cu often leaches from these agents to the marine environment (Skarbøvik et al., 2014). Although there is a slight increase in Cu concentration observed in sediments deposited after 1994 in core D3-3B (Figure 4.4.2), it is difficult to link it directly to fish farming activity because the increasing trend has been steady since 1926. In addition nearly all Cu concentrations measured in the core sediments indicate *background* conditions (Figure x). - Copper concentrations in core D2-6A are slightly higher than in core D3-3B and represent mainly *moderate* status conditions (Figure 4.4.1). Concentrations in sediments younger than 1994 are slightly lower than in background sediments from the early 1900s. Monitoring results undertaken by Aquaplan-niva during 2011-2015 show comparable Cu concentrations in surface sediments (Table 2.4.1).

However, although there are no signs of heavy organic loading observed in the inner Øksfjord, there are some parameters indicating a recent increasing trend which might be linked to fish farming activity. In core D2-6A, nTOC and TN concentrations slightly increased since 1995 and represent *moderate* conditions (Figure x). Also, an increase in *B. skagerrakensis* abundance observed in the post fish farming assemblages, could be the result

of increased fresh food supply to the benthic environment. *B. skagerrakensis* was also abundant in the living foraminiferal assemblages collected from the same site in September 2017 (12.1 % (average of 3 replicates), A. T. Klootwijk, unpublished data). The living assemblage also showed high abundances of *Stainforthia fusiformis* (average of 22.5 %). As previously mentioned, *S. fusiformis* is an opportunistic species which is often abundant in environments with enriched organic matter supply. The slightly higher diversity indices in the youngest assemblages could likewise be the result of increased food availability, which might reflect increased deposition of particulate organic matter resulting from fish farms in the surrounding.

The same general trends in nTOC and TN concentrations were observed in core D3-3B. This is substantiated by the increased abundance of the opportunistic *Stainforthia* group in the youngest assemblages representing deposits after the establishment of fish farming. The living assemblages displayed a significant dominance of *Stainforthia fusiformis* at this location (41.8 % (average of 3 replicates), A. T. Klootwijk, unpublished data). As in the D2 assemblages, this increase in the *Stainforthia* group in both the dead and living assemblages could indicate increased organic material (food) supply, which could by the result of increased deposition of particulate organic material from fish farm activity. The higher abundance of *S. fusiformis* found in the living assemblage compared to the *Stainforthia* group of the dead assemblages post fish farm establishment could likely be the result of the increased fish farm production since the early 2000's and increased dispersion and deposition of POM from the fish farms.

Although there are some indications of increased deposition of organic material which could be the result of particulate organic matter dispersal from the fish farms in Øksfjord, the ecological quality status (EcoQS) is representing *background* conditions at both locations.

5.5 Comparison with other fjords

This chapter compares results of this study with results of two other studies from Norwegian fjords with fish farm production. All studies are based on geochemical and micropaleontological analyses in dated sediment cores and aim to assess the impact of fish farming on the respective locations. Sediment accumulation rates, TOC content, C/N ratio, carbon accumulation rates, average sand content and diversity indices H'(log2) and ES(100) of benthic foraminifera found in the two Øksfjord cores, are compared to results from

Ornaheimsfjord (Sjetne, 2016) and Kaldfjord (Vågen, 2017) (Table 5.5.1). It should be noted that none of the cores were collected directly below the fish farms in any of the studies. Ornaheimsfjord is a side arm of Hardangerfjorden in western Norway and Kaldfjord is a semi-enclosed fjord situated on the northern coast of the island Kvaløya in the Tromsø municipality in northern Norway.

Both northern Norwegian fjords, Øksfjord and Kaldfjord, are characterized by low sediment accumulation rates. This might be due the scarce vegetation in northern areas and lower freshwater input in these fjords. The SARs of the FF-station in Ornaheimsfjord and the two locations in Kaldfjord have seen an increase since the onset of fish farming (Vågen 2018, Sjetne 2016) which is not evident in Øksfjord.

At the Kaldfjord stations there was also significant increase in nTOC concentrations and increased carbon accumulation during this time period. There is also a slight increase for these parameters post fish farm establishment in Øksfjord, but in a smaller magnitude. The relatively high average concentration on nTOC in D2-6A is thought to be of natural sources as there is little anthropogenic activity around the fjord, and the values are also relatively high and stable back to 1897. Although the Ornaheimsfjord study showed an increase in carbon accumulation post fish farm establishment, there was no apparent increase in nTOC, and the average nTOC content is also lower than the averages from the two locations in the two other fjords. C/N ratio-ranges for all three fjords indicates mainly marine derived organic material in the sediments, with the lowest average ratio found in the Øksfjord locations and the highest values found in the Kaldfjord location, indicating a higher terrestrial input in this fjord.

The diversity indices based on benthic foraminifera all indicated *good* or *background* EcoQS, and no significant decrease in diversity in the assemblages after fish farming establishment. The most abundant species (>10%) in the foraminiferal assemblages found in the analyzed sediments of all three fjords are listed in Table 5.5.2. Both locations in Kaldfjord and Øksfjord displayed an increase in the opportunistic species *S. fusiformis* in the most recent assemblages, indicating some degree of stress related to an increase of organic matter in the sediments, which is corroborated by the increased nTOC seen in these sediments. *B. skagerrakensis* showed an increase in abundance in the most recent assemblages in Øksfjord

D2-6A and Onarheimsfjorden FF-core, which could indicate increased phytodetritus input to the benthic system in the fjord related to increased dispersion of nutrient from the fish farms.

Table 5.5.1: Overview of various parameters in three Norwegian fjords (Øksfjord (this study), Ornaheimsfjord (Sjetne, 2016), Kaldfjord (Vågen, 2018): Average sedimentation rate, average TOC content range of C/N ratio, carbon accumulation rates, average sand content, and diversity indices ES(100) and H'(log2). Color refers to ecological quality status (EcoQS) according to table x.

	Øksfjord D2-6A (excluding redeposited layer)	Øksfjord D3-3B	Ornaheimsfjord (averages or max-min of two locations)	Kaldfjord (Stations IN/OUT)
Water depth (m)	240	157	127	111/138
Sill depth (m)	Approx. 130 m	Approx. 130 m.	Approx. 100 m (outer basin ridge) Approximately 190 m (main sill in Hardangerfjorden)	55 (internal fjord sill)/ >150
Average sediment accumulation rate	0.035	0.058	0.18	0.05/0.07
Average nTOC content	3.1	1.4	1.3	2.2/3.1
C/N ratio range	6.6	4.8 – 7.1	7 – 8.6	6.7 – 9.4/ 7.8 – 10.3
Carbon accumulation rate (g C/m2/yr	7.6 -12.4	8.1 – 9.6	13.8 – 41.8	8.4 – 30.4/ 14.1 – 32.3
Average sand content	14.8	37.4	6	24.3/33.4
H'(log2)	21.3	24.9	23	21.7/21.5
ES (100)	3.8	4	4.1	4/4

Table 5.5.2: Species of foraminifera with occurrence > 10% in at least one sample in Øksfjord D2-6A and D3-3B, Onarheimsfjorden FF-core (Sjetne, 2016) and Kaldfjord In-core and OUT-core (Vågen, 2018)

Øksfjord (D2-6A) 240 m	Øksfjord (D3-3B) 157 m	Onarheimsfjorden (FF-core) 127 m	Kaldfjord (IN-core) 111	Kaldjorden (OUT-core) 138
Brizalina skagerrakensis	*Bulimina marginata*	*Brizalina skagerrakensis*	*Bulimina marginata*	*Bulimina marginata*
Bulimina marginata	*Cassidulina laevigata*	*Bulimina marginata*	*Cassidulina reniforme*	*Cassidulina laevigata*
Cassidulina laevigata	*Cassidulina reniforme*	*Cassidulina laevigata*	*Elphidium excavatum*	*Cassidulina reniforme*
Cassidulina reniforme	*Hyalinea balthica*	*Eggereloides medius*	*Hyalinea balthica*	*Cassidulina neoteretis*
Cibicides refulgens	*Pullenia osloensis*	*Pullenia osloensis*	*Stainforthia fusiformis*	*Pullenia osloensis*
Hyalinea balthica	*Stainforthia* group	*Stainforthia fusiformis*		
Pullenia osloensis		*Textularia earlandi*		
Stainforthia group				
Trifarina angulosa				

6. Conclusions

- The radio nuclide signals in both cores displayed irregularities down-core which complicated the chronology models. In core D2-6A there was a monotonic feature in core interval 5-14 cm core depth which indicated an increased sedimentation accumulation rate from 1963 to 1967. The sudden shift in several parameters for this layer (grain size, heavy metals concentration, NTOC, TN, C/N, sediment isotopes and foraminiferal species assemblages) indicated that this layer was most likely influenced by a rapid depositional process, and that this sediment layer in part consisted of allochtonous sediments. The sediment accumulation rates in 0-5 cm and 15-19 cm core depth were stable at 0.034 and 0.037 g/cm2/yr respectively. The dating chronology placed the establishment of the fish farms in 1994 at 3-4 cm which gave only three data points post fish farm establishment. This provided a statistically weak basis for interpreting trends post fish farm establishment, and the comparison of environmental conditions before and after fish farm activity. The dating of the sediments above (1969 to present day) and below (1897-1960) the redeposited layer was thought adequate for determining the natural conditions at this location because of the insignificant anthropogenic activity historically in inner Øksfjord.

- In core D3-3B, the Pb-210 signal was generally very low, and disappeared completely below 6 cm core depth, and there was no 1963 maximum artificial fallout peak in the Cs-137 concentrations. The differences in grain size distribution and foraminiferal assemblages, together with an interpretation of the radio nuclide concentrations, suggested that these sediments also were redeposited. The sediment accumulation rate was stable from 1926 (5-6 cm) to present day (0.058 g/cm2/yr). The dating chronology placed the establishment of the fish farms in 2-3 cm core depth, which provided 2 data points post fish farm establishment. As in core D2-6A, provided this a statistically weak basis for interpreting trends post fish farm establishment. The 4 data points pre fish farm establishment were thought adequate as a basis for determining the reference conditions.

- In D2-6A, normalized total organic carbon (nTOC) content was classified as *poor* pre 1960 and *moderate* post 1969 according to the eceological quality status (EcoQS), indicating a relatively high natural influx of carbon to the sediments in this location. Increases in nTOC and TN in both cores indicated increased deposition of organic matter in recent times which could be a result of fish farm waste dispersion and depostion. The C/N ratio and stable isotope $\delta^{13}C$ and $\delta^{15}N$ signatures in both cores indicated that the organic matter was of mainly marine origin.

- There were no indications of significant increases in heavy metal concentrations in both cores, and thus no indication of increased deposition of copper as a result of leaching from antifouling agents used for impregnating the cage nets. The relatively high stable copper consentrations of Cu in the *in situ* sediment layers in core D2-6A were interpreted to be the result of a realatively high natural deposition.

- The generally higher concentrations of nTOC, TN and heavy metals in D2-6A compared to D3-3B indicated a difference in the depositional environmental in the two locations. This was suggested to be in relation to a longer residence time for supsended particualte matter due to the circular horizontal current pattern (eddy) in the water column above the D2 location.

- The ecological quality status (EcoQS) based on diversity indicies H'(log2) and ES(100) classified all assemblages in both cores as of *good* or *background* quality which indicate no heavy impact on the benthic community.

- Based on relative abundance (%) of benthic foraminiferal species, samples were grouped according to similarity in a MDS-ordination plot. Assemblages from 2013, 2004, 1995 and 1928 of core D2-6A grouped together, where assemblages from 2004 and 1995 displayed the greatest similarity. The two assemblages from the redeposited layer (1967 and 1963) both plotted separately. In D3-3B, assemblages from 2012, 1999, 1985 and 1926 were grouped together with the assemblages from 2012 and 1999 displaying greatest similarity. The ND (no dating)-assemblage plotted separately.

- The increased abundance of *Cibicides refulgens* and *Trifarina angulosa* in the 1963-assemblage in core D2-6A substantiated that the redeposited sediments in this layer were allochtonous, and possibly from a shallower, higher energy environment.

- In both cores there were indications of increased available nutrients in the sediments post fish farm activity based on variances in species composition. In D2-6A, this was indicated by the steady increase in abundance of *Brizalina Skagerrakensis* and *Bulimina marginata*, and the similar steady decrease in abundance of *Cassidulina reniforme*. The increased nutrients could be a result of increased phytoplancton blooms resulting from increased particulate organic material originating from the fish farms.

- Sedimentation accumulation rates, nTOC, carbon accumulation rates, C/N and diversity indicies H'(log2) and ES(100) were comparable with observations from two other Norwegian fjords with fish farm production (Onarheimsfjorden and Kaldfjord).

References

Alve, E. (1995). Benthic foraminiferal responses to estuarine pollution: a review. Journal of Foraminiferal Research, 25(3), 190-203.

Alve, E. (1996). Benthic foraminiferal evidence of environmental change in the Skagerrak over the past six decades. Norges Geologiske Undersokelse, 430, 85-94.

Alve, E., Lepland, A., Magnusson, J., & Backer-Owe, K. (2009). Monitoring strategies for re-establishment of ecological reference conditions: possibilities and limitations. Marine Pollution Bulletin, 59(8-12), 297-310.

Alve, E., Murray, J. W., & Skei, J. (2011). Deep-sea benthic foraminifera, carbonate dissolution and species diversity in Hardangerfjord, Norway: an initial assessment. Estuarine, Coastal and Shelf Science, 92(1), 90-102.

Akvaplan NIVA, Strømmodellering, APN Finnmark Hav. Retrieved september 20, 2018, from http://kart.akvaplan.niva.no/os

Appleby, P. G., & Oldfield, F. (1978). The calculation of lead-210 dates assuming a constant rate of supply of unsupported 210Pb to the sediment. Catena, 5(1), 1-8.

Coccioni, R., Frontalini, F., Marsili, A., & Mana, D. (2009). Benthic foraminifera and trace element distribution: a case-study from the heavily polluted lagoon of Venice (Italy). Marine Pollution Bulletin, 59(8-12), 257-267.

Dahl-Hansen, G & R. Velvin. 2007. Grieg Seafood Finnmark. Miljøundersøkelse i Øksfjorden, Loppa kommune 2007. Akvaplan-niva rapport 3806.01.

Dean, R. J., Shimmield, T. M., & Black, K. D. (2007). Copper, zinc and cadmium in marine cage fish farm sediments: an extensive survey. Environmental Pollution, 145(1), 84-95.

Directive 2000/60/EC of the European Parliament and of the Council of 23 October 2000 establishing a framework for Community action in the field of water policy

Directive 2008/56/EC of the European Parliament and of the Council of 17 June 2008 establishing a framework for community action in the field of marine environmental policy

Directorate of Fisheries. (2018a). Akvakultur/Akvakulturstatistikk/Laks, regnbueørret of ørret. Retrieved february 1, 2018, from https://www.fiskeridir.no/Akvakultur/Statistikk-akvakultur/Akvakulturstatistikk-tidsserier/Laks-regnbueoerret-og-oerret

Directorate of Fisheries. (2018a). Akvakultur/Akvakulturstatistikk/Statistiske publikasjoner/Foreløpig statistikk for akvakultur 2017.
Retrieved febraury 1, 2018, from https://www.fiskeridir.no/Akvakultur/Statistikk-akvakultur/Statistiske-publikasjoner/Statistikk-for-akvakultur

Duffield, C. J., Hess, S., Norling, K., & Alve, E. (2015). The response of Nonionella iridea and other benthic foraminifera to “fresh” organic matter enrichment and physical disturbance. Marine Micropaleontology, 120, 20-30.

Dolven, J. K., Alve, E., Rygg, B., & Magnusson, J. (2013). Defining past ecological status and in situ reference conditions using benthic foraminifera: a case study from the Oslofjord, Norway. Ecological indicators, 29, 219-233.

Enoksen, J.H., 2010: Environmental status: From ”natural” to polluted conditions in the Bunnefjord, inner Oslofjord. MSc thesis in Geosciences, University of Oslo, 75 pp.

Findlay, S. (1995). Importance of surface-subsurface exchange in stream ecosystems: The hyporheic zone. Limnology and oceanography, 40(1), 159-164.

Gowen, R. J. (1994). Managing eutrophication associated with aquaculture development. Journal of applied ichthyology, 10(4), 242-257.

Grass, G., Rensing, C., & Solioz, M. (2011). Metallic copper as an antimicrobial surface. Applied and environmental microbiology, 77(5), 1541-1547.

Gustafsson, M., & Nordberg, K. (1999). Benthic foraminifera and their response to hydrography, periodic hypoxic conditions and primary production in the Koljö fjord on the Swedish west coast. Journal of Sea Research, 41(3), 163-178.

Hald, M., & Steinsund, P. I. (1996). Benthic foraminifera and carbonate dissolution in the surface sediments of the Barents and Kara Seas. Berichte zur Polarforschung, 212, 285-307.

Husa, V., Grefsrud, E. S., Agnalt, A. L., Karlsen, Ø., Bannister, R., Samuelsen, O. B., & Grøsvik, B. E. (2016). Effekter av utslipp fra akvakultur på spesielle marine naturtyper, rødlista habitat og arter.

Holmer, M., Kristensen, E., (1992) Impact of marine fish cage farming on metabolism and sulphate reduction of underlying sediments: Marine Ecology Progress Series, 80, pp., 191-201

Hess, S., Alve, E., Trannum, H. C., & Norling, K. (2013). Benthic foraminiferal responses to water-based drill cuttings and natural sediment burial: results from a mesocosm experiment. Marine Micropaleontology, 101, 1-9.

Johnsen, I. A., Asplin, L. C., Sandvik, A. D., & Serra-Llinares, R. M. (2016). Salmon lice dispersion in a northern Norwegian fjord system and the impact of vertical movements. Aquaculture Environment Interactions, 8, 99-116.

Kartverket, norgeskart.no/Landkart. Retreived Oktober 2, 2108, from https://www.norgeskart.no/?_ga=2.12265779.628591531.1539457976-1954664810.1535364721#!?project=seeiendom&layers=1002,1015&zoom=4&lat=7197864.00&lon=396722.00

Kartverket, norgeskart.no/sjøkart. Retrieved Oktober 3, 2018, from https://www.norgeskart.no/?_ga=2.209014165.628591531.1539457976-1954664810.1535364721#!?project=seeiendom&layers=1008,1015&zoom=8&lat=7778941.56&lon=773430.19

Kihle, R. (1971). Foraminifera in five sediment cores in a profile across the Norwegian Channel south of Mandal. Norsk geol. Tidsskr, 51, 261-286.

Kutti, T., Ervik, A., & Høisæter, T. (2008). Effects of organic effluents from a salmon farm on a fjord system. III. Linking deposition rates of organic matter and benthic productivity. Aquaculture, 282(1-4), 47-53.

Kutti, T., Hansen, P. K., Ervik, A., Høisæter, T., & Johannessen, P. (2007). Effects of organic effluents from a salmon farm on a fjord system. II. Temporal and spatial patterns in infauna community composition. Aquaculture, 262(2-4), 355-366.

Kutti, T., Ervik, A., & Hansen, P. K. (2007). Effects of organic effluents from a salmon farm on a fjord system. I. Vertical export and dispersal processes. Aquaculture, 262(2-4), 367-381.

M-608/2016. Pettersen, R. Grenseverdier for klassifisering av vann, sediment og biota. Veileder, M-608/2016. Miljødirektoratet, Oslo/Trondheim. 24 s.

Majewski, W., & Zajaczkowski, M. (2007). Benthic foraminifera in Adventfjorden, Svalbard: Last 50 years of local hydrographic changes. The Journal of Foraminiferal Research, 37(2), 107-124.

Meyers, P. A. (1994). Preservation of elemental and isotopic source identification of sedimentary organic matter. Chemical geology, 114(3-4), 289-302.

Meyers, P. A. (1997). Organic geochemical proxies of paleoceanographic, paleolimnologic, and paleoclimatic processes. Organic geochemistry, 27(5-6), 213-250.

Ministry of Trade, Industry and Fisheries, Law of aquaculture, Chapter III. Environmental considerations. Retrieved February 2, 2018, from https://lovdata.no/dokument/NL/lov/2005-06-17-79

Molvær, J. Knutzen, J., Magnusson, J., Rygg, B., Skei, J., Sørensen, J. 1997. Klassifisering av miljøkvalitet i fjorder og kystvann. Veiledning 97:03. Miljødirektoratets rapportserie TA 1467/1997.

Murray, J. W. (1991). Ecology and distribution of benthic foraminifera. Biology of foraminifera, 221-254.

NGU, Bergrunn, Nasjonal bergrunnsdatabase, Bergrunn N250 med lineamenter. Retrieved September 20, 2018, from http://geo.ngu.no/kart/berggrunn/

NVE Atlas. Aktomhetsområde for snøskred og steinsprang. Retrieved January 10, 2018, from https://atlas.nve.no/Html5Viewer/index.html?viewer=nveatlas#

Nærings- og fiskeridepartementet, Lov om akvakultur, kapittel 3.

Pereira, P. M., Black, K. D., McLusky, D. S., & Nickell, T. D. (2004). Recovery of sediments after cessation of marine fish farm production. Aquaculture, 235(1-4), 315-330.
Rea, B. R., Whalley, W. B., & Raineyº, M. M. (1996). Evidence and implications from some plateaus in northern Norway. Geomorphology, 15, 109-121.

Peters, K. E., Sweeney, R. E., & Kaplan, I. R. (1978). Correlation of carbon and nitrogen stable isotope ratios in sedimentary organic matter 1. Limnology and Oceanography, 23(4), 598-604.

Sjetne, L. B. (2017). Organic carbon accumulation in Hardangerfjorden-A micropaleontological and geochemical study of benthic environmental impact from fish farming (Master's thesis).

Silvert, W., & Sowles, J. W. (1996). Modelling environmental impacts of marine finfish aquaculture. Journal of Applied Ichthyology, 12(2), 75-81.

Skarbøvik, E., Austnes, K., Allan, I., Stålnacke, P., Høgåsen, T., Nemes, A., . . . Beldring, S. (2014). Elvetilførsler og direkte tilførsler til norske kystområder – 2013. Retrieved March 2, 2018, from http://www.miljodirektoratet.no/Documents/publikasjoner/M264/M264.pdf

Stigebrandt, A. (2012). Hydrodynamics and circulation of fjords. In Encyclopedia of lakes and reservoirs (pp. 327-344). Springer, Dordrecht.

Sturt, B. A., Pringle, I. R., & Roberts, D. (1975). Caledonian nappe sequence of Finnmark, northern Norway, and the timing of orogenic deformation and metamorphism. Geological Society of America Bulletin, 86(5), 710-718.

Sætre, R. (Ed.). (2007). The Norwegian coastal current: oceanography and climate. Akademika Pub.

Syvitski, J. P. M., Burrell, D. C., & Skei, J. (1987). Fjords: processes and products. New York: Springer.

Torper, M. (2017). Den historiske utviklingen av organisk karbon og naturtilstanden i dypbassenget til Lurefjorden, Hordaland: En mikropaleontologisk og geokjemisk studie (Master's thesis).

Utarbeidelse av detaljerte faresonekart, Skredfare Loppa. NGI (2014) Dokumentnr: 20130620-01-R.

Norwegian Environmental Agency - Vann-nett.no/portal/waterbody/ecological status. Retrieved February 21, 2018, from https://vann-nett.no/portal/#/waterbody/0420030102-2-C

Valdemarsen, T., Quintana, C. O., Flindt, M. R., & Kristensen, E. (2015). Organic N and P in eutrophic fjord sediments–rates of mineralization and consequences for internal nutrient loading. Biogeosciences, 12(6), 1765-1779.

Norwegian Envirnmental Agency. Veileder 02:2013 – Revised 2015. Klassifisering av miljøtilstand i vann, Økologisk og kjemisk klassifiseringssystem for kystvann, grunnvann, innsjøer og elver.

Velvin, R & B-E. Bye, 2011. Grieg Seafood Finnmark. C-undersøkelse i Øksfjorden, Loppa kommune 2010. Akvaplan-niva rapport 5162

Velvin, R & B-E. Bye, 2012 a. Grieg Seafood Finnmark. C-undersøkelse i Øksfjorden, Loppa kommune 2011. Akvaplan-niva rapport 5573

Velvin, R & B-E. Bye, 2012 b. Grieg Seafood Finnmark. C-undersøkelse i Øksfjorden, Loppa kommune 2012. Akvaplan-niva rapport 6040.01

Velvin, R. & P-A. Emaus, 2008. Grieg Seafood Finnmark. C-undersøkelse i Øksfjorden, Loppa kommune 2008. Akvaplan-niva rapport 4299.

Velvin, R. & P-A. Emaus, 2009. Grieg Seafood Finnmark. C-undersøkelse i Øksfjorden, Loppa kommune 2009. Akvaplan-niva rapport 4743.

Velvin, R. & P-A. Emaus, 2013. Grieg Seafood Finnmark. C-undersøkelse i Øksfjorden, Loppa kommune 2013. Akvaplan-niva rapport 6692.01.

Velvin, R. & P-A. Emaus, 2014. Grieg Seafood Finnmark. C-undersøkelse i Øksfjorden, Loppa kommune 2013. Akvaplan-niva rapport 6692.01.

Velvin, R. & P-A. Emaus, 2015. Grieg Seafood Finnmark. C-undersøkelse i Øksfjorden, Loppa kommune 2014. Akvaplan-niva rapport 7252.01.

Velvin, R. & P-A. Emaus, 2016. Grieg Seafood Finnmark. C-undersøkelse i Øksfjorden, Loppa kommune 2015. Akvaplan-niva rapport 7850.01.

Vågen, H. K. (2018). Temporal changes of the benthic environmental conditions in a subarctic fjord with aquaculture activity-A geochemical and micropaleontological study (Master's thesis).

Appendicies:

Appendix A: Lab report from sediement dating

Radiometric Dating of six marine sediment cores from Kaldfjord and Øksfjord, northern Norway

P.G.Appleby and G.T.Piliposian
Environmental Radioactivity Research Centre
University of Liverpool

Methods

Dating by ^{210}Pb and ^{137}Cs was carried out on marine sediment cores 46-C, D-15 and D-35A from Kaldfjord and D2-6A, D3-3B and D4-36A from Øksfjord, northern Norway. Sub-samples from each core were analysed for ^{210}Pb, ^{226}Ra, and ^{137}Cs by direct gamma assay in the Liverpool University Environmental Radioactivity Laboratory, using Ortec HPGe GWL series well-type coaxial low background intrinsic germanium detectors (Appleby *et al*. 1986). ^{210}Pb was determined via its gamma emissions at 46.5 keV, and ^{226}Ra by the 295 keV and 352 keV γ-rays emitted by its daughter radionuclide ^{214}Pb following 3 weeks storage in sealed containers to allow radioactive equilibration. ^{137}Cs was measured by its emissions at 662 keV. The absolute efficiencies of the detectors were determined using calibrated sources and sediment samples of known activity. Corrections were made for the effect of self-absorption of low energy γ-rays within the sample (Appleby *et al.* 1992).

Results

The results of the radiometric analyses carried out on each core are given in Tables 1–6 and shown graphically in Figures 1.i–6.i. Supported ^{210}Pb activity was assumed to be equal to the measured ^{226}Ra activity, and unsupported ^{210}Pb activity calculated by subtracting supported ^{210}Pb from the measured total ^{210}Pb activity.

Øksfjord Core D2-6A

Lead-210 Activity

^{210}Pb/^{226}Ra equilibrium in this core (240 m water depth) is reached at a depth of around 25 cm (Figure 4.i(a)), similar to that in the Kaldfjord core D-35A. The unsupported ^{210}Pb record (Figure 4.i(b)) is dominated by a major non-monotonic feature between 5-13 cm that coincides almost exactly with a layer of dense sediment that appears to have been laid down during the relatively recent past. Since concentrations below this feature decline more or less exponentially with depth, sedimentation rates prior to this event appear to have been low and relatively uniform. Since concentrations

immediately above are similar to those immediately below, deposition of this layer may well have taken place over a relatively short period of time.

Artificial Fallout Radionuclides

The ^{137}Cs record in this core (Figure 4.i(c)) has two clearly defined peaks, the first between 13-16 cm and the second between 3-5 cm. Since they straddle the dense layer (lying between 5-13 cm), it follows that both may date from the period of maximum ^{137}Cs fallout in the early 1960s. Determining the precise 1963 depth is however complicated by the fact that high sedimentation rates associated with the formation of the dense layer may have distorted the ^{137}Cs record as well as the ^{210}Pb record. The maximum value of the ^{137}Cs/^{210}Pb activity ratio, sometimes a better estimate of the 1963 depth, lies between 7-10 cm.

Core Chronology

^{210}Pb dates calculated using the CRS model place 1963 at a depth of 15.5 cm, in relatively good agreement with suggestion that the deeper ^{137}Cs peak dates from the early 1960s. There are however significant uncertainties about dates either side of this feature. The ^{210}Pb record below 14 cm (below the dense layer) suggests a relatively uniform pre-1963 sedimentation rate, though the value given by the CRS model (0.034 ± 0.004 g cm^{-2} y^{-1}) is significantly lower than the value given by the CIC model (0.051 ± 0.008 g cm^{-2} y^{-1}). Further, whereas the CRS model suggests that the dense layer was associated with a prolonged (~20 year) episode of elevated sedimentation rates, the CIC model suggests that it was laid down over a much shorter period. The presence of relatively high ^{137}Cs concentrations in sediments in the second (3-5 cm) peak supports the latter view. The CRS calculations do however suggest that sedimentation rates were at their most intense over a relatively short (~5 year) period, and that the persistence of high sedimentation rates beyond this period may have been due to other factors such as sediment remobilisation. The chronology shown in Figure 4.ii and given in detail in Table 10 is an attempt to reconcile these various considerations. Because of the large uncertainties the results should however be regarded with some caution unless supported by other independent dating evidence. Information about the causes of the dense layer and their timing would be particularly useful.

Øksfjord Core D3-3B

Lead-210 Activity

This shallower (157 m water depth) core has a relatively short record, ^{210}Pb/^{226}Ra equilibrium being reached at a depth of around 6 cm (Figure 5.i(a)). Unsupported ^{210}Pb activity (Figure 5.i(b)) declines more or less exponentially with depth, though the record does disappear relatively abruptly below 6 cm.

Artificial Fallout Radionuclides

^{137}Cs concentrations in this core (Figure 5.i(c)) are extremely low and significantly above the limit of detection only in the uppermost 5 cm. There is no evidence of a peak recording the 1963 fallout maximum, though this may in part be due to the large standard errors in the measurements.

Core Chronology

^{210}Pb dates calculated using the CRS and CIC models both suggest a relatively constant sedimentation rate, with a mean value of 0.053 ± 0.006 g cm^{-2} y^{-1} (0.06 cm y^{-1}). These results, shown in Figure 5.ii and given in detail in Table 11, place 1963 at a depth of between 3.5-4.0 cm.

References

Appleby PG, 2001. Chronostratigraphic techniques in recent sediments, in *Tracking Environmental Change Using Lake Sediments Volume 1: Basin Analysis, Coring, and Chronological Techniques*, (eds W M Last & J P Smol), Kluwer Academic, pp171-203.

Appleby PG, PJ Nolan, DW Gifford, MJ Godfrey, F Oldfield, NJ Anderson & RW Battarbee, 1986. ^{210}Pb dating by low background gamma counting. *Hydrobiologia*, **141**:21-27.

Appleby PG & F Oldfield, 1978. The calculation of ^{210}Pb dates assuming a constant rate of supply of unsupported ^{210}Pb to the sediment. *Catena*, **5**:1-8

Appleby PG, N Richardson, & PJ Nolan, 1992. Self-absorption corrections for well-type germaniun detectors. *Nucl. Inst.& Methods B*, **71**: 228-233.

Table 4. Fallout radionuclide concentrations in the Øxsfjorden sediment core D2-6A

Depth		^{210}Pb						^{137}Cs	
		Total		Unsupported		Supported			
cm	g cm^{-2}	Bq kg^{-1}	±	Bq kg^{-1}	±	Bq kg^{-1}	±	Bq kg^{-1}	±
0.5	0.1	279.8	8.9	264.9	9.0	14.9	1.3	2.8	0.8
2.5	0.8	350.1	10.3	328.8	10.4	21.3	1.6	2.6	1.1
3.5	1.3	312.4	10.6	294.5	10.8	17.9	1.6	6.2	1.1
4.5	1.8	225.4	7.9	207.3	8.0	18.2	1.2	6.0	0.9
5.5	2.4	153.2	7.4	129.5	7.6	23.7	1.6	4.1	1.0
6.5	3.1	59.3	4.7	39.1	4.8	20.1	1.0	3.1	0.7
8.5	4.6	35.8	4.9	14.6	5.0	21.2	1.1	2.0	0.7

10.5	6.4	24.2	4.3	12.2	4.4	12.0	0.8	0.9	0.4
12.5	8.9	33.4	3.8	19.6	3.9	13.8	0.9	1.5	0.6
14.5	10.4	181.0	9.4	156.5	9.6	24.4	1.7	6.9	1.1
16.5	11.4	121.7	8.3	101.6	8.4	20.2	1.5	2.6	1.0
18.5	12.5	79.5	6.3	59.2	6.5	20.2	1.2	1.1	0.9
21.0	13.8	43.1	4.8	21.9	4.9	21.2	1.0	1.3	0.7
25.0	16.0	18.5	3.6	0.6	3.8	17.9	1.0	0.0	0.0
29.0	18.4	18.4	2.7	-1.6	2.9	20.0	0.9	0.0	0.0
33.0	20.8	18.4	2.9	-1.0	3.0	19.4	0.8	0.2	0.5
37.0	23.2	19.0	2.5	2.0	2.6	17.0	0.7	0.0	0.0

Table 5. Fallout radionuclide concentrations in the Øxsfjorden sediment core D3-3B

Depth		^{210}Pb						^{137}Cs	
		Total		Unsupported		Supported			
cm	g cm^{-2}	Bq kg^{-1}	±	Bq kg^{-1}	±	Bq kg^{-1}	±	Bq kg^{-1}	±
0.5	0.3	171.1	10.6	156.7	10.8	14.4	1.9	2.2	1.1
1.5	0.9	167.6	6.3	150.4	6.4	17.2	1.2	1.8	0.8
2.5	1.7	115.4	8.3	99.5	8.5	15.9	1.6	1.2	1.0
3.5	2.6	63.2	4.8	47.8	4.9	15.4	1.0	1.3	0.6
4.5	3.7	40.2	3.7	26.9	3.8	13.3	0.7	0.7	0.3
5.5	4.8	40.2	3.6	26.3	3.7	13.9	0.7	0.3	0.5
6.5	6.1	15.9	2.1	1.1	2.2	14.8	0.8	0.0	0.0
7.5	7.4	13.5	1.5	0.9	1.6	12.6	0.5	0.3	0.3
8.5	8.7	16.4	1.7	1.4	1.8	15.0	0.5	0.0	0.0
10.5	11.5	14.3	2.5	-1.7	2.7	16.1	0.8	0.1	0.5
12.5	14.2	14.9	1.9	-1.7	2.0	16.5	0.7	0.0	0.0

Table 10. ^{210}Pb chronology of the Øksfjord sediment core D2-6A

Depth		Chronology			Sedimentation Rate		
		Date	Age				
cm	g cm^{-2}	AD	y	±	g cm^{-2} y^{-1}	cm y^{-1}	± (%)
0.0	0.0	2017	0	0			
0.5	0.1	2013	4	1	0.037	0.11	8.3
2.5	0.8	1995	22	3	0.037	0.10	8.3
3.5	1.3	1983	34	4	0.037	0.08	8.3
4.5	1.8	1969	48	4	0.037	0.12	8.3
5.5	2.4	1967	50	4	0.358	0.56	
6.5	3.1	1965	52	4	0.986	1.31	
8.5	4.6	1964	53	4	2.065	2.46	
10.5	6.4	1964	53	4	2.553	2.38	
12.5	8.9	1963	54	4	1.039	1.05	
14.5	10.4	1960	57	4	0.034	0.12	12.4
16.5	11.4	1928	89	6	0.034	0.06	12.4
18.5	12.5	1897	120	9	0.034	0.06	12.4
21.0	13.8	1858	159	13	0.034	0.06	12.4

Table 11. ^{210}Pb chronology of the Øksfjord sediment core D3-3B

Depth		Chronology			Sedimentation Rate		
		Date	Age				
cm	g cm^{-2}	AD	y	±	g cm^{-2} y^{-1}	cm y^{-1}	± (%)
0.0	0.0	2017	0	0			
0.5	0.3	2012	5	2	0.053	0.09	11.8
1.5	0.9	1999	18	3	0.053	0.07	11.8
2.5	1.7	1985	32	5	0.053	0.06	11.8
3.5	2.6	1967	50	7	0.053	0.05	11.8
4.5	3.7	1948	69	9	0.053	0.05	11.8
5.5	4.8	1926	91	12	0.053	0.05	11.8

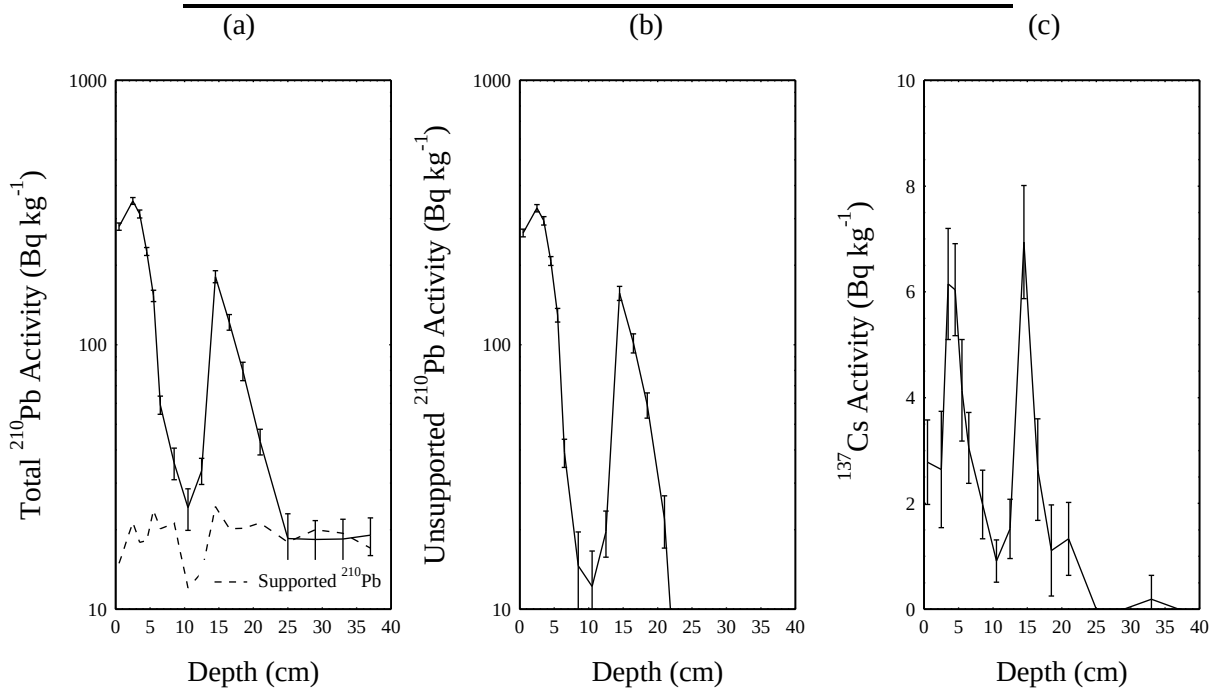

Figure 4.i. Fallout radionuclides in the Øxsfjorden sediment core D2-6A showing (a) total and supported ^{210}Pb, (b) unsupported ^{210}Pb, (c) ^{137}Cs concentrations versus depth.

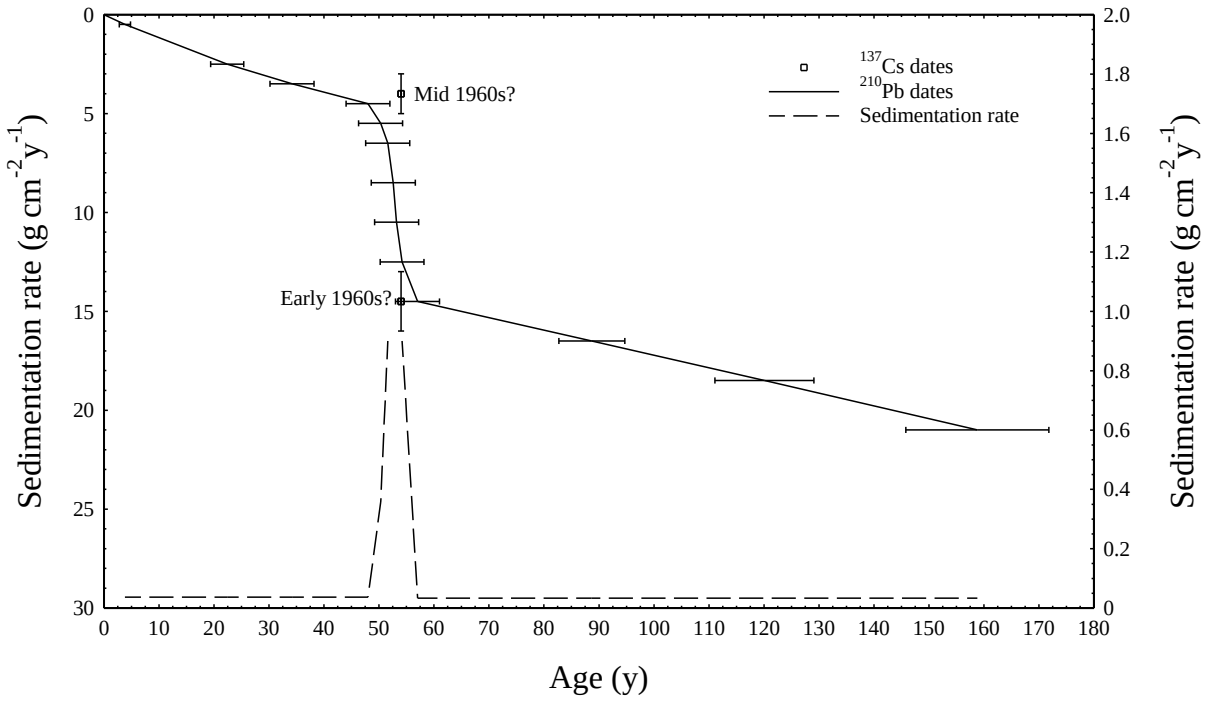

Figure 4.ii. Radiometric chronology of the Øxsfjorden sediment core D2-6A showing the possible ^{210}Pb dates and sedimentation rates, and the 1963 depths suggested by the ^{137}Cs fallout record.

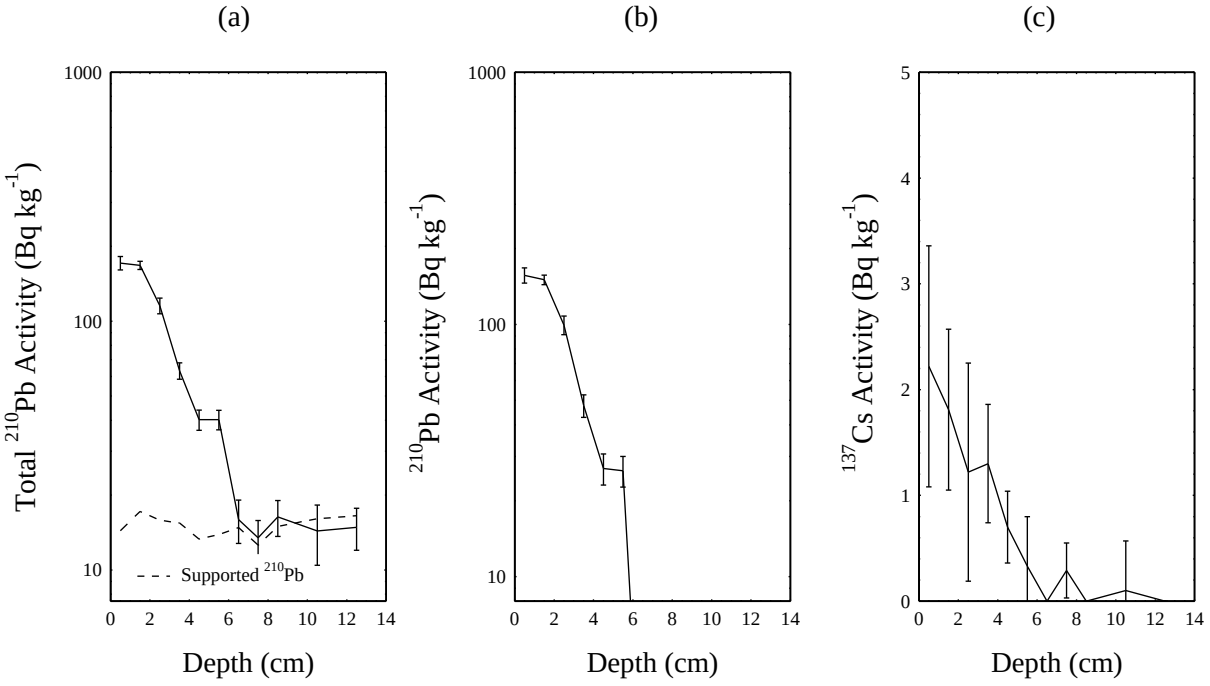

Figure 5.i. Fallout radionuclides in the Øxsfjorden sediment core D3-3B showing (a) total and supported ^{210}Pb, (b) unsupported ^{210}Pb, (c) ^{137}Cs concentrations versus depth.

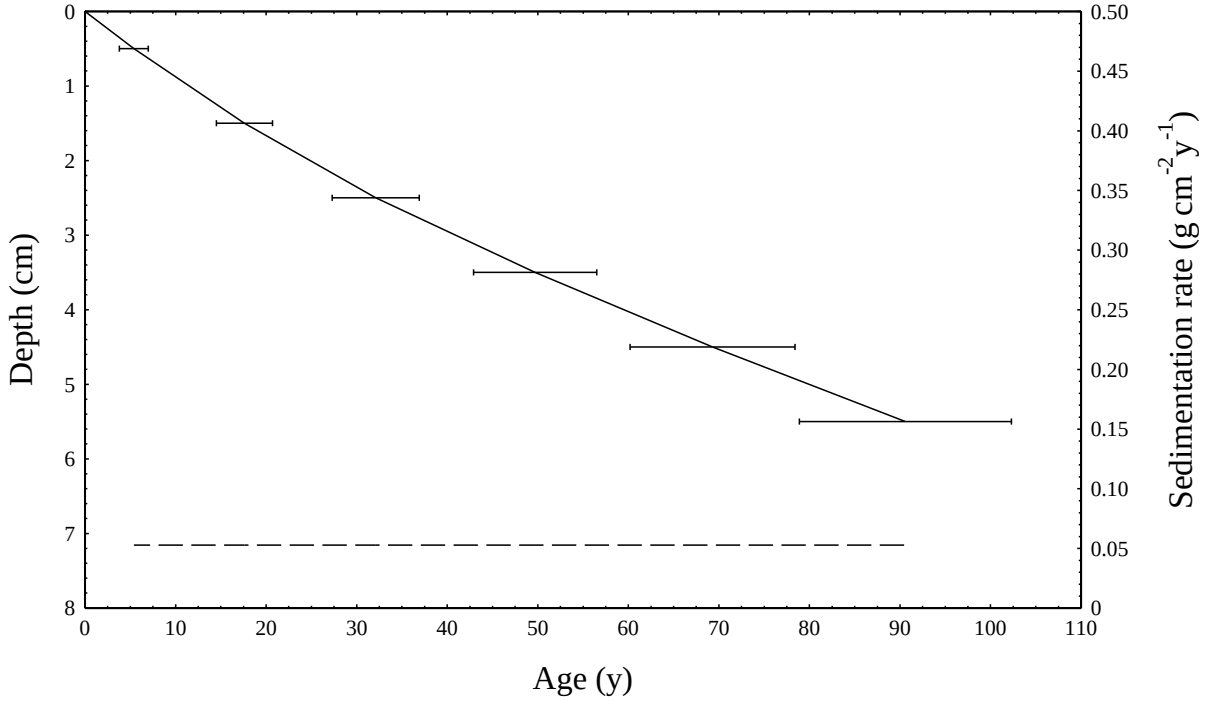

Figure 5.ii. Radiometric chronology of the Øxsfjorden sediment core D3-3B showing the ^{210}Pb dates and sedimentation rates.

Appendix B: Lab report for sediment isotopes

LABORATORY REPORT

Prepared for: University of Oslo	Contact: Dr Silvia Hess
Iso-Analytical Ref. No.: 180109-2	P.O. No.:
Material: Sediment, seaweed, fish food and jellyfish	Analysis: $\delta^{13}C$ and $\delta^{15}N$
Date Arrived: January 9, 2018	Report Date: March 12, 2018
Reported by: Ian Begley	Results File: 180109-2-results.xls

We have completed carbon and nitrogen isotope analysis of the 116 sediment, seaweed, fish food and jellyfish samples received from you on January 9, 2018.

The results for analysis of your samples can be found in the attached MS Excel worksheet with the filename 180109-2-results.xls.

Nitrogen isotope analysis of sediment samples

The technique used for nitrogen isotope analysis of your sediment samples was Elemental Analyser - Isotope Ratio Mass Spectrometry (EA-IRMS).

In brief, tin capsules containing sample or reference material are loaded into an auto-sampler on a Europa Scientific elemental analyser. From where they were dropped in sequence into a furnace held at 1000°C, where they are combusted in an oxygen rich environment, raising the temperature in the region of the sample to ~1700 °C. The gases produced on combustion are swept in a helium stream over combustion catalyst (Cr_2O_3), copper oxide wires to oxidize hydrocarbons and silver wool to remove sulfur and halides. The resultant gases, N_2, NO_x, H_2O, O_2 and CO_2 are swept through a reduction stage of pure copper wires held at 600 °C. This step removes O_2 and converts NO_x species to N_2. A magnesium perchlorate chemical trap is used to remove H_2O and a carbosorb trap used to remove CO_2. Nitrogen is resolved using a packed column gas chromatograph held at an isothermal temperature of 100 °C. The resultant chromatographic peak for N_2 enters the ion source of a Europa Scientific 20-20 IRMS where it is ionized and accelerated. Gas species of different mass are separated in a magnetic field then simultaneously measured using a Faraday cup collector array to measure the isotopomers of N_2 at m/z 28, 29, and 30.

Both references and samples are converted to N_2 and analysed using this method. The analysis proceeds in a batch process by which a reference is analysed followed by a number of samples and then another reference.

The reference material used during $\delta^{15}N$ analysis of your sediment samples was IA-R001 (wheat flour, $\delta^{15}N_{AIR}$ = 2.55 ‰). For quality control purposes check samples of IA-R001, IA-

R045 (ammonium sulfate, $\delta^{15}N_{AIR}$ = -4.71 ‰) and IA-R046 (ammonium sulfate, $\delta^{15}N_{AIR}$ = 22.04 ‰) were analysed during batch analysis of your samples.

IA-R001, IA-R045 and IA-R046 are calibrated against and traceable to IAEA-N-1 (ammonium sulfate, $\delta^{15}N_{AIR}$ = 0.4 ‰). IAEA-N-1 is an inter-laboratory comparison standard distributed by the International Atomic Energy Agency (IAEA), Vienna.

The measured □^{15}N values for the check samples are provided in the results file.

Carbon isotope analysis of sediment samples

Prior to carbon isotope analysis of your sediment samples it was necessary to remove the inorganic carbonate. Samples were acidified with 1M hydrochloric acid and left overnight to allow the inorganic carbon to be liberated as CO_2. The samples were then neutralized by repetitively washing with distilled water and subsequently oven dried at 60 °C in readiness for □^{13}C analysis.

The technique used for carbon isotope analysis of your sediment samples was Elemental Analyser - Isotope Ratio Mass Spectrometry (EA-IRMS).

In brief, tin capsules containing sample or reference material are loaded into an auto-sampler on a Europa Scientific elemental analyser. From where they were dropped in sequence into a furnace held at 1000°C, where they are combusted in an oxygen rich environment, raising the temperature in the region of the sample to ~1700 °C. The gases produced on combustion are swept in a helium stream over combustion catalyst (Cr_2O_3), copper oxide wires to oxidize hydrocarbons and silver wool to remove sulfur and halides. The resultant gases, N_2, NO_x, H_2O, O_2 and CO_2 are swept through a reduction stage of pure copper wires held at 600 °C. This step removes O_2 and converts NO_x species to N_2. A magnesium perchlorate chemical trap removes water. Carbon dioxide is separated from nitrogen by a packed column gas chromatograph held at an isothermal temperature of 100 °C. The resultant CO_2 chromatographic peak enters the ion source of the Europa Scientific 20-20 IRMS where it is ionised and accelerated. Gas species of different mass are separated in a magnetic field then simultaneously measured using a Faraday cup collector array to measure the isotopomers of CO_2 at m/z 44, 45, and 46.

Both references and samples are converted and analysed in this manner. The analysis proceeds in a batch process, whereby a reference is analysed followed by a number of samples and then another reference.

The reference material used during $\delta^{13}C$ analysis of your sediment samples was IA-R001 (wheat flour, $\delta^{13}C_{V\text{-}PDB}$ = of -26.43 ‰). For quality control purposes check samples of IA-R001, IA-R005 (beet sugar, $\delta^{13}C_{V\text{-}PDB}$ = -26.03 ‰) and IA-R006 (cane sugar, $\delta^{13}C_{V\text{-}PDB}$ = -11.64 ‰) were analysed during batch analysis of your samples.

IA-R001, IA-R005 and IA-R006 are calibrated against and traceable to IAEA-CH-6 (sucrose, $\delta^{13}C_{V\text{-}PDB}$ = -10.43 ‰). IAEA-CH-6 is an inter-laboratory comparison standard distributed by the International Atomic Energy Agency (IAEA), Vienna.

The measured $\delta^{13}C$ values for the check samples are provided in the results file.

Carbon and nitrogen isotope analysis of tissue samples

Carbon and nitrogen isotope analysis of your seaweed, fish food and jellyfish samples was undertaken by Elemental Analysis - Isotope Ratio Mass Spectrometry (EA-IRMS).

In this technique, samples and references are weighed into tin capsules, sealed, and loaded into an auto-sampler on a Europa Scientific elemental analyser. From where they are dropped in sequence into a furnace held at 1000 °C and combusted in the presence of oxygen. The tin capsules flash combust, raising the temperature in the region of the sample to ~1700 °C. The combusted gases are swept in a helium stream over combustion catalyst (Cr_2O_3), copper oxide wires (to oxidize hydrocarbons), and silver wool to remove sulfur and halides. The resultant gases, N_2, NO_x, H_2O, O_2, and CO_2 are swept through a reduction stage of pure copper wires held at 600 °C. This removes any oxygen and converts NO_x species to N_2. A magnesium perchlorate chemical trap is used to remove water. Nitrogen and carbon dioxide are separated using a packed column gas chromatograph held at a constant temperature of 65 °C. The resultant nitrogen peak enters the ion source of the Europa Scientific 20-20 IRMS first, where it is ionized and accelerated. Nitrogen gas species of different mass are separated in a magnetic field then simultaneously measured using a Faraday cup collector array to measure the isotopomers of N_2 at *m/z* 28, 29, and 30. After a delay the carbon dioxide peak enters the ion source and is ionized and accelerated. Carbon dioxide gas species of different mass are separated in a magnetic field then simultaneously measured using a Faraday cup collector array to measure the isotopomers of CO_2 at *m/z* 44, 45, and 46.

Both references and samples are converted to N_2 and CO_2 and analysed using this method. The analysis proceeds in a batch process by which a reference is analysed followed by a number of samples and then another reference.

The reference material used for $\delta^{13}C$ and $\delta^{15}N$ analysis of your samples was IA-R068 (soy protein, $\delta^{13}C_{V\text{-}PDB}$ = -25.22 ‰, $\delta^{15}N_{AIR}$ = 0.99 ‰).

IA-R068, IA-R038 (L-alanine, $\delta^{13}C_{V\text{-}PDB}$ = -24.99 ‰, $\delta^{15}N_{AIR}$ = -0.65 ‰) and a mixture of IAEA-C7 (oxalic acid, $\delta^{13}C_{V\text{-}PDB}$ = -14.48 ‰) and IA-R046 (ammonium sulfate, $\delta^{15}N_{AIR}$ = 22.04 ‰) were run as quality control check samples during analysis of your samples.

IA-R068 and IA-R038 are calibrated against and traceable to IAEA-CH-6 (sucrose, $\delta^{13}C_{V\text{-}PDB}$ = -10.43 ‰) and IAEA-N-1 (ammonium sulfate, $\delta^{15}N_{AIR}$ = 0.40 ‰). IA-R046 is calibrated against and traceable to IAEA-N-1. IAEA-C7, IAEA-CH-6 and IAEA-N-1 are inter-laboratory comparison standards distributed by the International Atomic Energy Agency, Vienna.

The $\delta^{13}C$ and $\delta^{15}N$ results for the check samples are included in the tabulated results.

Appendix C: Results from geochemical analysis

D2-6A

Core interval (cm)	Core depth (cm)	Sediment age (years AD)	Water content (%)	Sand content (% > 63 µm)	TOC (%)	nTOC (%)	TN (%)	C/N	d13CVPDB (‰)	d15NAir (‰)
0-1	0,5	2013	76,3	6,2	2,7	2,8	0,42	6,3	-22,67	5,3
1-2	1,5	2004	71,3	10,5	2,7	2,9	0,42	6,3	-22,45	5,3
2-3	2,5	1995	67,8	7,9	2,6	2,8	0,41	6,4	-22,41	5,2
3-4	3,5	1983	63,8	6,9	2,4	2,5	0,37	6,5	-22,35	5,3
4-5	4,5	1969	58,9	8,0	2,0	2,2	0,31	6,5	-22,36	5,3
5-6	5,5	1967	53,9	4,6	1,6	1,7	0,25	6,6	-22,35	5,3
6-7	6,5	1965	49,4	3,7	1,0	1,1	0,15	6,9	-22,18	5,3
7-8	7,5	1965	46,2	3,8	0,9	0,9	0,13	6,7	-22,17	5,3
8-9	8,5	1964	47,3	5,0	0,9	1,0	0,13	6,9	-22,30	5,5
9-10	9,5	1964	43,6	5,7	0,8	0,9	0,12	6,7	-22,35	5,7
10-11	10,5	1964	34,8	25,6	0,7	1,2	0,09	7,8	-23,20	5,2
11-12	11,5	1964	25,2	71,9	0,2	1,5	0,03	7,3	-22,18	5,5
12-13	12,5	1963	33,5	29,0	0,9	1,4	0,11	8,3	-22,28	5,5
13-14	13,5	1962	54,4	13,2	2,3	2,5	0,34	6,7	-21,95	5,1
14-15	14,5	1960	60,5	32,2	3,1	3,7	0,47	6,7	-22,03	5,1
15-16	15,5	1944	59,5	25,7	3,2	3,6	0,46	7,0	-21,89	5,0
16-17	16,5	1928	59,0	18,9	3,1	3,4	0,47	6,5	-21,80	5,0
17-18	17,5	1912	60,1	24,8	3,3	3,8	0,48	6,9	-21,81	5,1
18-19	18,5	1897	60,7	24,5	3,2	3,6	0,47	6,8	-21,74	5,1
19-20	19,5	ND	60,6							
20-22	21,0	ND	59,8							
22-24	23,0	ND	58,6							
24-26	25,0	ND	57,6							
26-28	27,0	ND	57,0							
28-30	29,0	ND	56,5							
30-32	31,0	ND	56,4							
32-34	33,0	ND	56,4							
34-36	35,0	ND	55,8							
36-38	37,0	ND	55,2							
38-40	39,0	ND	54,3							
40-42	41,0	ND	55,3							

Core interval	Cu (mg/kg)	Zn (mg/kg)	Cd (mg/kg)	Pb (mg/kg)	Hg* (mg/kg)
0-1	39,4	79,2	0,06	16,6	0,34
1-2	39,5	80,5	0,10	16,5	0,32
2-3	42,2	86,2	0,11	17,4	0,36
3-4	46,0	92,7	0,12	18,4	0,32
4-5	47,5	91,6	0,10	18,3	0,32
5-6	44,5	73,6	0,10	13,4	0,23
6-7	46,5	65,0	0,14	8,8	0,12
7-8	49,7	66,3	0,16	8,1	0,09
8-9	45,8	61,5	0,13	7,5	0,10
9-10	37,4	49,6	0,10	5,9	0,08
10-11	22,7	31,9	0,10	4,1	0,07
11-12	10,8	19,5	0,07	2,1	0,06
12-13	21,9	40,6	0,08	7,1	0,12
13-14	37,5	81,0	0,08	21,0	0,28
14-15	38,8	95,7	0,08	28,7	0,40
15-16	37,5	91,7	0,11	26,5	0,38
16-17	38,6	93,2	0,13	25,4	0,38
17-18	38,2	92,1	0,16	24,3	0,32
18-19	39,7	94,0	0,21	24,7	0,38

Background
Good
Moderate
Poor
Bad

D3-3B										
Core interval (cm)	**Core depth (cm)**	**Sediment age (years AD)**	**Water content (%)**	**Sand content (% > 63 µm)**	**TOC (%)**	**nTOC (%)**	**TN (%)**	**C/N**	**d13CVPDB (‰)**	**d15NAir (‰)**
0-1	0,5	2012	57,6	22,8	1,3	1,7	0,24	5,3	-22,81	5,2
1-2	1,5	1999	50,4	25,7	1,2	1,7	0,21	5,6	-22,69	5,1
2-3	2,5	1985	45,2	32,6	1,2	1,7	0,18	5,8	-22,45	5,1
3-4	3,5	1967	37,0	38,2	0,8	1,5	0,13	6,3	-22,20	5,1
4-5	4,5	1948	36,3	38,7	0,7	1,4	0,12	5,8	**-21,95**	5,1
5-6	5,5	1926	30,5	41,9	0,7	1,4	0,10	6,5	-22,02	5,2
6-7	6,5	ND	28,0	45,0	0,5	1,3	0,09	5,3	-22,06	5,2
7-8	7,5	ND	27,1	42,6	0,5	1,2	0,09	5,0	-21,90	5,3
8-9	8,5	ND	25,6	40,2	0,5	1,2	0,10	5,2	-21,98	5,1
9-10	9,5	ND	25,2	42,4	0,5	1,3	0,09	5,6	**-21,79**	5,1
10-11	10,5	ND	24,5	39,4	0,5	1,2	0,08	6,3	-21,96	5,1
11-12	11,5	ND	25,8	36,7	0,6	1,2	0,09	6,5	-22,44	5,1
12-13	12,5	ND	25,8	38,5	0,4	1,1	0,08	4,8	-21,69	5,3
13-14	13,5	ND	24,3	39,0	0,5	1,2	0,07	7,1	**-22,02**	5,4

Core interval (cm)	**Cu (mg/kg)**	**Zn (mg/kg)**	**Cd (mg/kg)**	**Pb (mg/kg)**	**Hg* (mg/kg)**
0-4 cm 1st analysis					
0-1	19,1	39,2	0,04	7,3	0,19
1-2	21,4	45,3	0,07	8,8	0,25
2-3	15,5	37,0	0,06	7,9	0,17
3-4	13,0	32,7	0,06	7,7	0,15
0-4 cm 2nd analysis					
0-1	19,3	40,5	0,05	8,0	0,24
1-2	22,8	49,8	0,07	9,9	0,25
2-3	25,5	60,9	0,08	13,5	0,27
3-4	14,8	37,5	0,07	9,1	0,18
0-4 cm 3rd analysis					
0-1	20,8	42,8	0,12	7,8	0,59
1-2	16,4	34,9	0,21	6,5	0,67
2-3	10,4	24,5	0,13	5,1	0,54
3-4	11,7	29,9	0,06	6,6	0,65
Final results (Mean of 1st, 2nd and 3rdanalysis 0-4 cm and first analysis of 4-14 cm)					
0-1	19,7	40,9	0,07	7,7	0,34
1-2	20,2	43,3	0,11	8,4	0,39
2-3	17,1	40,8	0,09	8,8	0,33
3-4	13,1	33,4	0,07	7,8	0,33
4-5	11,4	27,5	0,04	6,3	0,11
5-6	10,1	23,3	0,04	5,0	0,10
6-7	8,8	19,1	0,05	3,5	0,08
7-8	9,5	21,7	0,06	3,6	0,08
8-9	9,3	19,0	0,07	3,0	0,05
9-10	9,4	19,0	0,07	2,6	0,07
10-11	9,7	20,1	0,08	2,5	0,06
11-12	11,2	23,2	0,10	2,7	0,04
12-13	9,9	20,3	0,07	2,5	0,06
13-14	10,4	21,4	0,08	2,6	0,05

Appendix E: Foraminifera data, total individual counts

Øksfjord cores	Counts										
>63 µm			D2-6A					D3-3B			
Sediement depth (cm)	0,5	1,5	2,5	5,5	11,5	16,5	0,5	1,5	2,5	5,5	11,5
Sediment age (years AD)	2013	2007	1995	1967	1963	1928	2012	1999	1985	1926	ND
Sediment interval (cm)	0-1	1-2	2-3	5-6	11-12	16-17	0-1	1-2	2-3	5-6	11-12
Adercotryma glomeratum/wrighti	12	7	11	13	0	5	5	13	16	4	1
Ammoscalaria tenuimargo	0	0	0	0	0	0	0	5	3	1	0
Crobostomoides cassimargo	0	0	0	0	0	0	0	0	2	2	0
Cribrostomoides jeffreysii	0	0	0	0	0	0	2	3	2	0	0
Crobostomoides sp	0	0	0	0	0	0	0	0	2	0	0
Eggerella europea	1	0	1	0	0	0	1	1	0	0	0
Eggerelloides medius	4	4	3	4	0	2	9	6	10	2	1
Haplophragmoides bradyi	0	1	0	0	0	0	0	0	0	0	0
Haplophragmoides sphaeriloculum	0	0	1	0	0	1	3	6	1	4	0
Lagenammina arenulata	0	0	0	0	0	0	0	0	5	3	0
Lagenammina difflugiformis	0	0	0	2	1	0	0	0	0	0	0
Psammosphaere sp	1	0	0	0	0	0	0	0	0	0	0
Revurvoides contortus	0	0	2	5	0	1	0	9	8	7	2
Recurvoides laevigatum	15	7	0	0	0	0	0	0	0	0	0
Reophax fusiformis	2	3	0	0	0	0	0	1	0	3	0
Reophax rostrata	1	0	0	4	0	0	0	0	0	0	0
Reophax sp.	0	1	0	0	0	2	0	0	0	6	0
Reophax scorpiurus	0	4	0	0	0	0	9	1	0	0	0
Spiroplectammina biformis	0	0	17	1	0	1	10	14	4	0	0
Textularia contorta	1	1	1	0	0	0	0	1	0	1	0
Textularia earlandi	23	18	41	3	0	1	20	15	7	4	0
Textularia kattegatensis	0	0	0	0	0	0	0	1	1	0	0
Tritaxis conica	0	0	0	0	0	0	2	4	7	0	0
Trochammina globigeriniformis	0	0	0	0	0	0	2	0	2	1	0
Trochammina sp.	0	0	0	0	0	0	0	4	2	0	1
Astrononion gallowayi	2	2	12	1	2	2	0	0	0	1	2
Bolivina sp.	0	0	0	0	0	1	0	0	0	0	0
Bolivinellina pseudopunctata	3	6	9	5	3	9	11	4	0	1	0
Brizalina skagerrakensis	48	15	11	10	0	1	1	0	0	0	0
Buccella frigida	1	0	0	0	1	0	0	3	3	18	15
Bulimina marginata	44	35	31	73	22	10	48	47	54	46	28
Bulimina sp	0	0	0	0	0	0	1	0	0	0	0
Cassidulina laevigata	19	16	27	51	9	44	10	10	1	8	0
Cassidulina neoteretis	0	0	0	0	0	0	0	0	0	0	4
Cassidulina reniforme	22	33	50	26	25	60	6	9	5	17	55
Cassidulinoides bradyi	1	0	1	0	0	0	0	0	0	0	0
Cibicidoides bradyi	0	1	0	0	0	0	0	0	0	0	0
Cibicidoides mundulus	0	0	0	3	0	0	0	0	0	0	0
Cibicidoides sp	0	0	0	0	0	0	0	0	0	2	0
Cibicides lobatulus	19	4	8	0	3	0	1	2	2	0	1
Cibicides praecinctus	0	0	0	0	0	0	0	0	0	0	1
Cibicides refulgens	10	7	5	0	97	12	2	4	0	1	3
Cornuspira involvens	0	1	0	0	0	0	0	0	0	0	0
Cyclogyra invovlens	0	0	0	0	0	0	0	0	1	0	0
Discorbinella bertheloti	0	2	1	3	4	5	1	0	0	0	0
Elphidium albiumbilicatum	0	0	0	0	3	1	3	1	1	1	7
Elphidium excavatum	2	3	1	0	4	1	1	1	2	3	15
Elphidium sp.	0	1	1	0	0	1	1	0	0	2	1
Elphidium subarctica	0	4	1	0	3	5	2	3	2	0	0
Epistominella vitrea	3	11	34	0	3	2	5	7	1	2	3
Fissurina sp	0	0	0	0	2	0	0	0	0	0	0
Gavelinopsis praegeri	0	0	0	1	0	1	0	0	0	0	0
Globobuliminia turgida	9	5	3	11	1	5	0	0	0	1	0
Hyalinea balthica	12	7	10	36	17	15	12	10	5	9	31
Islandiella islandica	0	0	1	0	2	1	0	0	4	1	3
Lagena distoma	0	0	0	0	0	0	1	0	0	2	0
Lagena globosa	0	0	1	0	0	0	0	0	0	0	0
Lagena laevis	1	0	1	0	0	0	0	0	0	0	0
Lagena striata	0	0	0	0	1	0	0	0	0	0	0
Lagena sp.	0	0	0	0	0	1	0	0	0	0	0
Lenticulina sp.	0	1	0	0	0	0	0	0	0	0	0
Melonis barleeanum	0	2	0	0	2	0	0	0	0	0	1
Nonionella auricula	0	0	0	0	0	5	0	0	0	0	0
Nonionella iridea	1	8	0	6	1	0	1	0	1	0	0
Nonionella turgida	0	0	0	0	0	0	0	0	2	2	0
Nonionellina labradorica	14	17	24	12	3	7	6	5	4	9	7
Pullenia osloensis	22	39	64	0	4	31	13	13	4	6	14
Quinqueloculina sp.	1	0	0	5	0	0	0	0	0	0	0
Quinqueloculina stalkeri	0	1	1	0	0	1	0	0	0	0	0
Stainforthia concava	3	4	3	0	1	9	2	4	2	9	5
Stainforthia fusiformis + feylingi	23	32	60	11	6	42	32	49	37	27	11
Trifarina angulosa	1	3	3	0	27	1	0	1	6	7	3
Triloculina oblonga	0	0	1	0	0	0	0	0	0	0	0
calc unidetified	0	0	0	0	0	0	0	0	0	2	1
Sum picked	324	306	441	286	248	286	223	257	209	215	216
Ind / g sediment	1612	1798	3350	2419	2794	1208	3338	2410	2480	315	522
BFAR (ind/cm2/yr)	425,9	481,0	1047,6	123,1	2,4	190,9	176,9	127,7	131,4	16,7	
# species	32	35	34	22	27	33	31	32	34	35	25
%-calcareous tests	81,5	85,0	82,5	88,8	99,6	95,5	71,7	67,3	65,6	82,3	97,7
%-agglutinated tests	18,5	15,0	17,5	11,2	0,4	4,5	28,3	32,7	34,4	17,7	2,3
ES(100)	22,0	25,8	20,8	18,0	19,7	21,5	23,7	25,0	27,9	28,1	19,8
H'(log2)	4,12	4,31	4,00	3,50	3,29	3,78	4,02	4,12	4,10	4,32	3,63

Appendix E: Foraminifera data, concentration of tests (individuals/g sediment)

Øksfjord cores	Individuals per gram										
>63 µm			D2-6A					D3-3B			
Sediement depth (cm)	0,5	1,5	2,5	5,5	11,5	16,5	0,5	1,5	2,5	5,5	11,5
Sediment age (years AD)	2013	2007	1995	1967	1963	1928	2012	1999	1985	1926	ND
Sediment interval (cm)	0-1	1-2	2-3	5-6	11-12	16-17	0-1	1-2	2-3	5-6	11-12
Adercotryma glomeratum/wrighti	59,70	41,13	83,55	109,95	0,00	21,11	74,84	121,92	189,85	5,87	2,42
Ammoscalaria tenuimargo	0,00	0,00	0,00	0,00	0,00	0,00	0,00	46,89	35,60	1,47	0,00
Crobostomoides cassimargo	0,00	0,00	0,00	0,00	0,00	0,00	0,00	0,00	23,73	2,93	0,00
Cribrostomoides jeffreysii	0,00	0,00	0,00	0,00	0,00	0,00	29,94	28,13	23,73	0,00	0,00
Crobostomoides sp	0,00	0,00	0,00	0,00	0,00	0,00	0,00	0,00	23,73	0,00	0,00
Eggerella europea	4,98	0,00	7,60	0,00	0,00	0,00	14,97	9,38	0,00	0,00	0,00
Eggerelloides medius	19,90	23,50	22,79	33,83	0,00	8,44	134,72	56,27	118,66	2,93	2,42
Haplophragmoides bradyi	0,00	5,88	0,00	0,00	0,00	0,00	0,00	0,00	0,00	0,00	0,00
Haplophragmoides sphaeriloculum	0,00	0,00	7,60	0,00	0,00	4,22	44,91	56,27	11,87	5,87	0,00
Lagenammina arenulata	0,00	0,00	0,00	0,00	0,00	0,00	0,00	0,00	59,33	4,40	0,00
Lagenammina difflugiformis	0,00	0,00	0,00	16,92	11,27	0,00	0,00	0,00	0,00	0,00	0,00
Psammosphaere sp	4,98	0,00	0,00	0,00	0,00	0,00	0,00	0,00	0,00	0,00	0,00
Revurvoides contortus	0,00	0,00	15,19	42,29	0,00	4,22	0,00	84,40	94,93	10,27	4,83
Recurvoides laevigatum	74,63	41,13	0,00	0,00	0,00	0,00	0,00	0,00	0,00	0,00	0,00
Reophax fusiformis	9,95	17,63	0,00	0,00	0,00	0,00	0,00	9,38	0,00	4,40	0,00
Reophax rostrata	4,98	0,00	0,00	33,83	0,00	0,00	0,00	0,00	0,00	0,00	0,00
Reophax sp.	0,00	5,88	0,00	0,00	0,00	8,44	0,00	0,00	0,00	8,80	0,00
Reophax scorpiurus	0,00	23,50	0,00	0,00	0,00	0,00	134,72	9,38	0,00	0,00	0,00
Spiroplectammina biformis	0,00	0,00	129,12	8,46	0,00	4,22	149,69	131,29	47,46	0,00	0,00
Textularia contorta	4,98	5,88	7,60	0,00	0,00	0,00	0,00	9,38	0,00	1,47	0,00
Textularia earlandi	114,43	105,75	311,41	25,37	0,00	4,22	299,38	140,67	83,06	5,87	0,00
Textularia kattegatensis	0,00	0,00	0,00	0,00	0,00	0,00	0,00	9,38	11,87	0,00	0,00
Tritaxis conica	0,00	0,00	0,00	0,00	0,00	0,00	29,94	37,51	83,06	0,00	0,00
Trochammina globigeriniformis	0,00	0,00	0,00	0,00	0,00	0,00	29,94	0,00	23,73	1,47	0,00
Trochammina sp.	0,00	0,00	0,00	0,00	0,00	0,00	0,00	37,51	23,73	0,00	2,42
Astrononion gallowayi	9,95	11,75	91,14	8,46	22,53	8,44	0,00	0,00	0,00	1,47	4,83
Bolivina sp.	0,00	0,00	0,00	0,00	0,00	4,22	0,00	0,00	0,00	0,00	0,00
Bolivinellina pseudopunctata	14,93	35,25	68,36	42,29	33,80	38,00	164,66	37,51	0,00	1,47	0,00
Brizalina skagerrakensis	238,81	88,13	83,55	84,58	0,00	4,22	14,97	0,00	0,00	0,00	0,00
Buccella frigida	4,98	0,00	0,00	0,00	11,27	0,00	0,00	28,13	35,60	26,41	36,25
Bulimina marginata	218,91	205,63	235,46	617,41	247,87	42,22	718,50	440,77	640,76	67,49	67,67
Bulimina sp	0,00	0,00	0,00	0,00	0,00	0,00	14,97	0,00	0,00	0,00	0,00
Cassidulina laevigata	94,53	94,00	205,07	431,34	101,40	185,78	149,69	93,78	11,87	11,74	0,00
Cassidulina neoteretis	0,00	0,00	0,00	0,00	0,00	0,00	0,00	0,00	0,00	0,00	9,67
Cassidulina reniforme	109,45	193,88	379,77	219,90	281,67	253,33	89,81	84,40	59,33	24,94	132,93
Cassidulinoides bradyi	4,98	0,00	7,60	0,00	0,00	0,00	0,00	0,00	0,00	0,00	0,00
Cibicidoides bradyi	0,00	5,88	0,00	0,00	0,00	0,00	0,00	0,00	0,00	0,00	0,00
Cibicidoides mundulus	0,00	0,00	0,00	25,37	0,00	0,00	0,00	0,00	0,00	0,00	0,00
Cibicidoides sp	0,00	0,00	0,00	0,00	0,00	0,00	0,00	0,00	0,00	2,93	0,00
Cibicides lobatulus	94,53	23,50	60,76	0,00	33,80	0,00	14,97	18,76	23,73	0,00	2,42
Cibicides praecinctus	0,00	0,00	0,00	0,00	0,00	0,00	0,00	0,00	0,00	0,00	2,42
Cibicides refulgens	49,75	41,13	37,98	0,00	1092,87	50,67	29,94	37,51	0,00	1,47	7,25
Cornuspira involvens	0,00	5,88	0,00	0,00	0,00	0,00	0,00	0,00	0,00	0,00	0,00
Cyclogyra invovlens	0,00	0,00	0,00	0,00	0,00	0,00	0,00	0,00	11,87	0,00	0,00
Discorbinella bertheloti	0,00	11,75	7,60	25,37	45,07	21,11	14,97	0,00	0,00	0,00	0,00
Elphidium albiumbilicatum	0,00	0,00	0,00	0,00	33,80	4,22	44,91	9,38	11,87	1,47	16,92
Elphidium excavatum	9,95	17,63	7,60	0,00	45,07	4,22	14,97	9,38	23,73	4,40	36,25
Elphidium sp.	0,00	5,88	7,60	0,00	0,00	4,22	14,97	0,00	0,00	2,93	2,42
Elphidium subarctica	0,00	23,50	7,60	0,00	33,80	21,11	29,94	28,13	23,73	0,00	0,00
Epistominella vitrea	14,93	64,63	258,24	0,00	33,80	8,44	74,84	65,65	11,87	2,93	7,25
Fissurina sp	0,00	0,00	0,00	0,00	22,53	0,00	0,00	0,00	0,00	0,00	0,00
Gavelinopsis praegeri	0,00	0,00	0,00	8,46	0,00	4,22	0,00	0,00	0,00	0,00	0,00
Globobuliminia turgida	44,78	29,38	22,79	93,03	11,27	21,11	0,00	0,00	0,00	1,47	0,00
Hyalinea balthica	59,70	41,13	75,95	304,48	191,53	63,33	179,63	93,78	59,33	13,20	74,92
Islandiella islandica	0,00	0,00	7,60	0,00	22,53	4,22	0,00	0,00	47,46	1,47	7,25
Lagena distoma	0,00	0,00	0,00	0,00	0,00	0,00	14,97	0,00	0,00	2,93	0,00
Lagena globosa	0,00	0,00	7,60	0,00	0,00	0,00	0,00	0,00	0,00	0,00	0,00
Lagena laevis	4,98	0,00	7,60	0,00	0,00	0,00	0,00	0,00	0,00	0,00	0,00
Lagena striata	0,00	0,00	0,00	0,00	11,27	0,00	0,00	0,00	0,00	0,00	0,00
Lagena sp.	0,00	0,00	0,00	0,00	0,00	4,22	0,00	0,00	0,00	0,00	0,00
Lenticulina sp.	0,00	5,88	0,00	0,00	0,00	0,00	0,00	0,00	0,00	0,00	0,00
Melonis barleeanum	0,00	11,75	0,00	0,00	22,53	0,00	0,00	0,00	0,00	0,00	2,42
Nonionella auricula	0,00	0,00	0,00	0,00	0,00	21,11	0,00	0,00	0,00	0,00	0,00
Nonionella iridea	4,98	47,00	0,00	50,75	11,27	0,00	14,97	0,00	11,87	0,00	0,00
Nonionella turgida	0,00	0,00	0,00	0,00	0,00	0,00	0,00	0,00	23,73	2,93	0,00
Nonionellina labradorica	69,65	99,88	182,29	101,49	33,80	29,56	89,81	46,89	47,46	13,20	16,92
Pullenia osloensis	109,45	229,13	486,10	0,00	45,07	130,89	194,59	121,92	47,46	8,80	33,84
Quinqueloculina sp.	4,98	0,00	0,00	42,29	0,00	0,00	0,00	0,00	0,00	0,00	0,00
Quinqueloculina stalkeri	0,00	5,88	7,60	0,00	0,00	4,22	0,00	0,00	0,00	0,00	0,00
Stainforthia concava	14,93	23,50	22,79	0,00	11,27	38,00	29,94	37,51	23,73	13,20	12,08
Stainforthia fusiformis + feylingi	114,43	188,00	455,72	93,03	67,60	177,33	479,00	459,53	439,04	39,61	26,59
Trifarina angulosa	4,98	17,63	22,79	0,00	304,20	4,22	0,00	9,38	71,20	10,27	7,25
Triloculina oblonga	0,00	0,00	7,60	0,00	0,00	0,00	0,00	0,00	0,00	0,00	0,00
calc unidetified	0,00	0,00	0,00	0,00	0,00	0,00	0,00	0,00	0,00	2,93	2,42

Appendix F : Foraminifera data, relative species abundance (%)

Øksfjord cores	Relative species abundance (%)										
>63 µm			D2-6A					D3-3B			
Sediement depth (cm)	0,5	1,5	2,5	5,5	11,5	16,5	0,5	1,5	2,5	5,5	11,5
Sediment age (years AD)	2013	2007	1995	1967	1963	1928	2012	1999	1985	1926	ND
Sediment interval (cm)	0-1	1-2	2-3	5-6	11-12	16-17	0-1	1-2	2-3	5-6	11-12
Adercotryma glomeratum/wrighti	3,70	2,29	2,49	4,55	0,00	1,75	2,24	5,06	7,66	1,86	0,46
Ammoscalaria tenuimargo	0,00	0,00	0,00	0,00	0,00	0,00	0,00	1,95	1,44	0,47	0,00
Crobostomoides cassimargo	0,00	0,00	0,00	0,00	0,00	0,00	0,00	0,00	0,96	0,93	0,00
Cribrostomoides jeffreysii	0,00	0,00	0,00	0,00	0,00	0,00	0,90	1,17	0,96	0,00	0,00
Crobostomoides sp	0,00	0,00	0,00	0,00	0,00	0,00	0,00	0,00	0,96	0,00	0,00
Eggerella europea	0,31	0,00	0,23	0,00	0,00	0,00	0,45	0,39	0,00	0,00	0,00
Eggerelloides medius	1,23	1,31	0,68	1,40	0,00	0,70	4,04	2,33	4,78	0,93	0,46
Haplophragmoides bradyi	0,00	0,33	0,00	0,00	0,00	0,00	0,00	0,00	0,00	0,00	0,00
Haplophragmoides sphaeriloculum	0,00	0,00	0,23	0,00	0,00	0,35	1,35	2,33	0,48	1,86	0,00
Lagenammina arenulata	0,00	0,00	0,00	0,00	0,00	0,00	0,00	0,00	2,39	1,40	0,00
Lagenammina diffluguformis	0,00	0,00	0,00	0,70	0,40	0,00	0,00	0,00	0,00	0,00	0,00
Psammosphaere sp	0,31	0,00	0,00	0,00	0,00	0,00	0,00	0,00	0,00	0,00	0,00
Revurvoides contortus	0,00	0,00	0,45	1,75	0,00	0,35	0,00	3,50	3,83	3,26	0,93
Recurvoides laevigatum	4,63	2,29	0,00	0,00	0,00	0,00	0,00	0,00	0,00	0,00	0,00
Reophax fusiformis	0,62	0,98	0,00	0,00	0,00	0,00	0,00	0,39	0,00	1,40	0,00
Reophax rostrata	0,31	0,00	0,00	1,40	0,00	0,00	0,00	0,00	0,00	0,00	0,00
Reophax sp.	0,00	0,33	0,00	0,00	0,00	0,70	0,00	0,00	0,00	2,79	0,00
Reophax scorpiurus	0,00	1,31	0,00	0,00	0,00	0,00	4,04	0,39	0,00	0,00	0,00
Spiroplectammina biformis	0,00	0,00	3,85	0,35	0,00	0,35	4,48	5,45	1,91	0,00	0,00
Textularia contorta	0,31	0,33	0,23	0,00	0,00	0,00	0,00	0,39	0,00	0,47	0,00
Textularia earlandi	7,10	5,88	9,30	1,05	0,00	0,35	8,97	5,84	3,35	1,86	0,00
Textularia kattegatensis	0,00	0,00	0,00	0,00	0,00	0,00	0,00	0,39	0,48	0,00	0,00
Tritaxis conica	0,00	0,00	0,00	0,00	0,00	0,00	0,90	1,56	3,35	0,00	0,00
Trochammina globigeriniformis	0,00	0,00	0,00	0,00	0,00	0,00	0,90	0,00	0,96	0,47	0,00
Trochammina sp.	0,00	0,00	0,00	0,00	0,00	0,00	0,00	1,56	0,96	0,00	0,46
Astrononion gallowayi	0,62	0,65	2,72	0,35	0,81	0,70	0,00	0,00	0,00	0,47	0,93
Bolivina sp.	0,00	0,00	0,00	0,00	0,00	0,35	0,00	0,00	0,00	0,00	0,00
Bolivinellina pseudopunctata	0,93	1,96	2,04	1,75	1,21	3,15	4,93	1,56	0,00	0,47	0,00
Brizalina skagerrakensis	14,81	4,90	2,49	3,50	0,00	0,35	0,45	0,00	0,00	0,00	0,00
Buccella frigida	0,31	0,00	0,00	0,00	0,40	0,00	0,00	1,17	1,44	8,37	6,94
Bulimina marginata	13,58	11,44	7,03	25,52	8,87	3,50	21,52	18,29	25,84	21,40	12,96
Bulimina sp	0,00	0,00	0,00	0,00	0,00	0,00	0,45	0,00	0,00	0,00	0,00
Cassidulina laevigata	5,86	5,23	6,12	17,83	3,63	15,38	4,48	3,89	0,48	3,72	0,00
Cassidulina neoteretis	0,00	0,00	0,00	0,00	0,00	0,00	0,00	0,00	0,00	0,00	1,85
Cassidulina reniforme	6,79	10,78	11,34	9,09	10,08	20,98	2,69	3,50	2,39	7,91	25,46
Cassidulinoides bradyi	0,31	0,00	0,23	0,00	0,00	0,00	0,00	0,00	0,00	0,00	0,00
Cibicidoides bradyi	0,00	0,33	0,00	0,00	0,00	0,00	0,00	0,00	0,00	0,00	0,00
Cibicidoides mundulus	0,00	0,00	0,00	1,05	0,00	0,00	0,00	0,00	0,00	0,00	0,00
Cibicidoides sp	0,00	0,00	0,00	0,00	0,00	0,00	0,00	0,00	0,00	0,93	0,00
Cibicides lobatulus	5,86	1,31	1,81	0,00	1,21	0,00	0,45	0,78	0,96	0,00	0,46
Cibicides praecinctus	0,00	0,00	0,00	0,00	0,00	0,00	0,00	0,00	0,00	0,00	0,46
Cibicides refulgens	3,09	2,29	1,13	0,00	39,11	4,20	0,90	1,56	0,00	0,47	1,39
Cornuspira involvens	0,00	0,33	0,00	0,00	0,00	0,00	0,00	0,00	0,00	0,00	0,00
Cyclogyra invovlens	0,00	0,00	0,00	0,00	0,00	0,00	0,00	0,00	0,48	0,00	0,00
Discorbinella bertheloti	0,00	0,65	0,23	1,05	1,61	1,75	0,45	0,00	0,00	0,00	0,00
Elphidium albiumbilicatum	0,00	0,00	0,00	0,00	1,21	0,35	1,35	0,39	0,48	0,47	3,24
Elphidium excavatum	0,62	0,98	0,23	0,00	1,61	0,35	0,45	0,39	0,96	1,40	6,94
Elphidium sp.	0,00	0,33	0,23	0,00	0,00	0,35	0,45	0,00	0,00	0,93	0,46
Elphidium subarctica	0,00	1,31	0,23	0,00	1,21	1,75	0,90	1,17	0,96	0,00	0,00
Epistominella vitrea	0,93	3,59	7,71	0,00	1,21	0,70	2,24	2,72	0,48	0,93	1,39
Fissurina sp	0,00	0,00	0,00	0,00	0,81	0,00	0,00	0,00	0,00	0,00	0,00
Gavelinopsis praegeri	0,00	0,00	0,00	0,35	0,00	0,35	0,00	0,00	0,00	0,00	0,00
Globobuliminia turgida	2,78	1,63	0,68	3,85	0,40	1,75	0,00	0,00	0,00	0,47	0,00
Hyalinea balthica	3,70	2,29	2,27	12,59	6,85	5,24	5,38	3,89	2,39	4,19	14,35
Islandiella islandica	0,00	0,00	0,23	0,00	0,81	0,35	0,00	0,00	1,91	0,47	1,39
Lagena distoma	0,00	0,00	0,00	0,00	0,00	0,00	0,45	0,00	0,00	0,93	0,00
Lagena globosa	0,00	0,00	0,23	0,00	0,00	0,00	0,00	0,00	0,00	0,00	0,00
Lagena laevis	0,31	0,00	0,23	0,00	0,00	0,00	0,00	0,00	0,00	0,00	0,00
Lagena striata	0,00	0,00	0,00	0,00	0,40	0,00	0,00	0,00	0,00	0,00	0,00
Lagena sp.	0,00	0,00	0,00	0,00	0,00	0,35	0,00	0,00	0,00	0,00	0,00
Lenticulina sp.	0,00	0,33	0,00	0,00	0,00	0,00	0,00	0,00	0,00	0,00	0,00
Melonis barleeanum	0,00	0,65	0,00	0,00	0,81	0,00	0,00	0,00	0,00	0,00	0,46
Nonionella auricula	0,00	0,00	0,00	0,00	0,00	1,75	0,00	0,00	0,00	0,00	0,00
Nonionella iridea	0,31	2,61	0,00	2,10	0,40	0,00	0,45	0,00	0,48	0,00	0,00
Nonionella turgida	0,00	0,00	0,00	0,00	0,00	0,00	0,00	0,00	0,96	0,93	0,00
Nonionellina labradorica	4,32	5,56	5,44	4,20	1,21	2,45	2,69	1,95	1,91	4,19	3,24
Pullenia osloensis	6,79	12,75	14,51	0,00	1,61	10,84	5,83	5,06	1,91	2,79	6,48
Quinqueloculina sp.	0,31	0,00	0,00	1,75	0,00	0,00	0,00	0,00	0,00	0,00	0,00
Quinqueloculina stalkeri	0,00	0,33	0,23	0,00	0,00	0,35	0,00	0,00	0,00	0,00	0,00
Stainforthia concava	0,93	1,31	0,68	0,00	0,40	3,15	0,90	1,56	0,96	4,19	2,31
Stainforthia fusiformis + feylingi	7,10	10,46	13,61	3,85	2,42	14,69	14,35	19,07	17,70	12,56	5,09
Trifarina angulosa	0,31	0,98	0,68	0,00	10,89	0,35	0,00	0,39	2,87	3,26	1,39
Triloculina oblonga	0,00	0,00	0,23	0,00	0,00	0,00	0,00	0,00	0,00	0,00	0,00
calc unidetified	0,00	0,00	0,00	0,00	0,00	0,00	0,00	0,00	0,00	0,93	0,46

Appendix G: Foraminiferal species assemblage similarity (MDS) calcareous species

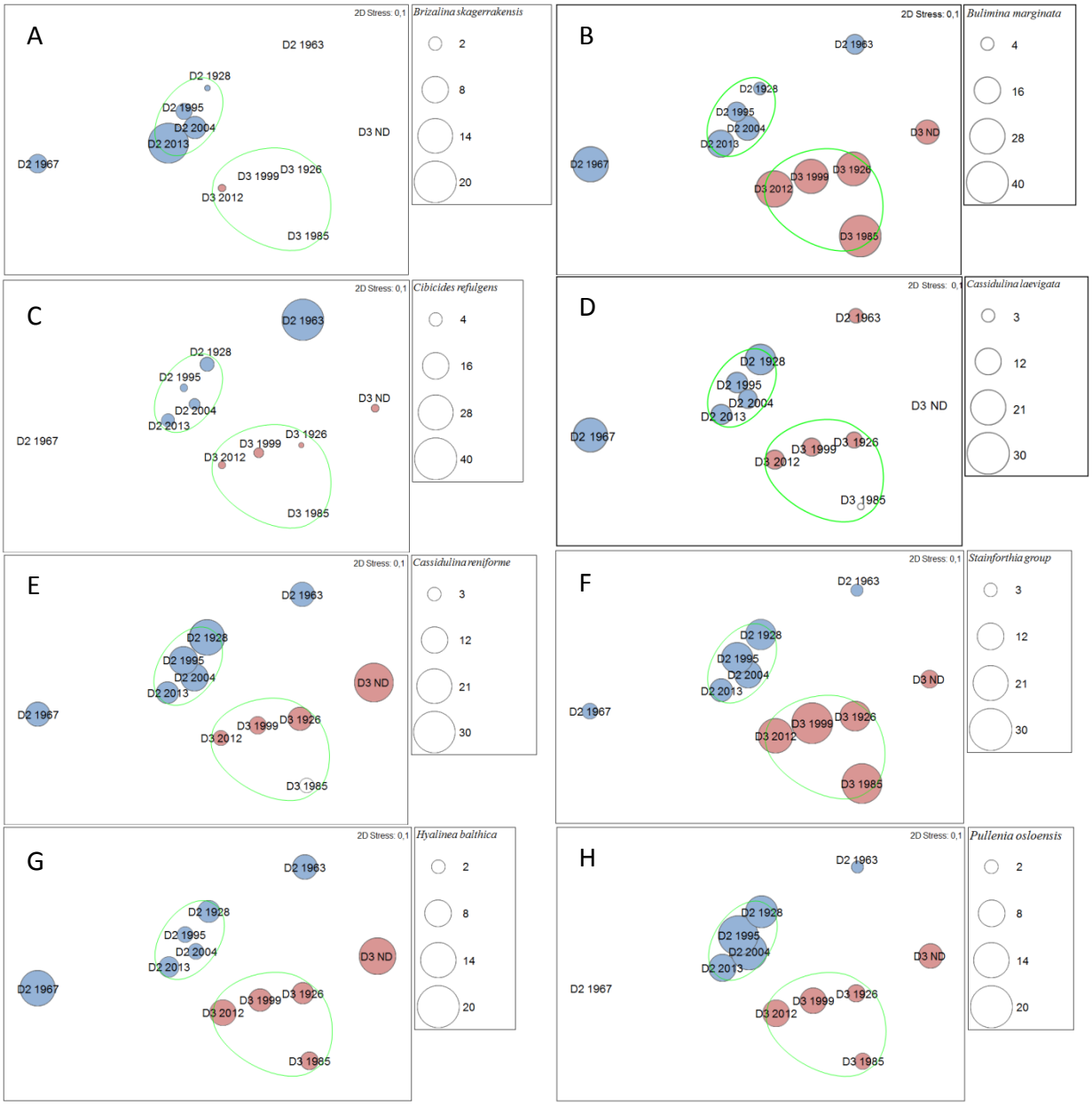

Appendix H: Foraminifera reference list, based on The World Register of Marine Species (WoRMS, 2018)

Adercotryma glomeratum (Brady) = *Lituola glomerata* Brady 1878.
Adercotryma wrighti Brönnimann & Whittaker 1987.
Ammoscalaria tenuimargo (Brady) = *Haplophragmium tenuimargo* Brady, 1882.
Astrononion gallowayi Loeblich & Tappan, 1953.
Bolivinellina pseudopunctata (Höglund) = *Bolivina pseudopunctata* Höglund, 1947.
Brizalina skagerrakensis (Qvale & Nigam) = *Bolivina skagerrakensis* Qvale & Nigam, 1985.
Buccella frígida (Cushman) = *Pulvinulina frigida* Cushman, 1922.
Bulimina marginata d'Orbigny, 1826.
Cassidulina laevigata d'Orbigny, 1826.
Cassidulina neoteretis Siendekrantz, 1995.
Cassidulina reniforme Nørvang, 1945.
*Cassidulinoides bradyi (*Normann) = *Cassidulina bradyi* Norman, 1881.
Cibicides lobatulus (Walker & Jacob*) = Echinus lobatulus* Walker & Jacob, 1798.
Cibicides praecinctus (Karrer) = *Rotalia praecincta* Karrer, 1868.
Cibicides refulgens de Monfort, 1808.
Cibicidoides bradyi (Trauth) = *Truncatulina bradyi* Trauth, 1918.
Cibicidoides mundulus (Brady, Parker & Jones) = *Truncatulina mundula* Brady, Parker & Jones, 1888.
Cornuspira involvens (Reuss) = *Operculina involvens* Reuss, 1850.
Cribrostomoides jeffreysii (Williamson) = *Nonionina jeffreysii* Williamson, 1858.
Cribrostomoides cassimargo
Cyclogyra involvens (Reuss) = *Operculina involvens* Reuss, 1850.
Discorbinella bertheloti (d'Orbigny) = *Rosalina bertheloti* d'Orbigny, 1839.
Eggerella europea (Christiansen) = *Verneuilina europeum* Christiansen, 1958.
Eggerelloides medius (Höglund) = *Verneuilina media* Höglund, 1947.
Elphidium albiumbilicatum (Weiss) = *Nonion pauciloculum* (Cushman) subsp. *albiumbilicatum* Weiss, 1954.
Elphidium excavatum (Terquem) = *Polystomella excavata* Terquem, 1875.
Elphidium subarctica Cushman, 1944.
Epistominella vitrea Parker, 1953.
Gavelinopsis praegeri (Heron-Allen & Earland) = *Discorbina preagreri* Heron-allen & Earland, 1913.
Globobulimina turgida Bailey = *Bulimina turgida* Bailey, 1851.
Haplophragmoides bradyi (Robertson) = *Trochammina bradyi* Robertson, 1891.
Haplophragmoides sphaeriloculum Cushman, 1917.
Hyalinea balthica (Schröter in Gmelin) = *Nautilus balthicus* Schröter in Gmelin, 1791.
Islandiella islandica Nørvang, 1945.
Lagenammina arenulata (Skinner) = *Reophax difflugiformis var. arenulata* Skinner, 1961.
Lagena dístoma Parker & Jones, 1864.
Lagena globosa (Montagu) = *Vermiculum globosum* Montagu, 1803.
Lagena laevis (Montagu) = *Vermiculum laeve* Montagu, 1803.
Lagena striata (d'Orbigny) = *Oolina striata* d'Orbigny, 1839.
Lagenammina arenulata (Skinner) = *Reophax difflugiformis subsp. arenulata* Skinner, 1961

Lagenammina difflugiformis (Brady) = *Reophax difflugiformis* Brady, 1879
Melonis barleeanum (Williamson) = *Nonionina barleeana* Williamson, 1858.
Nonionella auricula Heron-Allen & Earland, 1930
Nonionella iridea Heron-Allen & Earland, 1932.
Nonionella turgida (Williamson) = *Rotalina turgida* Williamson,1858.
Nonionellina labradorica (Dawson) = *Nonionina scapha* var. *labradorica* Dawson, 1860.
Pullenia osloensis Feyling-Hanssen, 1954.
Quinqueloculina stalkeri Loeblich & Tappan, 1953
Recurvoides laevigatum Höglund, 1947
Reophax fusiformis (Williamson) = *Proteonina fusiformis* Williamson, 1858.
Reophax rostrata Höglund, 1947
Reophax scorpiurus Montfort, 1808.
Recurvoides contortus Earland, 1934
*Spiroplectammina biformis (*Parker & Jones) = *Textularia agglutinans* var. *biformis* Parker & Jones, 1865.
Stainforthia concava (Höglund) = *Virgulina concava* Höglund 1947.
Stainforthia feylingi Knudsen & Seidenkrantz, 1994
Stainforthia fusiformis (Williamson) = *Bulimina pupoides* d'Orbigny var. *fusiformis* Williamson 1858
Textularia contorta Höglund, 1947
Textularia earlandi Parker, 1952.
Textularia kattegatensis Höglund, 1948.
Trifarina angulosa (Williamson) = *Uvigerina angulosa* Williamson, 1858.
Triloculina oblonga (Montagu) = *Vermiculum oblongum* Montagu, 1803.
Tritaxis conica (Parker & Jones) = *Valvulina conica* Parker & Jones, 1865.
Trochammina globigeriniformis (Parker & Jones*) = Ammoglobigerina globigeriniformis* Parker & Jones, 1865.

Appendix I: Fish farm production data (provided by Odd Leknes, Grieg Seafood)

Brutto tilvekst i perioden	Fôrmengde i perioden	Utgående År															
Lokalitet	Data	2005	2006	2007	2008	2009	2010	2011	2012	2013	2014	2015	2016	2017			
Auskarnes Ø 10275	Brutto tilvekst i perioden	776 284	464 460	1 887 219	1 404 379	627 782	3 075 943	924 832	1 909 562	2 394 655	1 182 279	2 249 464	122 075	0			
	Fôrmengde i perioden	1 154 027	534 247	2 138 111	2 038 234	624 555	3 786 579	1 013 516	1 982 677	2 939 119	1 305 617	2 874 983	217 010	0			
Kjøsen 27015	Brutto tilvekst i perioden			671 498	2 523 089	599 898	813 834	2 475 831	96 259	2 282 855	1 550 888	0	113 770	2 343 837			
	Fôrmengde i perioden			639 301	3 050 813	1 030 673	826 270	2 798 358	116 172	2 487 579	2 020 041	0	117 545	2 794 655			
Steinviknes 10825	Brutto tilvekst i perioden	90 746	2 056 747	674 841	423 653	3 152 976	782 218	2 532 337	857 180	1 763 304	1 724 494	0	0	1 818 229			
	Fôrmengde i perioden	89 000	2 472 210	1 364 783	565 273	3 811 535	705 715	2 950 654	1 080 900	1 847 231	2 363 483	0	0	2 085 067			
Storvik 13316	Brutto tilvekst i perioden		1 305 328	2 962 930	793 629	1 540 416	2 071 394	717 275	2 800 032	727 558	630 597	2 234 576	577 489	0			
	Fôrmengde i perioden		1 328 808	4 192 308	819 792	1 607 305	2 845 817	741 191	3 243 164	765 609	764 571	2 875 746	527 452	0			
Total	Brutto tilvekst i perioden	867 030	3 826 535	6 196 488	5 144 751	5 921 072	6 743 388	6 650 275	5 663 033	7 168 372	5 088 258	4 484 040	813 333	4 162 066			
	Fôrmengde i perioden	1 243 027	4 335 265	8 334 503	6 474 112	7 074 068	8 164 381	7 503 720	6 422 913	8 039 538	6 453 712	5 750 729	862 007	4 879 722			

Lokalitet	I bruk			Ikke i bruk		
Lokalitet	Fra og med	Til og med	Dager	Fra og med	Til og med	Dager
Auskarnes Ø 10275	13.05.2009	04.07.2011	783	05.07.2011	17.09.2011	75
Auskarnes Ø 10275	18.09.2011	28.10.2013	771	29.10.2013	22.03.2014	145
Auskarnes Ø 10275	23.03.2014	03.05.2016	772	04.05.2016	05.09.2017	489
Danielsnes 31137	12.09.2010	16.11.2012	796	17.11.2012	02.12.2013	381
Danielsnes 31137	03.12.2013	08.09.2015	644	09.09.2015	29.06.2016	295
Danielsnes 31137	30.06.2016	05.09.2017	432			
Kjøsen 27015	12.12.2009	16.01.2012	766	17.01.2012	28.09.2012	256
Kjøsen 27015	29.09.2012	23.09.2014	724	24.09.2014	02.11.2016	771
Kjøsen 27015	03.11.2016	05.09.2017	306			
Olaneset 10795	27.08.2011	10.09.2013	745	11.09.2013	09.11.2013	60
Olaneset 10795	10.11.2013	17.09.2015	676	18.09.2015	18.10.2016	396
Olaneset 10795	19.10.2016	05.09.2017	321			
Skognes 10823	06.11.2010	02.03.2013	847	03.03.2013	31.05.2013	90
Skognes 10823	01.06.2013	22.12.2013	205	23.12.2013	05.09.2017	1 352
Steinviknes 10825	20.06.2010	18.07.2012	760	19.07.2012	25.11.2012	130
Steinviknes 10825	26.11.2012	13.10.2014	687	14.10.2014	25.06.2017	985
Steinviknes 10825	26.06.2017	05.09.2017	71			
Storvik 13316	08.04.2011	20.06.2013	805	21.06.2013	08.05.2014	322
Storvik 13316	09.05.2014	22.04.2016	714	23.04.2016	05.09.2017	500